

# Indicative significance of water environment in zeolitic structure – a study using experimentally grown cancrinite and analcime

EWA SŁABY

*Institute of Geochemistry, Mineralogy and Petrology of the University of Warsaw,  
PL-02-089 Warszawa, Al. Żwirki i Wigury 93. E-mail: eslaby@geo.uw.edu.pl*

## ABSTRACT:

SŁABY, E. 1999. Indicative significance of water environment in zeolitic structure – a study using experimentally grown cancrinite and analcime. *Acta Geol. Polon.*, **49** (1), 25-65. Warszawa.

Cancrinite and analcime were synthesized in the two hydrothermal systems: acid plagioclase –  $\text{Na}_2\text{CO}_3$  –  $\text{H}_2\text{O}$  and basic plagioclase –  $\text{Na}_2\text{CO}_3$  –  $\text{H}_2\text{O}$  under widely varying temperatures and salt concentrations in the solution. The IR,  $^1\text{H}$  MAS NMR, DTG/TG analyses were carried out to determine water position in the crystals. Additionally IR spectra were recorded during subsequent dehydration and rehydration processes. The results of the investigations indicate that the water environment in both minerals is sensitive to the conditions of crystal formation. Crystallization temperature is the most important factor influencing water position. The water sites in the analcime and cancrinite crystals depend on structure modifications. Variations of the structure result from different chemical composition of the source material, structure of the substrates and the salt concentration in the solution. The structures formed under lower temperatures incorporate more water than those formed at high temperatures. In the cancrinite and analcime two main types of water,  $\text{H}_2\text{O}(\text{I})$  and  $\text{H}_2\text{O}(\text{II})$ , appear. Other  $\text{OH}_m$  groups can also be recognized. The position of water  $\text{H}_2\text{O}(\text{II})$  is better defined than that of  $\text{H}_2\text{O}(\text{I})$ .  $\text{H}_2\text{O}(\text{II})$  is the most sensitive indicator of thermal conditions of the formation of cancrinite as well as analcime. The amount of  $\text{H}_2\text{O}(\text{II})$  equals that of  $\text{H}_2\text{O}(\text{I})$  in the products of low temperature ( $300^\circ\text{C}$ ) syntheses. In crystals synthesized at high temperature ( $550^\circ\text{C}$ ) the presence of  $\text{H}_2\text{O}(\text{II})$  is very limited.

## INTRODUCTION

In the last few years much more attention has been focused on water environment in the zeolitic structure. A lot of research work has also been done on analcime- and cancrinite-family minerals. The most important aspects of this research are the following:

- refining of the water position in the structure;
- recognising of the water environment: dynamic motion, self-diffusion, thermal behaviour in the structure;
- research on the oxygen and hydrogen isotope composition of structurally incorporated water;

- experimental work on the oxygen isotope fractionation between water in the system and water in zeolitic mineral;
- research on the dehydration process of the mineral structure.

There are many petrologic implication of the results from the three last topics. Many investigations have been carried out on analcime crystals and almost no data are available for cancrinite family minerals. The most important petrologic requirement is to obtain the answer to the question: Does the water environment and the behaviour of the water molecule in the structure indicate the origin of the crystal?

The research work on the isotopic composition of the channel water and on the dehydration process seems to give quantitative constraints on the origin of zeolites. The oxygen isotope composition of the channel water in the analcime structure suggests that analcimes may be also the best oxygen isotope low-temperature geothermometer (KARLSSON & CLAYTON 1990). Analcime-water fractionation is nearly independent over the entire stability range of analcime and very similar to water-calcite fractionation. The temperature could be then calculated using the water-calcite fractionation curve. Much more questionable is an attempt to use isotopic composition to determine the precise origin of the analcime (KARLSSON & CLAYTON 1991, LUHR & KYSER 1989). Analcimes described by KARLSSON & CLAYTON (1991) on isotopic constraints as secondary, are in the opinion of PEARCE (1993) primary.

Perhaps more promising are considerations of the dehydration kinetics of the zeolitic structure. GIAMPAOLO & LOMBARDI (1994) have noticed difference in the bonding energies within analcimes crystallized in different genetic environments. PUTNIS & *al.* (1994) and LINE & *al.* (1995) have continued the research work on the dehydration kinetics in analcimes of different origin: hydrothermal analcimes (H) and analcimes (X) formed from leucite crystals. According to results obtained by these authors, the H<sub>2</sub>O bonding energies in the crystals depend on porosity. The higher porosity in X analcime promotes acceleration of water movement during the dehydration process. Similarly, the Na drift under electron beam is much faster in the X-type of analcime. However the results are not comprehensive as, under certain circumstances, the dehydration process may act as an indicator of analcime origin. It could be admitted that the water shows order-disorder in analcime structure. Order-disorder of elements in the structure could depend on crystallization conditions.

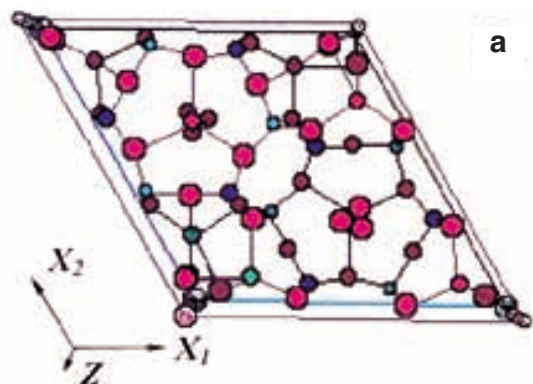
While reviewing the above data one can formulate a question: is the water environment in the zeolitic structure sensitive to the physico-chemical conditions of the crystallization process? Establishing such a relation could have a significant petrographic meaning for the reconstruction of the genetic conditions of parageneses contacting the zeolite minerals. The aim of the present research work was to crystallize zeolitic structures with different ordering of the channel water under various hydrothermal conditions and determine the water environment in there, in order to prove the relation.

Syntheses over a narrow range of hydrothermal conditions have been chosen in order to avoid argument that differences in water environment could appear only in strictly different genetic events. If there is any variability in the water position in the structure build over a narrow range of physico-chemical conditions there must also be in any other environment. Zeolites are formed generally under hydrothermal low-temperature conditions. In the experiment higher temperature runs have been preferred because approaching equilibrium in the process is then relatively fast. Two minerals with zeolitic-type structure were chosen for this purpose: analcime and cancrinite. Both of them are usually products of the dissolution of aluminosilicates under hydrothermal conditions. Both of them show order-disorder in water orientation. They could crystallize together under certain conditions. The structure of both of them has been repeatedly determined using a variety of techniques, including neutron diffraction. Some additional information about the dynamic as well as about the thermal behaviour of the channel water has been published in the last few years. The main reason however is that information is lacking regarding the influence of the crystallizations conditions on water environment in analcime and cancrinite minerals.

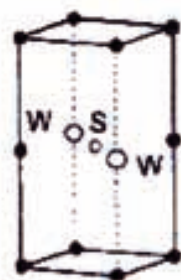
## CANCRINITE AND ANALCIME STRUCTURE

Minerals of the cancrinite family appear in many silica-deficient and alkali-rich rocks. They are usually products of the hydrothermal alteration of nepheline or feldspar (GUNNER & BURR 1946). The nepheline could be primary magmatic crystals or a plagioclase alteration product in hydrothermal solution (CERMIGNANI & ANDERSON 1983, ANDERSON & CERMIGNANI 1991). The family comprises minerals with similar framework and different channel ions. The name cancrinite is used for two minerals: cancrinite and basic (hydroxyl) cancrinite. In cancrinite channel Na, Ca and CO<sub>3</sub> ions are found whereas in basic cancrinite the carbonate ions are replaced by an OH-group. The ideal formula for cancrinite is Na<sub>6</sub>Ca<sub>2</sub>[Al<sub>6</sub>Si<sub>6</sub>O<sub>24</sub>](CO<sub>3</sub>)<sub>2</sub>·2H<sub>2</sub>O.

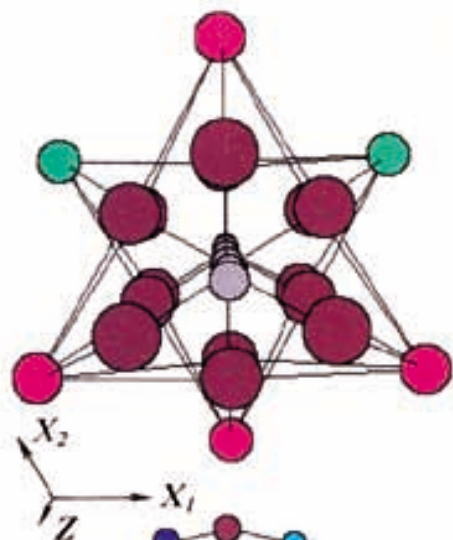
The crystal structure of cancrinite was first determined by JARCHOW (1965). The basic units of the hexagonal cancrinite structure (P6<sub>3</sub>) are 4-, 6- and 12-membered rings of alternating silicon and aluminium tetrahedra. The aluminium and silicon cations are fully ordered (Text-fig. 1a). The structure consists of small "undecahedral" ε-cages and



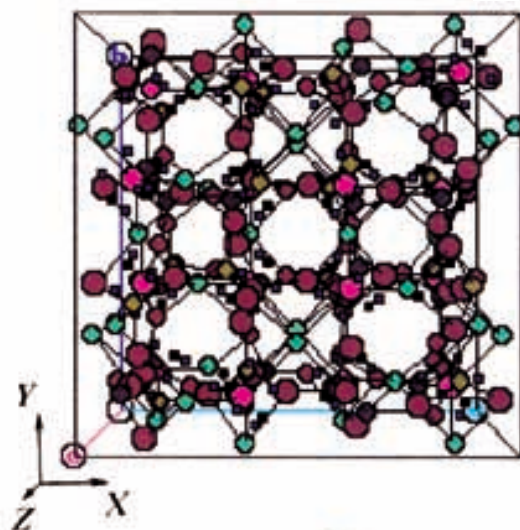
a



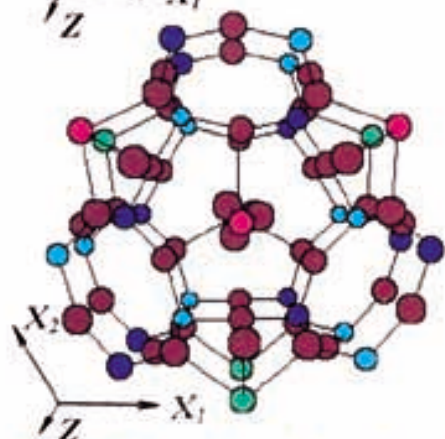
a



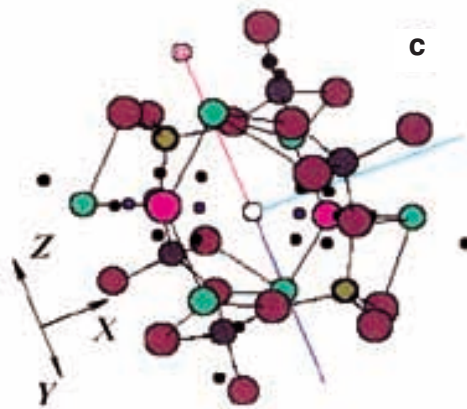
b



b



c



c



Fig. 1

Fig. 2

Fig. 1. Crystal structure of cancrinite

a – Unit cell showing four-, six-, and twelve-membered rings; b – Detail showing centre of 12-membered ring of silicon and aluminium tetrahedra; c – Detail showing water environment (oxygens around Na1 position) in the cell

Fig. 2. Crystal structure of cubic analcime

a – The S and W sites in the prismatic cage; b – Cell unit; c – Detail showing water environment in the analcime structure

large continuous channels. Each  $\epsilon$ -cage is formed of five 6-membered rings and six 4-membered rings. The 6-membered rings show stacking in an ABAB... sequence, which in turn leads to 12-membered rings forming large continuous channels with  $\text{CO}_3^{2-}$  groups along  $c$  (Text-fig. 1b). The  $\epsilon$ -cage is occupied by  $\text{Na} \cdot \text{H}_2\text{O}$  cluster (Text-fig. 1c). The Na takes the Na1 site and water is disordered around 3-fold axis (GRUNDY & HASSAN 1982, EMIRALIEV & JAMZIN 1982). In the  $\text{H}_2\text{O(I)} - \text{Na1} - \text{H}_2\text{O(II)}$  chain, one water molecule is closer to the Na cation than the other (HASSAN 1996a, b). During heating the chain expands. Both distances become equal. The sodium moves towards the plane of the six-membered ring. The tetrahedra in the ring are forced to rotate, which makes the ring configuration more planar (HASSAN 1996b). The water leaves the structure continuously but with variable intensity, due to the differences in  $\text{H}_2\text{O(I)}$  and  $\text{H}_2\text{O(II)}$  bonding in the structure, thus two weak maxima appear at  $\sim 300^\circ\text{C}$  and  $\sim 680^\circ\text{C}$ . The water loss causes an increase in  $c$  parameter (HASSAN 1996b). Besides the water molecules, the  $\text{OH}_m$  ( $m=1,2,3$ ) complexes are found in the 12-membered channel (GALITSKI & *al.* 1978).

The Na2 is located in the large channel. The calcium cation could occupy the Na2 site or could be incorporated into the  $\text{CaCO}_3$  clusters. The ions in the large channel intend to build superstructure with supercell up to  $\sim 41 \text{ \AA}$  ( $8 \times c=5.117 \text{ \AA}$ ). The satellite reflections pointing to the superstructure were commonly observed by JARCHOW (1965) and by FOIT, JR & *al.* (1973). HASSAN & BUSECK (1992) in their excellent paper explained the origin of the superstructure in details presenting the supercell model and calculating the supercell parameters.

Analcime crystals are found in a number of different environments. Due to the conditions of formation they are divided into five groups: P-type (primary), H-type (hydrothermal), S-type (sedimentary), M-type (metamorphic), L(X)-type (formed by exchange conversion of leucite). The ideal formula for analcime is  $\text{NaAlSi}_2\text{O}_6 \cdot \text{H}_2\text{O}$ . Hydrothermal analcime is inferred to have been formed by dissolution of aluminosilicates and crystallization from hydrothermal solution. The source material could include plagioclase, nepheline and volcanic glass.

The crystal symmetry of analcimes varies from cubic to monoclinic. The crystal structure of cubic analcimes was first determined by TAYLOR (1930) and refined many times. MAZZI & GALLI (1978) checked the symmetry of anisotropic crystals and

found tetragonal and orthorhombic symmetry. The difference in symmetry results from different ordering and site occupancies of aluminium and silicon. The crystal structure of monoclinic analcimes was determined by PECHAR (1988). The basic module in the analcime cubic and tetragonal structure is termed prismatic cage (Text-fig. 2a-b). It is composed of four-membered rings and additional tetrahedra are located on the two opposite edges. The extra-framework sites inside the prism and on the "missing" edges are called S and W respectively (MERLINO 1984). These sites attract special attention because the analcime structure contains water molecules and sodium atoms there (Text-fig. 2c).

Almost every element in the analcime structure is distributed in a disordered way. Sodium atoms have a disordered distribution (16 Na atoms over 24 sites available of them). The 32 silicon and 16 aluminium atoms have a similarly disordered distribution. The water molecule could be shifted towards the sodium position when sodium occupancy is low. There are three sodium sites surrounding each water position. To account for the stoichiometric unit one of them must be empty and the vacant sites filled by hydrogen atoms (MAZZI & GALLI 1978). Because of variously distributed sodium vacancy the hydronium atoms occupied in disordered way some among 96 positions. The H atoms are also not arranged around the oxygen atom in an ordered way (FERRARIS & *al.* 1971). Water molecules show dynamic disorder in the motion both at higher, as well as at lower temperatures (LINE & *al.* 1994). Removal of a water molecule from the structure causes migration of sodium atoms. After the redistribution of the sodium atoms one-third of their sites are free and two-thirds have the fourfold plane trapezoidal coordination (BAKAKIN & *al.* 1994).

## THE EXPERIMENT

### Assumption and performance

The type of zeolitic structure that crystallizes in hydrothermal environments depends on many factors including: source material, chemical composition of the fluid, time, temperature and others. Many papers deal with zeolite hydrothermal synthesis in the system  $\text{Na}_2\text{O-SiO}_2\text{-Al}_2\text{O}_3\text{-H}_2\text{O}$  (with or without carbonate anions). This review includes only those works which influenced the design of my experiment. The aim of the experiment was to crystallize

minerals with cancrinite and analcime structure under various conditions in a closed system.

BARTH-WIRSCHING & HÖLLER (1989) summarised the conditions of zeolite formation in the closed system. The most pronounced factor influencing the type of zeolite that forms is the pH of the solution and the Si/Al ratio in the source material. The temperature is of equal significance. A highly alkaline environment and a high temperature of the synthesis can influence the water content in the zeolite structure.

The source material is of great importance in the planning of an experiment. Using material with Si/Al ratio 1:1 one can obtain minerals belonging to the cancrinite-sodalite family (BUHL 1991, HERMELER & *al.* 1991, MUNDUS & *al.* 1996, GERSON & ZHENG 1997, ZHENG & *al.* 1997). If the silicon content is higher analcime appears instead of sodalite (ABE & *al.* 1973, UEDA & KOIZUMI 1979, DUBANSKA & RYKL 1983, PECHAR 1989). Variation in the Si/Al (assuming Si>Al) of the source material leads to the growth of metastable analcime phases (KHUNDADZE & *al.* 1970). The starting material used in the synthesis differs significantly from experiment to experiment. Many experiments deal with natural minerals (albite, nepheline, corundum, *etc.*), rocks (shales and tuffs) or gel mixtures. The type of material affects the reaction kinetics. The grain size also affects the kinetics of zeolite crystallization. The yield of zeolite in the high-temperature synthesis increases if the substrate is coarse-grained (LO 1987).

The composition of the cancrinite like minerals that appear in hydrothermal system depends on the solution composition. A high NaOH (> 8M) concentration, with the addition of Na<sub>2</sub>CO<sub>3</sub> promotes natrodavyne and cancrinite crystallization (BUHL 1991). There are two types of both of them. Lowering of the NaOH concentration results in the appearance, in turn, of: sodalite, intermediate phase, and cancrinite (HERMELER & *al.* 1991).

Taking into account all the results of previous researches, I decided to conduct the new experiment under the following conditions:

- to set up the experiment under P-T conditions close to that of a natural hydrothermal system
- to take as a source material natural minerals with various Si:Al ratios (~1, >1),
- to use diluted Na<sub>2</sub>CO<sub>3</sub> solution in order to avoid intermediate and natrodavyne member of the cancrinite family,
- to run the experiment in the temperature range >300°C to avoid crystallization of low-symmetry zeolite phases,

– to establish the solution to mineral ratio at the start of the experiment of W/M=10 (single runs were conducted with W/M=5),

– to run the experiment always under constant pressure below 2 kbar.

As a source material natural acid and basic plagioclase were used. The Si:Al ratio in basic plagioclase almost approaches the value 1. In acid plagioclases (oligoclases) Si>>Al. Pure end members (albite and anorthite) were not used because they appear rather seldom in the igneous rocks. They both have different structures from those of oligoclase and labradorite, which could influence the reaction kinetics. Clear oligoclase crystals (Na<sub>0.74-0.76</sub>K<sub>0.02</sub>Ca<sub>0.23-0.21</sub> [Al<sub>1.27-1.24</sub>Si<sub>2.74-2.77</sub>O<sub>8</sub>]) (grain size 2 mm) without any indications of alteration and with no visible inclusions were separated from Tatra Mts. granite. Anorthosite from the NE part of Poland was the source for basic plagioclase (Ca<sub>0.63-0.56</sub>Na<sub>0.36-0.43</sub>K<sub>0.02</sub> [Al<sub>1.62-1.55</sub>Si<sub>2.38-2.44</sub>O<sub>8</sub>]) (grain size 2 mm). As in the case of the acid plagioclases only clear crystals of basic plagioclase (grain size 2 mm) were selected as a starting material. The hydrothermal medium used in the experiment was variably diluted Na<sub>2</sub>CO<sub>3</sub> solution of the molalities: 0.1, 0.5 and 1. Single runs were carried out with saturated and oversaturated 1-2M NaHCO<sub>3</sub> solutions. For every source material and every diluted solution 2 – 3 syntheses were performed at 550°C, 520°C, 480°C, 450°C, 400°C, 360°C, 330°C and 300°C (±10°C). The duration of the synthesis was chosen arbitrarily as 30 days. The run duration time was longer than that used to establish equilibrium between plagioclase and carbonate solution under similar temperature conditions by CERMIGNANI & ANDERSON (1983). Some runs were performed during 4, 8, 12, 20 and 40 days. The pressure was fixed at 1.8 kbar.

Cone seal pressure vessels made from Rene 41 with 12 mm inner diameter and 240 mm inner length were used in a perpendicular arrangement with the cup at the bottom. The arrangement gave rise to thermal gradient of 100°C between the top and the bottom. Four copper containers with 8 mm inner diameter and 20 mm inner length were fixed in an autoclave. The temperature in each container was measured in blind runs at 2 kbar using pressure tight welded shielded Ni-CrNi thermocouples and at the same time the temperature was monitored by means of an external Ni-CrNi thermocouple. Each Cu-container was then filled with starting material and solution usually in the proportion 1:10, placed in a cold seal vessel and heated in a furnace, usually for 30 days. The temperature was monitored continuously. The temperature of the reaction

was extrapolated from the autoclave calibration curve. The system was cooled by air. Before and after treatment the containers were weighed to ensure that no change in mass had occurred.

The products of plagioclase alteration were checked by microprobe analyses and X-ray powder diffraction. Chemical compositions were determined by means of an ARL Microprobe with wavelength-dispersive spectrometers (WDS) under the following conditions: 4s counting time (peak), 4s counting time (background), 6-8 $\mu$ m beam diameter, 15 kV excitation voltage, 15 nA specimen current. Microprobe analyses were made using the following standards: (101) albite for Na, Al, Si, (102) almandine for Fe and Mg, (141) sanidine for K and Ba, (140) strontium titanate (synthetic) for Sr, (135) plagioclase for Ca. The relative errors for the measured elements (Na, K, Ca, Si,

Al) were 0.5-1%. Data corrections were performed with a standard ZAF program.

X-ray powder diffraction data were collected on a Siemens D-500 (crystal graphite monochromator,  $\text{CuK}\alpha_1$  radiation). The data were collected in step-scan mode, from 10 to 80 $^\circ$ 2 $\theta$ . The 2 $\theta$  step size was 0.05 by the counting time 10s/step. External standard quartz were used. The least-squares refinement of lattice parameters was performed by using Treor. Quantitative analyses were performed using X-RAYAN program and the JCPDS data base (selected standards: analcime 19-1180, cancrinite 34-176, nepheline 35-424). To check the reaction progress changes in intensities of selected peaks in the source material and reaction products were used. The selected peaks were the following: (2 $\theta$ )19.170 (I=85) for cancrinite, 23.215(I=100) for nepheline, 15.863 (I=60) for analcime,

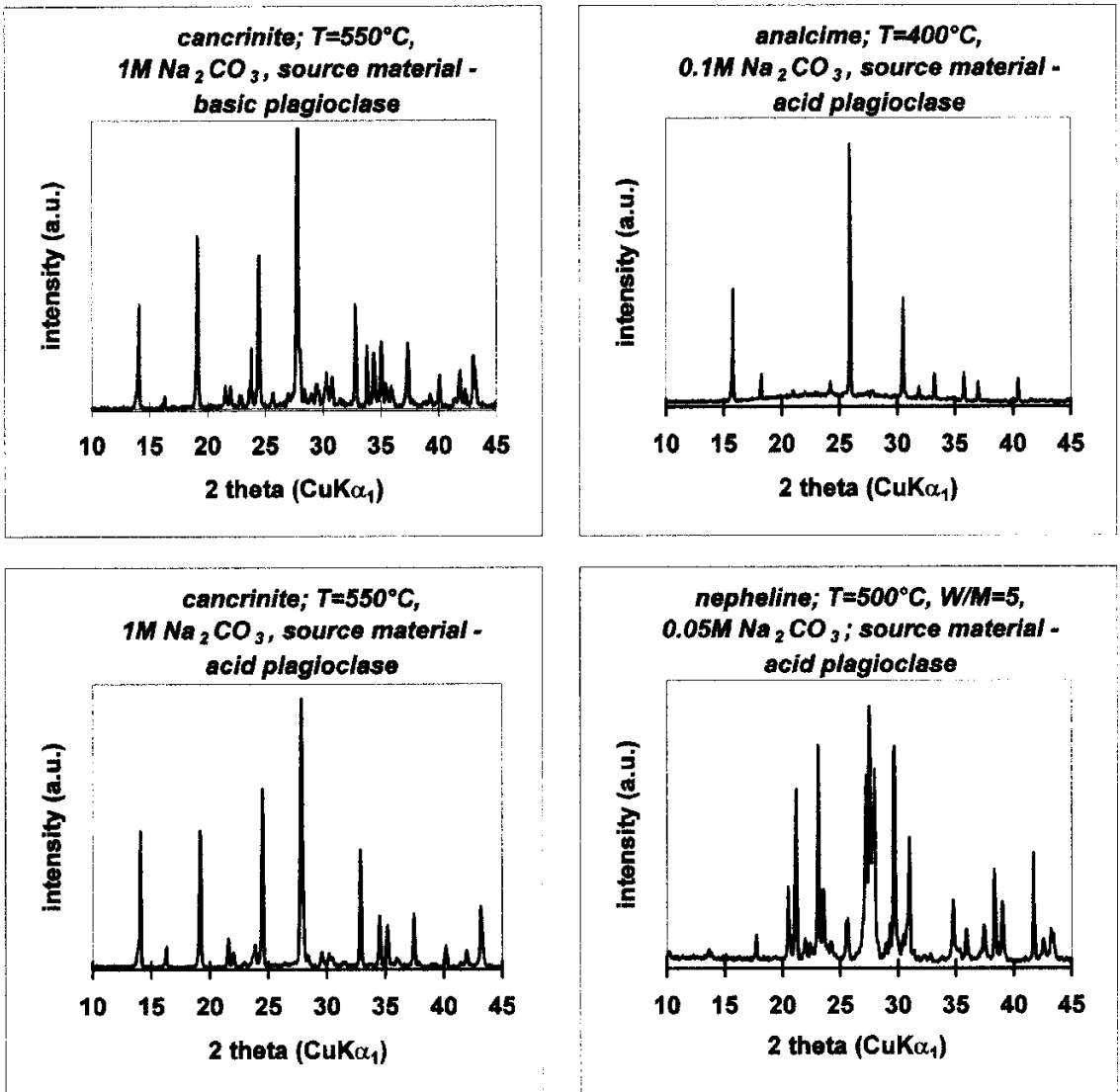


Fig. 3. The X-ray powder pattern (main peak area) of plagioclase alteration products (a.u. – arbitrary units)

a

Source material - basic plagioclase			Source material - acid plagioclase		
T(°C) of synthesis	Na <sub>2</sub> CO <sub>3</sub> concentration in the solution W/M=10	Products	T(°C) of synthesis	Na <sub>2</sub> CO <sub>3</sub> concentration in the solution W/M=10	Products
300	1M	cc, ab, rel	300	1M	cc, (an), ab, rel
400	1M	cc, ab, rel	400	1M	cc, (an), ab, rel
500	1M	cc, ab, rel	500	1M	cc, ab, rel
550	1M	cc, ab, rel	550	1M	cc, ab, rel
300	0.5M	cc, ab, rel	300	0.5M	an, ab, rel
400	0.5M	cc, ab, rel	400	0.5M	cc, ab, rel
500	0.5M	cc, ab, rel	500	0.5M	cc, ab, rel
550	0.5M	cc, ab, rel	550	0.5M	cc, ab, rel
300	0.1M	cc, ab, rel	300	0.1M	an, ab, rel
400	0.1M	cc, ab, rel	400	0.1M	an, ab, rel
500	0.1M	cc, ab, rel	500	0.1M	an, (cc), ab, rel
550	0.1M	cc, ab, rel	550	0.1M	an, ab, rel

Explanations: cc - cancrinite, an - analcime, ab - albite, rel - relicts of plagioclase, W/M - water to mineral ratio, symbols in brackets - small amount of mineral

b

Source material	T(°C) of synthesis	Na <sub>2</sub> CO <sub>3</sub> concentration in the solution	W/M ratio	Reaction time (days)	Products
acid plagioclase	300	0.5M	10	4	an, ab, rel
acid plagioclase	400	0.5M	10	4	an, (cc), ab, rel
acid plagioclase	500	0.5M	10	4	an, (cc/ne), ab, rel
acid plagioclase	600	0.5M	10	4	cc, (ne), ab, rel
acid plagioclase	300	0.5M	10	8	an, ab, rel
acid plagioclase	400	0.5M	10	8	an, (cc), ab, rel
acid plagioclase	500	0.5M	10	8	cc, ab, rel
acid plagioclase	600	0.5M	10	8	cc, ab, rel
acid plagioclase	300	0.5M	10	12	an, ab, rel
acid plagioclase	400	0.5M	10	12	an, cc, ab, rel
acid plagioclase	500	0.5M	10	12	cc, ab, rel
acid plagioclase	600	0.5M	10	12	cc, ab, rel
acid plagioclase	300	0.05M	10	4	an, ab, rel
acid plagioclase	400	0.05M	10	4	an, ab, rel
acid plagioclase	500	0.05M	5	8, 12	ne, ab, rel
basic plagioclase	500	0.05M	10	5	cc (ne), ab, rel
basic plagioclase	600	0.05M	10	5	cc (ne), ab, rel

Explanations: cc - cancrinite, an - analcime, ab - albite, rel - relicts of plagioclase, W/M - water to mineral ratio, symbols in brackets - small amount of mineral

c

Source material	T(°C) of synthesis	Salt concentration in the solution	W/M ratio	Reaction time (days)	Products
acid plagioclase	300	0.1M	10	30	an, ab, rel
acid plagioclase	400	0.1M	10	30	an, ab, rel
acid plagioclase	500	1M	10	20	cc, ab, rel
acid plagioclase	600	1M	10	20	cc, ab, rel
acid plagioclase	700	1M	10	12	cc, ab, rel
acid plagioclase	600	1M	5	12	ne, ab, rel

Explanations: an - analcime, cc - cancrinite, ne - nepheline, ab - albite, rel - plagioclase relicts

Table 1. Selected runs - conditions and products

a - Synthesis time 30 days; b - Synthesis time less than 30 days; c - Runs with NaHCO<sub>3</sub> solution as a medium

21.953 (I=50) for acid plagioclase, 21.953 (I=100) and 22.043 (I=45) for sodian anorthite. The results were compared with the reaction progress measured directly in the samples embedded in epoxy and polished.

From the total number of 300 runs, 200 were selected for consideration because of their reproducible results. 80 samples from the last ones were chosen for the further investigation.

## Products

The products of basic and acid plagioclase alteration are listed in Table 1a. The X-ray powder patterns of the main alteration products are shown in Text-fig. 3. The only crystals with zeolitic structure growing as a decay product of basic plagioclase is cancrinite. Cancrinite crystals appear as a product of every reaction, independently of the temperature of the run and also of the concentration of  $\text{Na}_2\text{CO}_3$  in the solution. They are accompanied by a small amount of albite, which is detectable only by X-ray

powder diffraction (Text-fig. 4). Perhaps some of the albite domains were captured by the growing cancrinite crystals. Lowering of the solution to mineral ratio (W/M) causes nepheline crystallization (Text-fig. 4). Runs with a duration of 30 days usually converted  $\sim 90 \pm 10$  vol% of plagioclase into zeolite and albite. The progress of the reaction in some runs with the same duration reached only 60 vol% of the source material.

The alteration process of acid plagioclase in carbonate solution resulted in analcime and cancrinite crystallization (Table 1a). The appearance of analcime depends on many factors. Its synthesis is favoured by lower temperatures (300-400°C) and lower carbonate concentrations in the solution (0.1M  $\text{Na}_2\text{CO}_3$ ). Analcime has also been found as a product of plagioclase decay in more concentrated solution (0.5M  $\text{Na}_2\text{CO}_3$ ) in the higher temperature runs (500°C) of short duration (4 days). Continuing of the reaction for an additional four days gave cancrinite as the only product (Text-fig. 5). This effect was not noticeable in short-time reactions of calcic plagioclase even with diluted

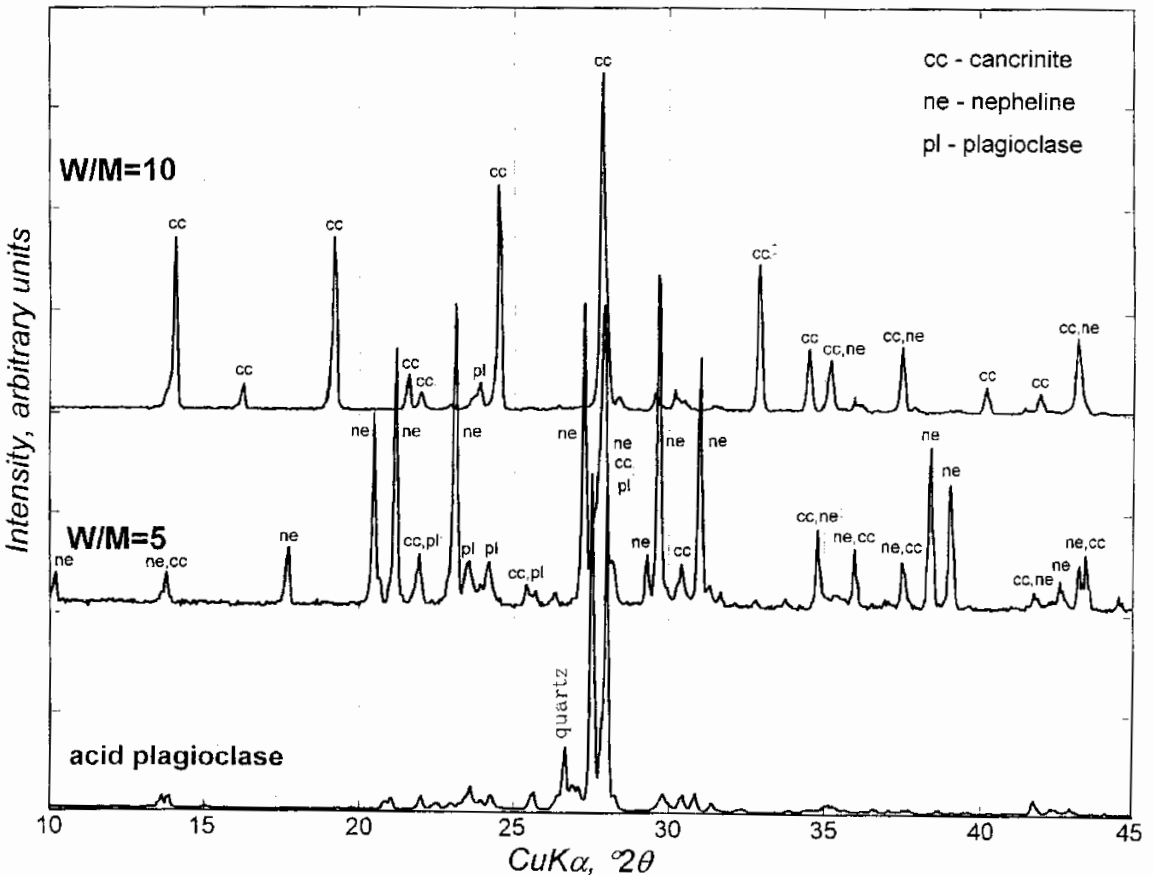


Fig. 4. The X-ray powder pattern of acid plagioclase decay by W/M=5 and W/M=10

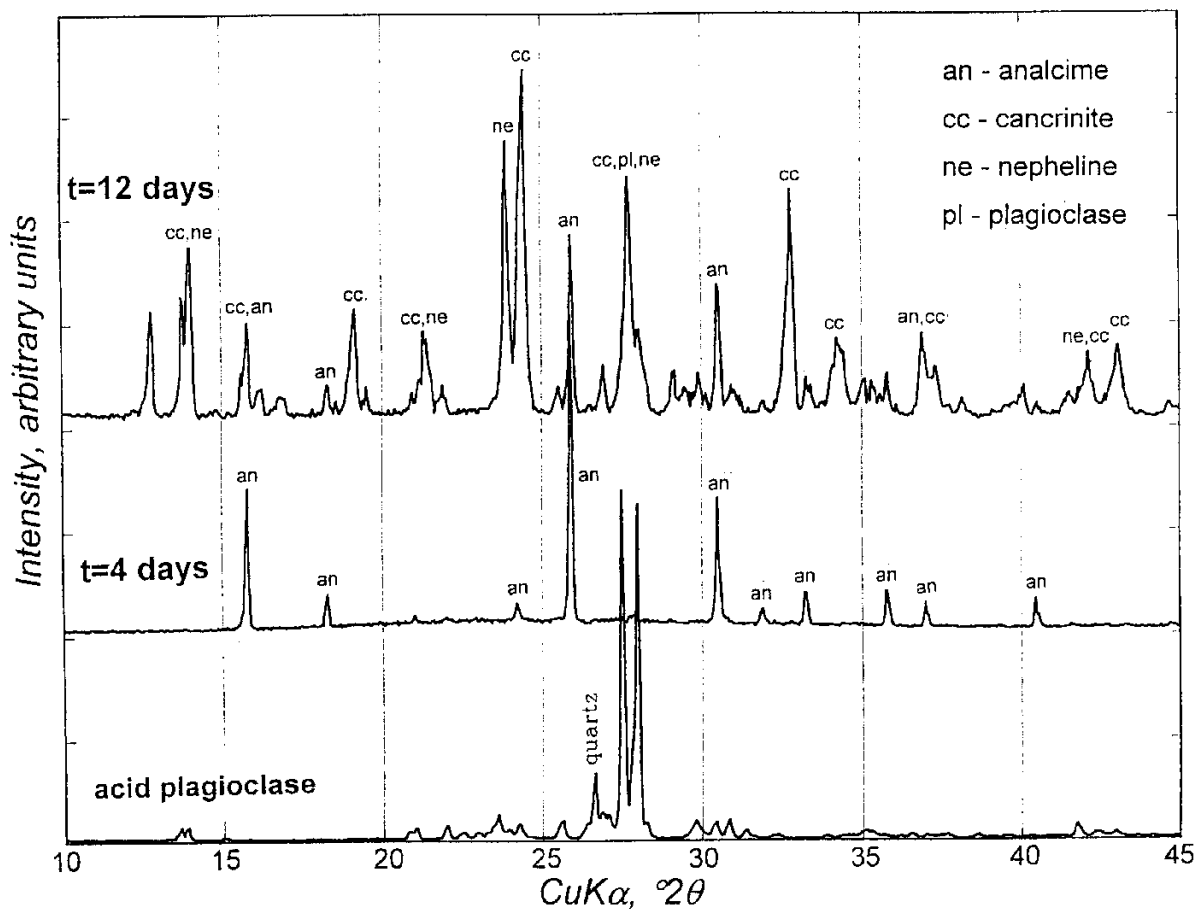


Fig. 5. The X-ray powder pattern of acid plagioclase alteration products after 4 and 12 days reaction in the 0.5M  $\text{Na}_2\text{CO}_3$  solution

(0.1M  $\text{Na}_2\text{CO}_3$ ) solution (Table 1b). The product of the reaction remained cancrinite. Runs with a duration of 30 days usually converted  $\sim 80 \pm 10$  vol% of plagioclase into crystals with zeolitic structure and albite. Sometimes 100 vol% of source material was transformed to analcime in a short time (see for 4 days run Text-fig. 4). Alteration of plagioclase in  $\text{NaHCO}_3$  solution gave similar results (Table 1c).

Taking into consideration all the described observations I can conclude that the reaction progress in all the runs was controlled by the local density, distribution of microcracks and crystal defects in the plagioclase. The dissolution rate of the plagioclase was mostly controlled by the precipitation rate of the zeolite minerals. A similar dissolution mechanism controlled by processes on the mineral surface was described by ALEKSEYEV & *al.* (1997), HOCHHELLA & *al.* (1988), and HELLMANN (1994, 1995).

Stability of both the cancrinite and analcime phases greatly depends on the silicon and alumi-

um activity in the system. The activity of silicon was especially high in the low temperature reaction of acid plagioclase with carbonate solution, because the composition of the source material and because of the mechanism of silica transport in alkaline solutions (ANDERSON & BURNHAM 1983). This phenomenon was more pronounced in the short-time reaction where the plagioclase dissolution was non-stoichiometric. Plagioclase in contact with alkaline solution may repolymerize silanol groups so the reaction step is silicon detachment (BRADY & WALTHER 1989, CASEY & *al.* 1989). The silicon activity decreases with temperature in comparison to the aluminium activity, which in turn inhibits analcime crystallization. Increasing temperature enhances the aluminium activity. There is a strong connection between sodium and aluminium activity. Sodium forms complexes with  $\text{Al}(\text{OH})_4^-$ . The degree of sodium-aluminium complexing increases with temperature growth (ANDERSON & BURNHAM 1983, DIAKONOV & *al.* 1994). Sodium controls the

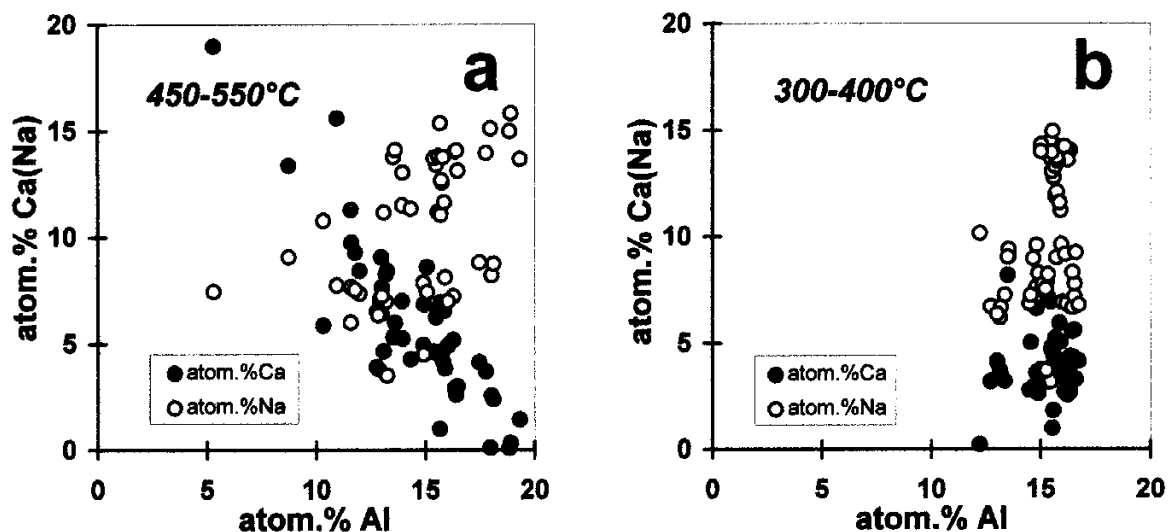


Fig. 6. The studied Ca, Na versus Al contents in the plagioclase alteration products

a – High temperature runs; b – Low temperature runs

	Run conditions: T(°C) / Na <sub>2</sub> CO <sub>3</sub> concentration in the solution / source material: b.p. - basic plagioclase, a.p. - acid plagioclase / product - cc (cancrinite), an (analcime), ne (nepheline)									
	550 / 1M / b.p. / cc	350 / 1M / b.p. / cc	550 / 0.5M / b.p. / cc	350 / 0.5M / b.p. / cc	550 / 0.1M / b.p. / cc	550 / 0.1M / b.p. / cc	550 / 1M / a.p. / cc	350 / 1M / a.p. / cc	350 / 0.1M / a.p. / an	500 / 0.05M / a.p. / ne
<b>Chemical analyses (wt%)</b>										
SiO <sub>2</sub>	35.01	35.16	34.23	34.72	35.53	35.13	35.13	34.27	54.32	38.55
Al <sub>2</sub> O <sub>3</sub>	29.22	29.40	29.01	30.85	29.72	30.63	29.69	29.29	23.18	33.90
FeO	0.21	0.27	0.17	0.21	0.56	0.09	0.06	0.35	0.02	0.44
MgO	0.02	0.04	0.00	0.01	0.05	0.02	0.01	0.05	0.00	0.00
CaO	8.11	2.55	6.01	3.77	6.02	3.71	7.20	4.63	0.32	0.14
Na <sub>2</sub> O	18.12	19.40	18.54	18.97	17.00	18.35	16.34	18.33	13.71	20.42
K <sub>2</sub> O	0.09	0.01	0.24	0.14	1.20	0.16	0.16	0.13	0.37	1.50
BaO	0.00	0.00	0.00	0.00	0.00	0.10	0.11	0.00	0.05	0.00
<b>Total</b>	<b>90.78</b>	<b>86.83</b>	<b>88.21</b>	<b>88.67</b>	<b>90.08</b>	<b>88.19</b>	<b>88.70</b>	<b>87.07</b>	<b>91.74</b>	<b>94.94</b>
<b>Cations in formula unit</b>										
Si <sup>4+</sup>	5.67	5.87	5.69	5.68	5.77	5.76	5.75	5.73	2.00	7.79
Al <sup>3+</sup>	5.58	5.74	5.68	5.95	5.69	5.92	5.73	5.77	1.00	8.08
Fe <sup>+2</sup>	0.03	0.04	0.02	0.03	0.08	0.01	0.01	0.05	0.00	0.07
Mg <sup>+2</sup>	0.00	0.01	0.00	0.00	0.01	0.00	0.00	0.01	0.00	0.00
Ca <sup>+2</sup>	1.41	0.46	1.07	0.66	1.05	0.65	1.26	0.83	0.01	0.03
Na <sup>+</sup>	5.69	6.28	5.97	6.02	5.35	5.83	5.19	5.94	0.97	8.00
K <sup>+</sup>	0.02	0.00	0.05	0.03	0.25	0.03	0.03	0.03	0.02	0.39
Ba <sup>+2</sup>	0.00	0.00	0.00	0.00	0.00	0.01	0.01	0.00	0.00	0.00
<b>cations</b>	<b>18.40</b>	<b>18.40</b>	<b>18.48</b>	<b>18.37</b>	<b>18.19</b>	<b>18.22</b>	<b>17.99</b>	<b>18.37</b>	<b>4.00</b>	<b>24.36</b>
<b>charge</b>	<b>48.00</b>	<b>48.00</b>	<b>48.00</b>	<b>48.00</b>	<b>48.00</b>	<b>48.00</b>	<b>48.00</b>	<b>48.00</b>	<b>14.00</b>	<b>64.00</b>

Table 2. Chemical composition of plagioclase decay products (selected analyses)

transport of aluminium in the system. The chemical composition of plagioclase dissolution products displays a positive correlation between sodium and aluminium. The correlation is seen however, only in the case of high-temperature runs, which corroborates ANDERSON & BURNHAM'S observations (Text-fig. 6a-b).

The silicon and aluminium concentration in the system are not the only factors which constrain cancrinite and analcime crystallization. Another factor seems to be the  $\text{CO}_3^{2-}$  concentration in the solution. Analcime appears even under high temperature in the 30 day runs (source material – acid plagioclase) with diluted carbonate solutions (0.1M  $\text{Na}_2\text{CO}_3$ ). More concentrated solutions favour cancrinite formation, although occasionally the reaction products contain very fine analcime crystals (reaction of acid plagioclase with 0.5M  $\text{Na}_2\text{CO}_3$  solution performed under  $450^\circ\text{C}$ ).

Dissolution of basic and acid plagioclase led to different phase formation due to differences in the chemical composition of both feldspars and the chemical composition of reacting solution. Reaction progress in the dissolution – precipitation process was influenced by the structure of both plagioclases and by defects in their structure. The dissolution process was faster in the case of basic than of acid plagioclase. Sodium-rich solution delayed albite cell decomposition, so that the anorthite compound dissolved first. Anorthite cells possess isolated from one another silica and alumina tetrahedra. Hydrolysis of the Si-O and Al-O bonds disrupts the structure more quickly than that of albite, which contains linked silicon tetrahedra (CASEY & *al.* 1989). The transformation path from basic and acid plagioclase to cancrinite (analcime) is shown in Text-fig. 7a-c. As the reaction progresses the domains of altered plagioclase become impoverished in calcium and enriched in silicon and sodium. The aluminium behaviour is different in the high- and low-temperature dissolution – precipitation processes of both acid and basic plagioclase.

Microprobe analyses of cancrinite, analcime and nepheline crystals demonstrate some differences in the chemical composition depending on the synthesis conditions, this being particularly the case with the cancrinite crystals (Table 2). The Al-Si framework of cancrinite, analcime and nepheline is perfectly crystallized. There is almost no difference in the silicon and aluminium content regardless of the reaction conditions. High temperature synthesis promotes calcium incorporation into cancrinite crystals so they are rich in calcium and relatively poor in

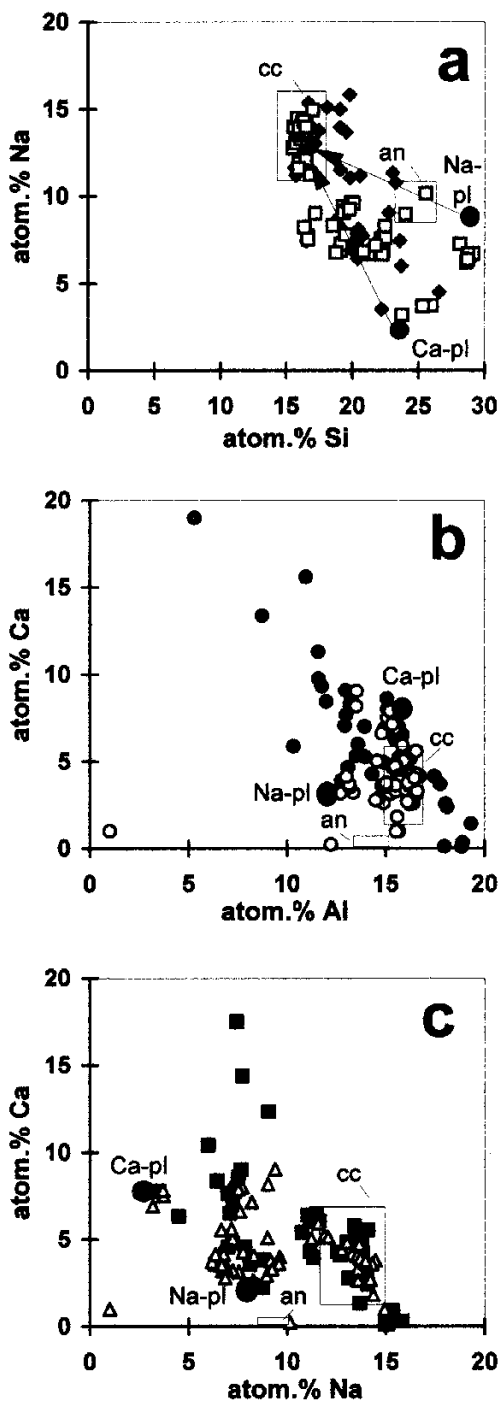


Fig. 7. Chemical composition of plagioclase alteration products a – Silicon versus sodium (open square – runs at  $T=300\text{--}400^\circ\text{C}$ , filled rhombus – runs at  $T=450\text{--}550^\circ\text{C}$ ; Ca-pl – basic plagioclase, Na-pl – acid plagioclase, cc – cancrinite, an – analcime); b – Aluminium versus calcium (open circles – runs at  $T=300\text{--}400^\circ\text{C}$ , filled circles – runs at  $T=450\text{--}550^\circ\text{C}$ ; Ca-pl – basic plagioclase, Na-pl – acid plagioclase, cc – cancrinite, an – analcime); c – Sodium versus calcium (square – runs at  $T=300\text{--}400^\circ\text{C}$ , triangle – runs at  $T=450\text{--}550^\circ\text{C}$ ; Ca-pl – basic plagioclase, Na-pl – acid plagioclase, cc – cancrinite, an – analcime)

sodium. In contrast, crystals formed under low temperature are rich in sodium and relatively poor in calcium. This tendency appears repeatedly in all run series for 1M, 0.5M and 0.1M Na<sub>2</sub>CO<sub>3</sub> solution, and for both types of source material. Microprobe analyses of zeolite are often erroneous due to sodium mobility under the electron beam. I believe that this is not the case with analysed synthetic crystals. According to the microprobe data the analcimes are filled with sodium and the cancrinite show differences in sodium content in a systematic way.

The habit of synthesized cancrinite and nepheline crystals did not depend on the crystallization conditions. However, the habit of the analcimes changed with the temperature of the run and the concentration of the solutions. The most dominant form of cancrinite crystals was a single hexagonal prism or a combination of two prisms (Pl. 1, Figs 1-3). Combination of a hexagonal prism with a hexagonal pyramid truncated by a pedion (Pl. 1, Fig. 4) was rarely observed. Cancrinites grow as single crystals or crystal clusters (Pl. 1, Figs 5-6). Nepheline crystallized in the form of a short hexagonal prism (Pl. 1, Figs 7-8).

Crystals of naturally occurring analcimes H are usually a combination of cube {100} and deltoid-icositetrahedron {211} faces. Almost all synthesized analcimes showed a similar morphology. An increase in alkalinity of solution and run temperature favoured {211} faces relative to {100} (Pl. 2, Figs 1-6). The last ones disappeared at 450°C and at solution concentration of 1M Na<sub>2</sub>CO<sub>3</sub>. The tendency was more pronounced for temperature increases than for increases in alkalinity. Analcimes grown in NaHCO<sub>3</sub> solution displayed a more complex morphology (Pl. 2, Fig. 7). Precise determination of the observed combination was very difficult. It is probable that the additionally grown faces belonged to tetrakis hexahedron. These results corroborate the observations of HÖLLER & WIRSCHING (1980) and GHOBARKAR & FRANKE (1986). The habit of analcimes produced by syntheses of short duration due to deformation of the crystal is difficult to assign (Pl. 2, Fig. 8).

For further research only samples converted at least in 80 vol. % to zeolite were selected.

## IR SPECTROSCOPY INVESTIGATIONS

Infrared investigations can provide useful information about zeolite structure. They give data about the vibration of the structural units through which the IR beam passes. In the present case the information concerns the aluminosilicate frame-

work composition, cation type and location, behaviour of the water molecule, as well as other groups in the structure sensitive to IR. Additional data about structural changes due to thermal treatment obtained from the IR measurements could be very helpful determining the exact location of the water.

In the IR spectrum of zeolite some regions can be related to certain building units of the structure. Absorption bands in the 3750-3000 cm<sup>-1</sup> region are usually attributed to the stretching vibration of hydroxyl groups. According to NAKAMOTO & *al.* (1955) and KUBICKI & *al.* (1993) this region extends to 2000 cm<sup>-1</sup>. If the ~1650 cm<sup>-1</sup> band (water bending vibration) also appears in the spectrum it is not clear whether the bands in the 2000-3750 cm<sup>-1</sup> region are from structural OH groups or molecular water. Vibration of CO<sub>3</sub><sup>-2</sup> groups are assigned to the ~1500 cm<sup>-1</sup> region. The intensities and positions of the bands may give information about the environment and amount of the group in the zeolite channel. The mid-infrared region (1250-400 cm<sup>-1</sup>) corresponds to the vibration of primary building units ([TO<sub>4</sub>], T=Si, Al) and secondary building units (rings of tetrahedra, polyhedra etc.) of the structure. Asymmetric stretching of internal tetrahedra in the zeolite structure are assigned to 1250-950 cm<sup>-1</sup>, symmetric stretching of internal tetrahedra to 720-650 cm<sup>-1</sup>, T-O bending to 420-500 cm<sup>-1</sup>. In the cancrinite family minerals the mid-infrared (700-500 cm<sup>-1</sup>) region is characterised by the triplet of bands. The bands reflect the bending vibration of Si-O-Al. The Si-O-Al angle is involved in the cell parameter expansion, so positions of these bands correlate with the cell unit parameters (BALLIRANO & *al.* 1996). The cell parameters depend, among others, on the contents of cation and anion groups. The triplet gives potential information about the structure saturation with cations.

In the present IR investigations special attention was paid to three regions: 2000-4000 cm<sup>-1</sup>, 1400-1500 cm<sup>-1</sup> and 500-700 cm<sup>-1</sup>.

Crystals of cancrinite and analcime in the 80 selected samples were carefully separated from the plagioclase relicts. The infrared absorption spectra were measured with an IR Nicolet (Magna - IR 550) spectrometer. The samples were prepared as KBr pellets (1:100 - sample/KBr). Usually the range of recorded spectra was set to be 4000-400 cm<sup>-1</sup>. For selected samples the range was expanded to 300 cm<sup>-1</sup>. The OH stretching vibration region in 40 recordings of the spectra was deconvoluted by means of square interpolation assuming Gauss shaped bands. For every band in the deconvoluted spectrum half-

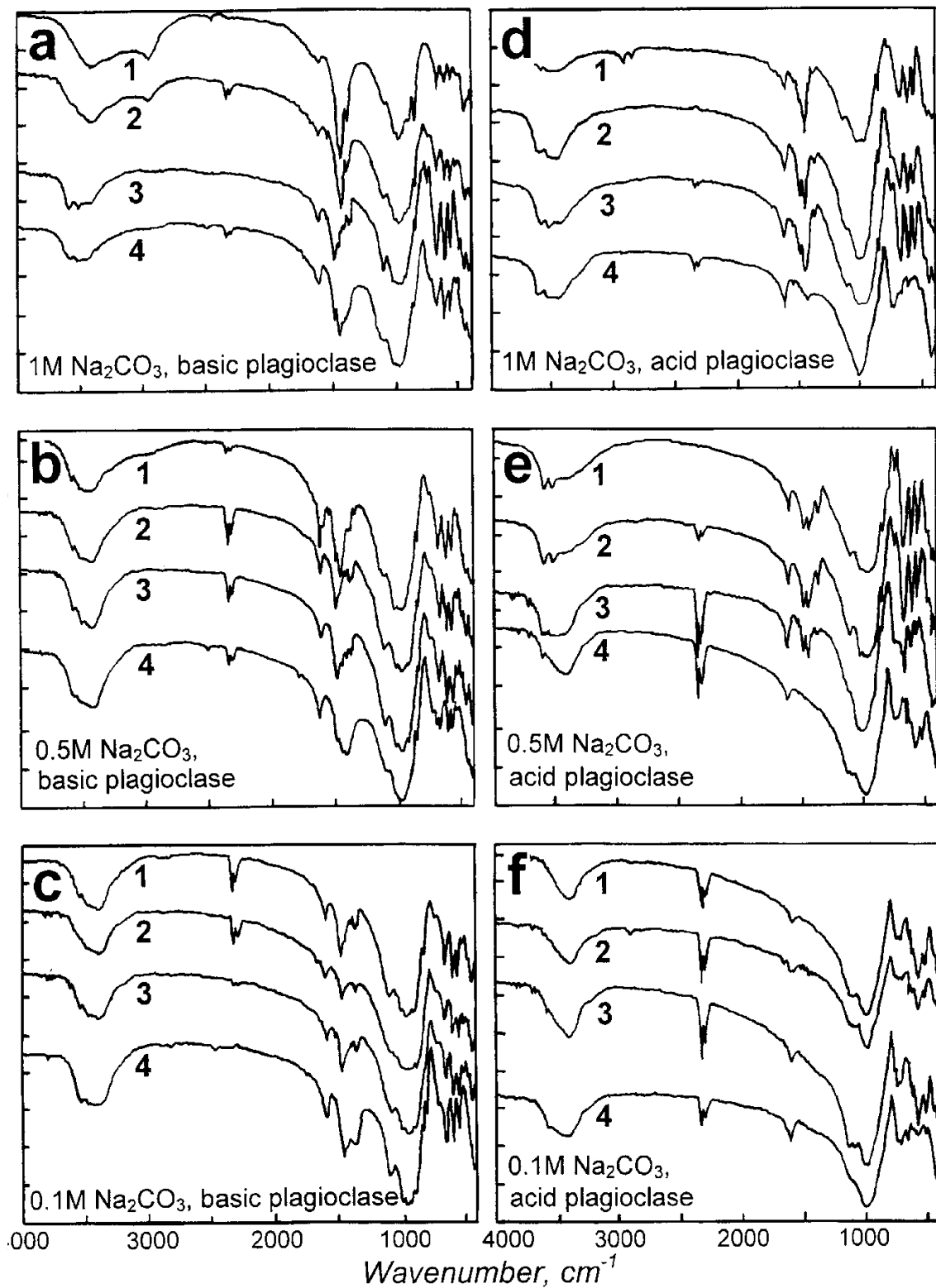


Fig. 8. The IR spectra of B-cancrinite, A-cancrinite and analcime (run temperature:  
 1 – T=550°C, 2 – T=500°C, 3 – T= 400°C, 4 – T=300°C)

a – B-cancrinite, b – B-cancrinite, c – B-cancrinite, d – A-cancrinite, e – A-cancrinite, f – analcime

width, relative shift, maximum and integrated intensities were assigned. The relative shift  $\alpha = (v_o - v) / v_o$  was used in the calculation of H–O1 bond lengths in the OH group (SOKOLOV 1964). Other parameters of the entity O1 – H....O2 in particular O1....O2, H....O2 distances were determined by means of KUBICKI & al. (1993) diagrams.

## Raw data

### Water stretching and bending vibration region

The frequencies of structural OH groups in cancrinite crystals, being products of basic and acid plagioclase decay, varied over a wide range. For

the sake of simplicity, the former products will be called **B-cancrinite** and the latter **A-cancrinite**. Hydrogen-bonded water is seen in almost all samples near 3600 cm<sup>-1</sup>, 3450 cm<sup>-1</sup> and 3280 cm<sup>-1</sup> (Table 3). Maximum intensities appear around a broad band at 3450 cm<sup>-1</sup> and sharp band at 3600 cm<sup>-1</sup> (Text-figs 8, 10 and 11). The maximum peak at ~3450 cm<sup>-1</sup> in the broad band is accompanied by many other peaks of lower intensity. The presence of the broad band usually indicates a non-uniform water environment, which could be caused by the variable locations of the water molecules and / or OH groups or by various interacting forces between the water / OH groups and the surrounding cations and anions.

a	T(°C) of synthesis	Na <sub>2</sub> CO <sub>3</sub> concentration in the solution	Band position (cm <sup>-1</sup> ) OH groups	Band position (cm <sup>-1</sup> ) "triplet"
	550	1M	3716, 3421, 3310, 2980	689, 628, 584
	500	1M	3602, 3534, 3454, 3316 3595, 3520, 3262	689, 629, 582 689, 626, 581
	450	1M	3599, 3527, 3441, 3290, 2978	686, 629, 585
	400	1M	3730, 3612, 3527, 3454, 3263 3620, 3503, 3448, 3263	692, 629, 585 683, 626, 577
	350	1M	3714, 3612, 3533, 3477, 3296	695, 634, 581
	550	0.5M	3454, 3270	697, 648, 566
	500	0.5M	3707, 3599, 3533, 3441	689, 629, 587
	400	0.5M	3710, 3606, 3533, 3448, 3289	689, 632, 579
	350	0.5M	3619, 3540, 3441	693, 639, 588
	550	0.1M	3448, 3270	709, 636, 577
	500	0.1M	3592, 3533, 3447, 3270	689, 630, 583
	400	0.1M	3599, 3540, 3448, 3277	689, 630, 590
	350	0.1M	3592, 3539, 3467, 3300	689, 630, 596
b	T(°C) of synthesis	Na <sub>2</sub> CO <sub>3</sub> concentration in the solution	Band position (cm <sup>-1</sup> ) OH groups	Band position (cm <sup>-1</sup> ) "triplet"
	550	1M	3592, 3528, 3463, 3263	692, 630, 588
	500	1M	3620, 3443, 3277, 2934	645, 586, 542
	400	1M	3610, 3530, 3447, 3218	692, 628, 581
	350	1M	3615, 3457, 3319	691, 623, 541
	550	0.5M	3609, 3530, 3432, 3252	688, 628, 576
	500	0.5M	3600, 3536, 3442, 3317, 3267	684, 625, 575
	400	0.5M	3603, 3537, 3454, 3281	694, 627, 582

Table 3. Frequencies of structural OH groups and „triplet” in cancrinite (run duration 30 days); a) Source material - basic plagioclase (B-cancrinite, selected samples); b) Source material - acid plagioclase (A-cancrinite, selected samples)

B-cancrinites grown in the more concentrated solution (1M Na<sub>2</sub>CO<sub>3</sub>) under high temperature conditions (550°C) display a very wide OH stretching vibration region. The spectra very rarely indicate a sharp band at ~3600 cm<sup>-1</sup>. The region is composed of many broad bands. The first one has a relatively very low frequency at ~2980 cm<sup>-1</sup> (Text-figs 8a and 10). Reducing the run temperature (400°C) causes the bands to shift towards higher frequencies. Instead of a set of broad bands, two sharp bands at ~3600 cm<sup>-1</sup> and ~3520 cm<sup>-1</sup>, accompanied by one broad band, appear (Text-figs 8a and 10). The intensities of both of the sharp bands are higher than that of 3450 cm<sup>-1</sup>. B-cancrinites grown at 350-300°C show only one sharp band at ~3600 cm<sup>-1</sup>. The second one (~3520 cm<sup>-1</sup>) can be resolved only with difficulty and belongs to the broad band. Simultaneously the intensity of both of the sharp bands is distinctly reduced.

The IR spectra of B-cancrinite crystallized from solutions of lower Na<sub>2</sub>CO<sub>3</sub> concentration (at 550°C) resemble low temperature products synthesized in concentrated 1M Na<sub>2</sub>CO<sub>3</sub> solution. They are characterised by a very broad band with the maximum around 3450 cm<sup>-1</sup>, with two poorly resolved sharp bands in the higher frequency area (Text-figs 8b-c and 10).

The IR spectra of A-cancrinites show different characteristics in the OH stretching vibration area than those of B-cancrinites (Text-figs 8d-e and 11; Table 3b). The biggest difference concerns crystals grown in the concentrate solution under high temperature conditions (1M Na<sub>2</sub>CO<sub>3</sub>, 550-500°C). For A-cancrinite the low frequency bands (<3000 cm<sup>-1</sup>) are absent from the spectra. The remaining part of the OH stretching vibration region is characterised by a broad band with two local maxima around 3530 cm<sup>-1</sup> and 3460 cm<sup>-1</sup> and one sharp band at

~3600 cm<sup>-1</sup> of slightly lower intensity (Text-figs 8d and 11). Decrease of synthesis temperature results in variable behaviour of the ~3530 cm<sup>-1</sup> and 3600 cm<sup>-1</sup> bands in the cancrinite spectra. The bands display variable intensities from sample to sample. Sometimes the first one is more intense, at other times the second one. In the low-temperature A-cancrinite (1M Na<sub>2</sub>CO<sub>3</sub>, 350-300°C) the maximum intensity is shown by the ~3450 cm<sup>-1</sup> band.

The IR spectra of A-cancrinite originating from 0.5M Na<sub>2</sub>CO<sub>3</sub> solution (550-500°C) look like the spectra of B-cancrinite resulting from lower temperature syntheses (450-400°C) in concentrated 1M Na<sub>2</sub>CO<sub>3</sub> solution. Two distinct peaks appear, with maximum intensities at ~3600 cm<sup>-1</sup> and ~3530 cm<sup>-1</sup>. Towards low frequencies the spectrum possesses the shape of a broad band. In the IR spectra of crystals grown under lower temperature, the intensities of the 3600 cm<sup>-1</sup> and the 3530 cm<sup>-1</sup> bands decrease markedly and that of the 3450 cm<sup>-1</sup> band increases (Text-figs 8e and 11).

Analcimes are mostly products of plagioclase reaction with 0.5 and 0.1M Na<sub>2</sub>CO<sub>3</sub> solution. Their spectra mainly show one tripartite broad band (Text-fig. 8f; Table 4). Usually the maximum intensity is seen around 3450 cm<sup>-1</sup>. In some spectra a sharp band at ~3600 cm<sup>-1</sup> has been noticed. The lower the run temperature and solution concentration the better is this band resolved. Analcime created due to reaction in 0.5M solution and at T=450°C shows four bands in the OH stretching vibration area. It is somewhat doubtful if the mineral represents a pure phase because there is a trace of a 1480 cm<sup>-1</sup> band in its IR spectrum.

All IR spectra of B and A-cancrinite and analcime show the water bending band at ~1650 cm<sup>-1</sup>. The intensity of the band seems to be lower in the B-cancrinite grown at 550°C than that in the A-cancrinite.

### CO<sub>3</sub><sup>2-</sup> vibration region

The environment of the CO<sub>3</sub><sup>2-</sup> molecule in the cancrinite structure is different in the low and high temperature crystals. The differences apply above all to band intensities. The band intensity in IR absorption spectrum is described by the Lambert-Beer law:

$$I=I_0 \exp(-\alpha x)$$

where (I<sub>0</sub>) is intensity of incident radiation, (x) is the sample thickness and (α) absorption coefficient. Assuming that wafer thickness and absorption ratio of a single absorption centre are uniform between samples, the intensity of vibration of the

T(°C) of synthesis	Na <sub>2</sub> CO <sub>3</sub> concentration in solution	Band position (cm <sup>-1</sup> )
450	0.5M	3615, 3543, 3456, 3308
350	0.5M	3621, 3454, 3280
550	0.1M	3559, 3431, 3277
500	0.1M	3585, 3430, 3270
400	0.1M	3632, 3422, 3294
350	0.1M	3621, 3545, 3450

Table 4. Frequencies of structural OH groups in analcime (run duration 30 days; selected samples)

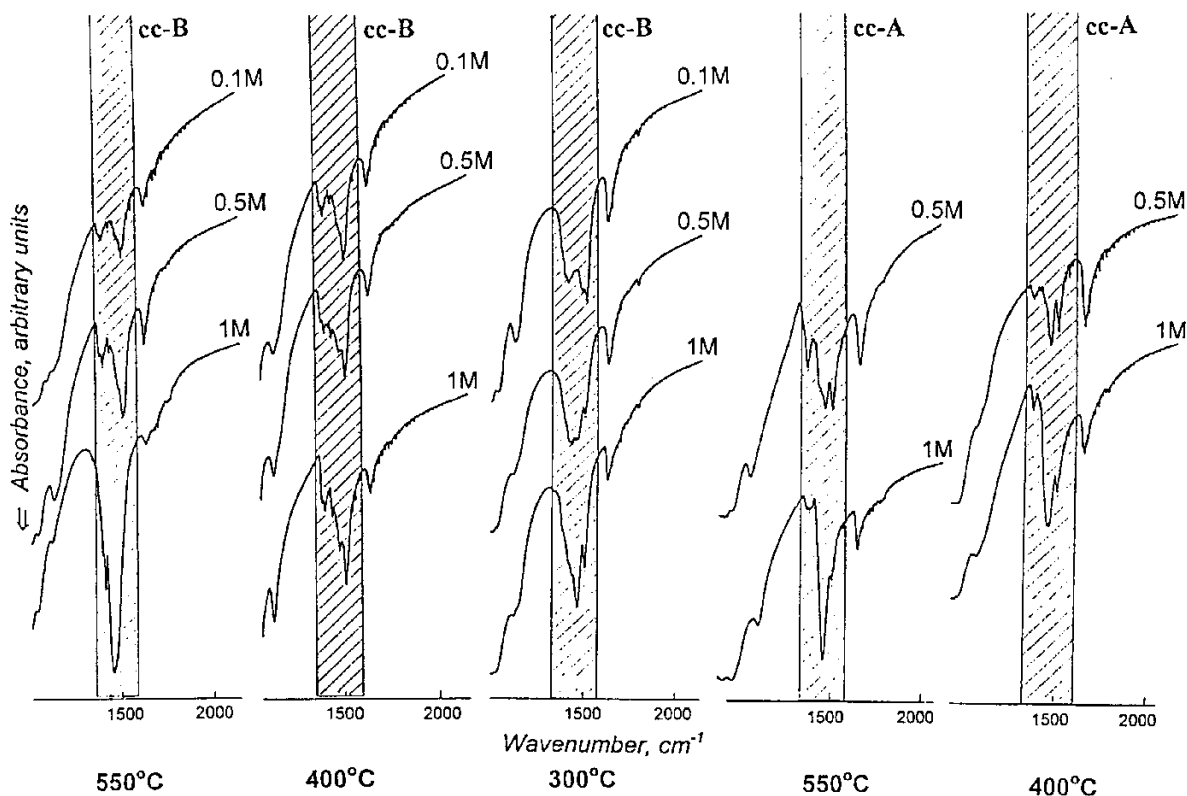


Fig. 9. The  $\text{CO}_3^{2-}$  vibrational range (striped area); Explanations: cc-B – B-cancrinite, cc-A – A-cancrinite; 0.1M, 0.5M, 1M –  $\text{Na}_2\text{CO}_3$  concentration in the solution

$\text{CO}_3^{2-}$  groups is proportional to the group content in the structure.

The structure of B-cancrinite synthesized under high temperature conditions is more filled with  $\text{CO}_3^{2-}$  groups than that crystallized in low temperature runs (Text-fig. 9). The higher the temperature and solution concentration used for the synthesis the more intense is the band at  $\sim 1480 \text{ cm}^{-1}$  and the more it is shifted towards lower frequencies ( $550^\circ\text{C}$ , 1M  $\text{Na}_2\text{CO}_3$   $\sim 1462 \text{ cm}^{-1}$ ;  $350^\circ\text{C}$ , 0.1M  $\text{Na}_2\text{CO}_3$   $\sim 1486 \text{ cm}^{-1}$ ). Actually the vibration spectrum of  $\text{CO}_3^{2-}$  in the high temperature B-cancrinite is split into two bands:  $\sim 1462 \text{ cm}^{-1}$  (maximum intensity) and  $\sim 1410 \text{ cm}^{-1}$ . The same band area shows three peaks in the crystals formed under lower temperature ( $400\text{--}450^\circ\text{C}$ ):  $\sim 1507 \text{ cm}^{-1}$  (usually maximal intensity),  $\sim 1468 \text{ cm}^{-1}$  and  $\sim 1420 \text{ cm}^{-1}$  (Text-fig. 9). The lowest temperature runs produced B-cancrinites whose  $\text{CO}_3^{2-}$  vibration band commonly shows more than three peaks (Text-fig. 9). BALLIRANO & *al.* (1996) found a strong positive correlation between anion content in the cancrinite-like minerals and  $c$  cell parameter expansion. The  $c$

cell parameter calculated for B-cancrinites support this. B-cancrinites with a very intensive  $\sim 1500 \text{ cm}^{-1}$  vibration band show a more expanded  $c$  cell parameter (Table 5).

A similar pattern of  $\text{CO}_3^{2-}$  vibration area is seen in the A-cancrinite (Text-fig. 9); in this case the

T( $^\circ\text{C}$ ) of synthesis	Solution composition	Cell parameters	
		a ( $\text{\AA}$ )	c ( $\text{\AA}$ )
550	1M $\text{Na}_2\text{CO}_3$	12.634	5.140
400	1M $\text{Na}_2\text{CO}_3$	12.620	5.124
350	1M $\text{Na}_2\text{CO}_3$	12.583	5.117
500	0.5M $\text{Na}_2\text{CO}_3$	12.603	5.119
400	0.5M $\text{Na}_2\text{CO}_3$	12.613	5.121
350	0.5M $\text{Na}_2\text{CO}_3$	12.584	5.106
500	0.1M $\text{Na}_2\text{CO}_3$	12.624	5.132
400	0.1M $\text{Na}_2\text{CO}_3$	12.603	5.116
350	0.1M $\text{Na}_2\text{CO}_3$	12.583	5.114
550	1M $\text{NaHCO}_3$	12.574	5.101

Table 5. B-cancrinite unit cell parameters

interaction between the carbonate groups and their environment in the channel is also more complex in minerals formed under low temperatures than under high temperatures.

### 500-700 $\text{cm}^{-1}$ region

In this region a triplet of bands in the cancrinite-like minerals appears. The position of the first band (with the lowest frequency) of the triplet correlates with the *a* cell parameter (BALLIRANO & *al.* 1996). The correlation is negative, that is, increasing *a* value is accompanied by a shift towards lower frequencies. Expansion of the *a* cell parameter depends on cation content in the structural unit. The position of the first band of triplet in the B- and A-cancrinite is shown in Table 3. Generally the frequencies of the first band correlate well with the sum of cations in the formula unit (*see* Tables 3 and 2 for comparison). A weak correlation between three variables: the sum of cations, *a* cell parameter, and the position of the first band is also observable (*see additionally* Table 5). Precise determination of the interconnection between these three variables proved to be very difficult because of a very narrow range of the frequency data values.

### Deconvoluted spectra

The shape of the raw IR spectra is characterised by the presence of one broad band in the OH stretching vibration area in all samples. Actually the band consists of many overlapping peaks. The real parameters of a single band could be obtained by using the deconvolution method. The technique allows us to obtain some additionally information on the hydrogen bond in the water molecule. The specific aim of the deconvolution of the OH stretching vibration area was to determine the following:

- the total number of bands, their frequencies, true maximum intensity,
- O1-H.....O2 spatial relation, especially the O1-H bond distance for every fitted peak (NOVAK 1974, KUBICKI & *al.* 1993),
- real integrated intensity (peak area), which correlates with water concentration in the structure (LIBOWITZKY & ROSSMAN 1997).

The OH stretching frequencies correlate with OH bond lengths, H bond angles and H bond distances. The best correlation with band position is shown by the H-O1 and the H.....O2 length when

the H bond is less than  $\sim 2 \text{ \AA}$ . In the zeolite structure O2 is usually bonded to silicon or aluminium. The free water molecule has an O1-H distance of  $0.96 \text{ \AA}$  and a frequency of  $3583 \text{ cm}^{-1}$ . A lower OH frequency is caused by a closer approach of the H atom to the O2 atom. Both the O1-H and H...O2 distances become almost equal. The hydrogen electron density is shared between both oxygen atoms (KUBICKI & *al.* 1993). The O1-H...O2 angle and OH stretching frequencies do not correlate well. There is almost no correlation over a wide range  $70\text{-}160^\circ$ . The O1-H...O2 angle deformation of the water molecule is thus difficult to determine. Another useful value is the integrated intensity. LIBOWITZKY & ROSSMAN (1997) have proved that only the integrated intensity (peak area) correlates linearly with water content in the structure, whereas peak heights do not correlate.

The results of the deconvolution of the OH stretching vibration area include: linear absorption data (maximum intensity), integral intensity (peak area) and band frequencies ( $\text{cm}^{-1}$ ). The results are presented in Tables 6-8 and in the Text-figs. 10-11.

Comparing all deconvoluted spectra of OH stretching vibration area in the B-cancrinite one can observe that lower run temperatures generally result in a band shift towards higher frequencies. This is especially well seen in the movement of the  $\sim 3600 \text{ cm}^{-1}$  band: from  $\sim 3591 \text{ cm}^{-1}$  for high temperature to  $\sim 3606 \text{ cm}^{-1}$  for low temperature samples. The peak area of the band increases in size with decrease in the run temperature. The composition of the solution, in which the cancrinite is crystallized, does not significantly influence position of this band. The integrated intensity of another constituents, the sharp band, the position of which after deconvolution is found to be  $\sim 3540 \text{ cm}^{-1}$ , varies slightly with run conditions.

High carbonate concentration in the solution seems to influence the position of the broad band in some cancrinite spectra. Spectra of high temperature B-cancrinites (1M  $\text{Na}_2\text{CO}_3$  solution) are good examples to illustrate this tendency. B-cancrinite crystallized under  $550^\circ\text{C}$  shows the OH stretching vibration area extending up to  $2798 \text{ cm}^{-1}$  (Text-fig. 10c and Table 6a). Three intense broad bands are present between  $2978 - 3450 \text{ cm}^{-1}$  in the deconvoluted region. They could be attributed either to the hydrogen of the water molecule bonded to different oxygen atom in the framework, or to cations (Na) occupying different sites. The lower the band frequency the longer is the H-O1 distance and relatively shorter the H.....O2 distance. The hydrogen

a	T (°C) of the synthesis; phase	Wavenumber (cm <sup>-1</sup> ) (Maximal intensity = 1) <u>Integrated intensity</u>									
		2700					3800				
	550 B-cancrinite Fig.10c	2798 (0.12) <u>30.10</u>	2978 (0.67) <u>107.64</u>		3237 (0.75) <u>277.99</u>	3450 (0.77) <u>195.27</u>					3716 (0.08) <u>5.75</u>
	500 B-cancrinite		2954 (0.13) <u>27.70</u>	3172 (0.28) <u>92.61</u>	3222 (0.18) <u>34.20</u>	3459 (0.93) <u>270.45</u>	3512 (0.06) <u>8.72</u>		<b>3591</b> <b>(0.24)</b> <b>0.02</b>		
	450 B-cancrinite		2968 (0.48) <u>99.06</u>		3240 (0.54) <u>161.81</u>	3457 (0.88) <u>247.53</u>	3527 (0.08) <u>0.12</u>		<b>3597</b> <b>(0.24)</b> <b>0.01</b>		
	400 B-cancrinite Fig.10f				3249 (0.18) <u>32.73</u>	3449 (0.97) <u>250.69</u>	3534 (0.37) <u>34.01</u>			<b>3600</b> <b>(0.72)</b> <b>88.78</b>	3730 (0.11) <u>6.32</u>
	350 B-cancrinite Fig.10i				3282 (0.33) <u>58.34</u>	3480 (0.95) <u>167.27</u>	3530 (0.20) <u>0.01</u>			<b>3605</b> <b>(0.74)</b> <b>126.91</b>	3714 (0.10) <u>8.96</u>

b	T (°C) of the synthesis; phase	Wavenumber (cm <sup>-1</sup> ) (Maximal intensity = 1) <u>Integrated intensity</u>									
		2700					3800				
	550 B-cancrinite				3231 (0.13) <u>22.40</u>	3450 (0.95) <u>268.14</u>					
	500 B-cancrinite Fig.10b				3217 (0.12) <u>21.92</u>	3437 (0.99) <u>272.04</u>	3531 (0.18) <u>0.09</u>		<b>3597</b> <b>(0.37)</b> <b>34.31</b>		3707 (0.13) <u>15.67</u>
	400 B-cancrinite Fig.10e				3267 (0.22) <u>35.65</u>	3428 (0.96) <u>200.05</u>	3536 (0.52) <u>22.59</u>			<b>3611</b> <b>(0.49)</b> <b>81.54</b>	3710 (0.08) <u>4.90</u>
	350 B-cancrinite Fig.10h				3254 (0.20) <u>34.02</u>	3432 (0.98) <u>215.58</u>	3523 (0.22) <u>2.46</u>			<b>3606</b> <b>(0.63)</b> <b>104.70</b>	

c	T (°C) of the synthesis; phase	Wavenumber (cm <sup>-1</sup> ) (Maximal intensity = 1) <u>Integrated intensity</u>									
		2700					3800				
	550 B-cancrinite			3153 (0.05) <u>8.48</u>	3242 (0.15) <u>15.34</u>	3442 (0.99) <u>249.58</u>					
	500 B-cancrinite Fig.10a				3242 (0.18) <u>23.97</u>	3442 (0.99) <u>217.41</u>	3524 (0.11) <u>1.62</u>		<b>3596</b> <b>(0.41)</b> <b>55.73</b>		
	400 B-cancrinite Fig.10d				3247 (0.21) <u>36.17</u>	3421 (0.90) <u>186.67</u>		3566 (0.60) <u>95.72</u>	<b>3591</b> <b>(0.12)</b> <b>0.25</b>		3730 (0.05) <u>3.10</u>
	350 B-cancrinite Fig.10g				3263 (0.24) <u>38.17</u>	3433 (0.98) <u>205.74</u>	3522 (0.26) <u>2.73</u>		<b>3595</b> <b>(0.06)</b> <b>0.09</b>	<b>3601</b> <b>(0.70)</b> <b>112.92</b>	

Table 6. Position of the absorption bands in the OH stretching vibration range after deconvolution; a) Crystals grown from basic plagioclase in 1M Na<sub>2</sub>CO<sub>3</sub> solution; b) Crystals grown from basic plagioclase in 0.5M Na<sub>2</sub>CO<sub>3</sub> solution; c) Crystals grown from basic plagioclase in 0.1M Na<sub>2</sub>CO<sub>3</sub> solution

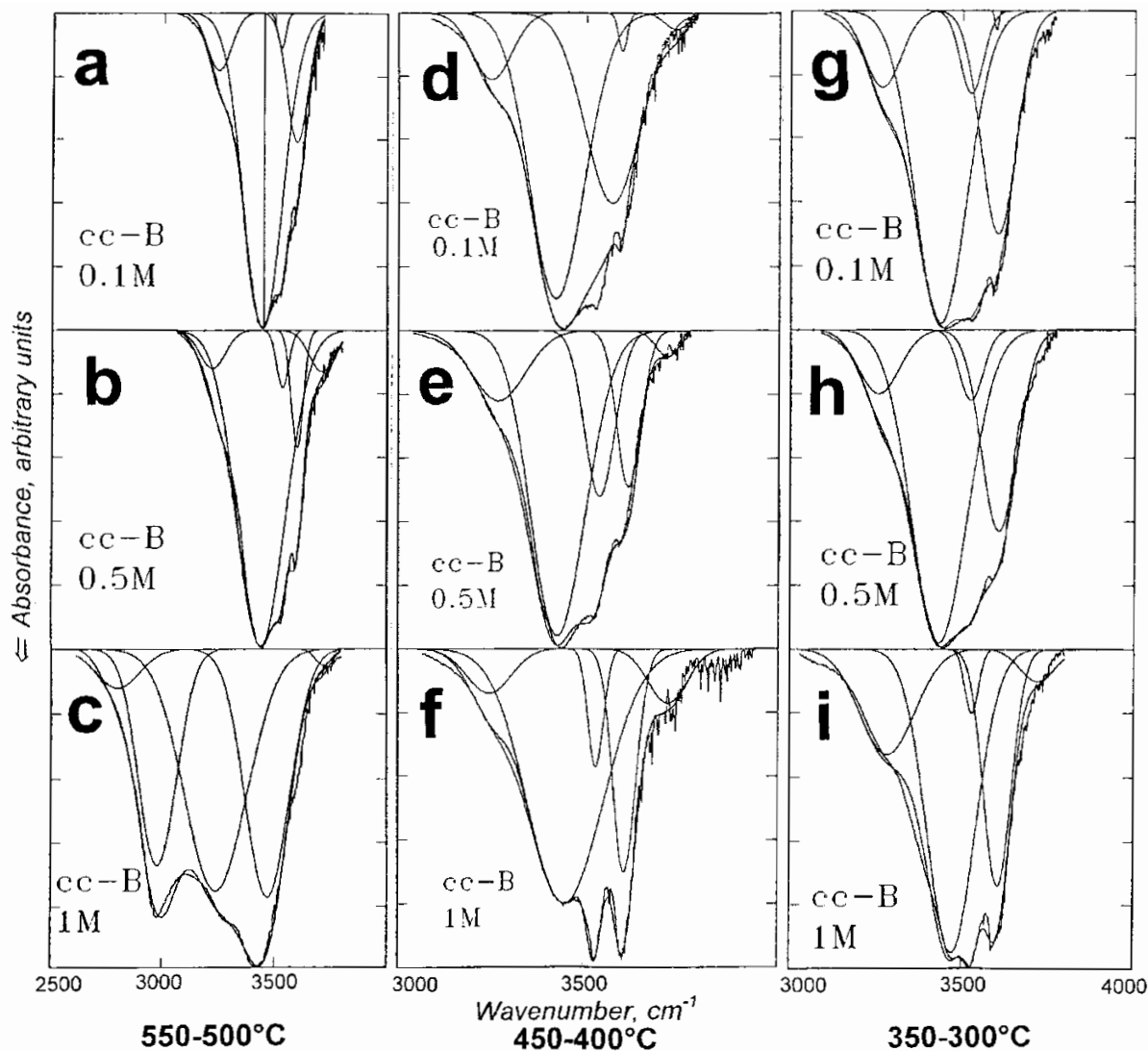


Fig. 10. Deconvoluted OH vibrational range of basic plagioclase decay products (see Table 6 for the value of maximal intensity and integrated intensity of the bands) Explanations: cc-B – B-cancrinite; 0.1M, 0.5M, 1M –  $\text{Na}_2\text{CO}_3$  concentration in the solution

bonding O1-H...O2 gets stronger. According to the KUBICKI & *al.* (1993) calculation for hypothetical aluminosilicate the H-O1 distance is  $1.0\text{\AA}$  for  $2798\text{ cm}^{-1}$ . According to NAKAMOTO & *al.* (1955) data determined for various minerals the calculated H-O1 distance is longer:  $2.7\text{\AA}$  for  $2798\text{ cm}^{-1}$ . The strength of the bonding decreases towards higher frequencies. The integrated intensities are almost the same in all the bands in the spectrum (Text-fig. 10c and Table 6a). The low frequency bands below  $3000\text{ cm}^{-1}$  could also originate from the C-H bond.

The broad band in all other samples of B-cancrinite may be differentiated generally into two parts but, together with sharp bands and one broad band at  $\sim 3730\text{ cm}^{-1}$ , the whole spectrum usually

consists of five components (Text-fig. 10a-i and Table 6a-c). The integrated intensities of the bands in the  $3200\text{--}3500\text{ cm}^{-1}$  area become differentiated. The most intense is the band  $\sim 3450\text{ cm}^{-1}$ . The band is slightly shifted towards lower frequencies in low temperature samples. The integrated intensity of this band is also somewhat reduced in low temperature B-cancrinites. The band at  $\sim 3450\text{ cm}^{-1}$  is accompanied by another two bands (seldom by three or four bands) with much smaller area. Of those additional bands the position and area of the  $\sim 3240\text{ cm}^{-1}$  band varies distinctly with run conditions. Its frequency and integrated intensity is shifted towards higher values in low temperature B-cancrinites. Although some of the peak areas increase

a	T (°C) of the synthesis; phase	Wavenumber (cm <sup>-1</sup> ) (Maximal intensity = 1) <u>Integrated intensity</u>									
		2700					3800				
	550 A-cancrinite Fig.11c				3258 (0.2) <u>27.89</u>	3447 (0.90) <u>197.58</u>	3524 (0.05) <u>0.01</u>	3572 (0.50) <u>50.46</u>	<b>3592</b> <b>(0.33)</b> <b>0.01</b>		
	500 A-cancrinite				3268 (0.20) <u>32.18</u>	3432 (0.96) <u>182.03</u>		3557 (0.40) <u>52.01</u>		<b>3626</b> <b>(0.30)</b> <b>1.49</b>	
	400 A-cancrinite Fig.11f				3218 (0.10) <u>19.54</u>	3447 (0.90) <u>265.51</u>	3527 (0.25) <u>4.83</u>			<b>3607</b> <b>(0.55)</b> <b>46.85</b>	
	350 A-cancrinite Fig.11i				3260 (0.24) <u>40.20</u>	3442 (0.96) <u>220.91</u>		3566 (0.50) <u>42.41</u>		<b>3636</b> <b>(0.60)</b> <b>93.01</b>	
b	T (°C) of the synthesis; phase	Wavenumber (cm <sup>-1</sup> ) (Maximal intensity = 1) <u>Integrated intensity</u>									
		2700					3800				
	550 A-cancrinite Fig.11b			3198 (0.2) <u>38.47</u>		3447 (0.80) <u>268.61</u>	3527 (0.30) <u>0.01</u>			<b>3607</b> <b>(0.55)</b> <b>99.19</b>	
	450 analcime				3254 (0.20) <u>34.31</u>	3444 (0.90) <u>217.79</u>		3564 (0.50) <u>57.83</u>		<b>3633</b> <b>(0.60)</b> <b>70.20</b>	
	400 A-cancrinite Fig.11e				3250 (0.10) <u>19.39</u>	3442 (0.96) <u>227.97</u>		3564 (0.50) <u>49.75</u>		<b>3631</b> <b>(0.50)</b> <b>73.70</b>	
	350 analcime Fig.11h				3268 (0.20) <u>28.56</u>	3437 (0.98) <u>205.90</u>		3562 (0.40) <u>33.13</u>		<b>3636</b> <b>(0.30)</b> <b>41.91</b>	
c	T (°C) of the synthesis; phase	Wavenumber (cm <sup>-1</sup> ) (Maximal intensity = 1) <u>Integrated intensity</u>									
		2700					3800				
	550 analcime Fig.11a				3268 (0.20) <u>33.05</u>	3439 (0.99) <u>202.10</u>		3555 (0.30) <u>29.95</u>			
	500 analcime				3268 (0.20) <u>22.95</u>	3439 (1.00) <u>199.78</u>		3556 (0.30) <u>29.95</u>			
	400 analcime Fig.11d				3272 (0.20) <u>29.10</u>	3437 (0.98) <u>201.50</u>		3562 (0.30) <u>39.70</u>		<b>3632</b> <b>(0.30)</b> <b>12.78</b>	
	350 analcime Fig.11g				3253 (0.10) <u>14.32</u>	3442 (0.97) <u>228.07</u>		3564 (0.40) <u>27.38</u>		<b>3629</b> <b>(0.40)</b> <b>48.64</b>	

Table 7. Position of the absorption bands in the OH stretching vibration range after deconvolution; a) Crystals grown from acid plagioclase in 1M Na<sub>2</sub>CO<sub>3</sub> solution; b) Crystals grown from acid plagioclase in 0.5M Na<sub>2</sub>CO<sub>3</sub> solution; c) Crystals grown from acid plagioclase in 0.1M Na<sub>2</sub>CO<sub>3</sub> solution

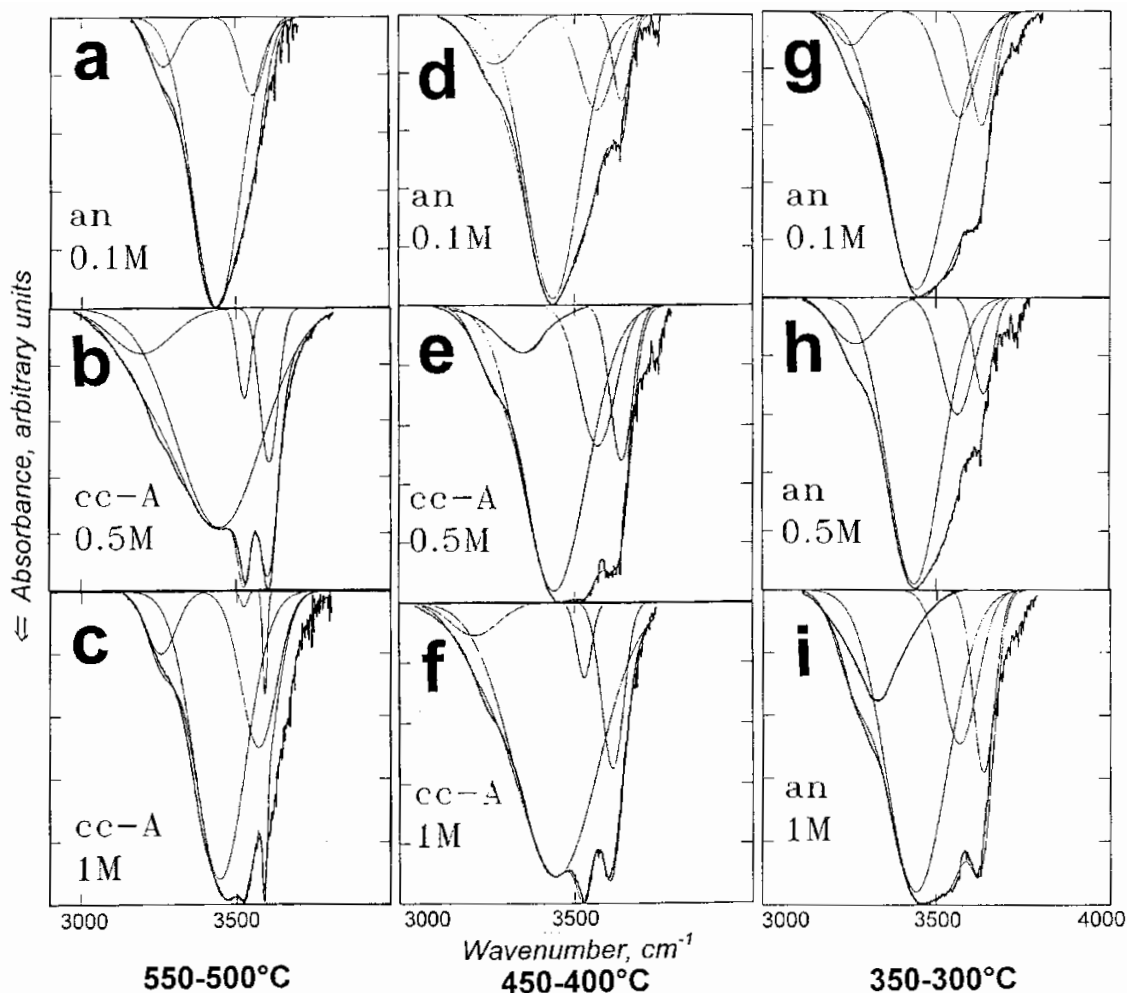


Fig. 11. Deconvoluted OH vibrational range of acid plagioclase decay products (see Table 7 for the value of maximal intensity and integrated intensity of the bands) Explanations: cc-A – A-cancrinite, an – analcime; 0.1M, 0.5M, 1M –  $\text{Na}_2\text{CO}_3$  concentration in the solution

and others decrease, depending on the synthesis conditions the sum of integrated intensities generally tend to rise in the samples crystallized under low temperatures and in diluted solution (Table 6). The range of O1-H distance in the hydrogen bond calculated for the deconvoluted  $3200 - 3500 \text{ cm}^{-1}$  region is also narrower:  $0.98 \text{ \AA}$  ( $\sim 3240 \text{ cm}^{-1}$ ) –  $0.96 \text{ \AA}$  ( $3530 \text{ cm}^{-1}$ ). The O1-H groups participate in a weak hydrogen bonding. The H...O2 distance increases up to  $\sim 3 \text{ \AA}$  (NAKAMOTO & *al.* 1955).

The lower the temperature of the run and the more dilute the solution reacting with the basic plagioclase, the more is the structure of the B-cancrinite filled with water. The lower the temperature of the run and the more dilute the solution reacting with the basic plagioclase, the weaker is the hydrogen bonding of the water molecule in the cancrinite structure.

The arrangement of the OH stretching vibration bands in the A-cancrinite show some differences but also some similarities to the spectra of B-cancrinite. The high temperature A-cancrinites do not display bands in the low frequency area (Text-fig. 11c and Table 7a). The main region  $3250 - 3600 \text{ cm}^{-1}$  can be differentiated into 3-4 parts (Text-fig. 11b, c, e, f, i and Table 7a-b). The main broad peak appears as in B-cancrinite around  $3440 \text{ cm}^{-1}$ . Its integrated intensity increases with reduction in run temperature (Table 7a-b). One of the accompanying bands, a peak around  $\sim 3560 \text{ cm}^{-1}$  (sharp peak), is absent in B-cancrinite. Its integrated intensity decreases in low temperature run products. The  $\sim 3600 \text{ cm}^{-1}$  band (sharp peak) position maintains the tendency of that in the B-cancrinite. Crystals formed under lower temperature and due to reaction with

a diluted solution show a shift of this band towards higher frequencies. The peaks have more expanded areas than those of high temperature reaction products. In the high temperature A-cancrinite (550°C) grown from the more concentrated solution (1M Na<sub>2</sub>CO<sub>3</sub>) this band displays a very reduced peak area, with the position below 3600 cm<sup>-1</sup> (Text-fig. 11c and Table 7a). The O1-H distance in the hydrogen bonding in A-cancrinites in comparison to that in B-cancrinites varies in a narrower range 98-95 Å. The last value is the length of the OH distance in a free water molecule. The water in A-cancrinite is bonded with a weak hydrogen bonding.

Spectra of analcime crystallized at high temperature reveal three bands in the deconvoluted region: ~3260 cm<sup>-1</sup>, ~3440 cm<sup>-1</sup> and 3550 cm<sup>-1</sup>

(Text-fig. 11a and Table 7c). The maximum integrated intensity is obtained for the ~3440 cm<sup>-1</sup> band. Low temperature analcimes additionally show a ~3636 cm<sup>-1</sup> band, its integrated intensity increases with decreasing run temperature. The ~3636 cm<sup>-1</sup> band appears in the spectrum of analcime crystallized below 400°C (Text-fig. 11d, g, h and Table 7a-c). Low temperature analcimes seem to contain more water than those produced under high temperature conditions (*see for integrated intensity* Table 7a-c).

Runs with short duration as well as with solution composition 0.1M NaHCO<sub>3</sub> do not significantly change the arrangement of the OH stretching vibration area (Table 8). In some analcimes from short duration runs the ~3260 cm<sup>-1</sup> peak disappears (SEABY & *al.* 1995).

T(°C) / Solution composition / Time of the run (days) / phase	Wavenumber (cm <sup>-1</sup> ) (Maximal intensity = 1) <u>Integrated intensity</u>									
	2700								3800	
600 / 1M NaHCO <sub>3</sub> / 30 / cancrinite				3268 (0.29) <u>51.27</u>	3421 (0.80) <u>175.89</u>		3553 (0.68) <u>106.13</u>	<b>3592</b> (0.14) <u>0.01</u>		3717 (0.08) <u>3.81</u>
600 / 1M NaHCO <sub>3</sub> / 30 / nepheline*				3270 (0.20) <u>48.12</u>	3455 (0.92) <u>205.87</u>					3725 (0.04) <u>3.39</u>
400 / 0.1M NaHCO <sub>3</sub> / 30 / analcime				3248 (0.10) <u>24.72</u>	3442 (0.95) <u>226.01</u>		3564 (0.50) <u>49.48</u>		<b>3629</b> (0.40) <u>62.87</u>	
400 / 1M Na <sub>2</sub> CO <sub>3</sub> / 8 / cancrinite				3245 (0.14) <u>28.46</u>	3450 (0.80) <u>207.97</u>	3530 (0.37) <u>34.01</u>			<b>3605</b> (0.70) <u>0.48</u>	3715 (0.17) <u>32.31</u>
400 / 0.5M Na <sub>2</sub> CO <sub>3</sub> / 8 / analcime				3228 (0.07) <u>12.77</u>	3468 (0.99) <u>292.69</u>		3565 (0.12) <u>4.22</u>		<b>3627</b> (0.40) <u>69.29</u>	
500 / 0.5M Na <sub>2</sub> CO <sub>3</sub> / 12 / cancrinite			3150 (0.16) <u>30.01</u>	3270 (0.27) <u>25.55</u>	3460 (0.99) <u>343.38</u>				<b>3610</b> (0.20) <u>34.22</u>	
500 / 0.1M Na <sub>2</sub> CO <sub>3</sub> / 8 / nepheline*				3290 (0.20) <u>48.58</u>	3440 (0.90) <u>192.39</u>		3580 (0.43) <u>72.38</u>			3720 (0.15) <u>11.89</u>

\* products of runs with W/M=5

Table 8. Position of the absorption bands in the OH stretching vibration range after deconvolution. Selected samples of crystals grown under various conditions (source material - acid plagioclase)

## INTERACTION WITH WATER

**Dehydration and rehydration – IR study**

Six cancrinite samples and one analcime sample were calcinated under vacuum up to 600°C. After dehydration (dehydroxylation) the activated wafers were treated with water. The dehydration and rehydration process was monitored by using IR spectra.

Before activation the samples were pre-treated for 1h in vacuum at 24°C. The activations were performed in a step mode from 25 – 600°C with the step size 5°C/min. The IR data were collected at every 8th step. After calcination the samples remained for 4h in vacuum at a temperature of 600°C. Well dehydrated samples were treated with water. Adsorption was also performed in a step mode under the following conditions: 0.01mbar (water pressure)/1min, 0.01mbar/10min, 0.1mbar/1min, 0.1mbar/10min, 1mbar/1min, 1mbar/10min, 5mbar/1min, 5mbar/10min, 10mbar/1min, 10mbar/10min, 10mbar/30min, 10mbar/1h. IR data were collected after every step of the above sequence. After the adsorption the samples were kept for 0.5h in vacuum at 40°C to remove excess water adsorbed at the crystal surface.

The selected B-cancrinite crystals were products of the syntheses performed under the following conditions: at 550°C in 1M Na<sub>2</sub>CO<sub>3</sub> solution, at 300°C in 1M Na<sub>2</sub>CO<sub>3</sub> solution, as well as in 0.1M Na<sub>2</sub>CO<sub>3</sub> solution. The A-cancrinite selected for the activation and adsorption process were products of syntheses at 550°C in 1M and 0.5M Na<sub>2</sub>CO<sub>3</sub> solution, as well as at 400°C in 1M Na<sub>2</sub>CO<sub>3</sub> solution. The analcime sample originated from the run at 400°C with 0.1M Na<sub>2</sub>CO<sub>3</sub> solution.

The evacuation process of all of the cancrinites shows some similarities. Dehydration occurs in two steps. The process causes first the low frequency bands (broad band) to disappear, then the two (or one) sharp peaks follow (~3530-3540 and ~3600 cm<sup>-1</sup>). In the water bending area the ~1630-1650 cm<sup>-1</sup> band splits into two or more peaks before vanishing. The adsorption process takes place differently in various samples.

*B-cancrinite crystallized at T=300°C in 0.1M Na<sub>2</sub>CO<sub>3</sub> solution*

Among the selected cancrinite samples the structure the most filled with water belongs to B-cancrinite crystallized at low temperature (300°C

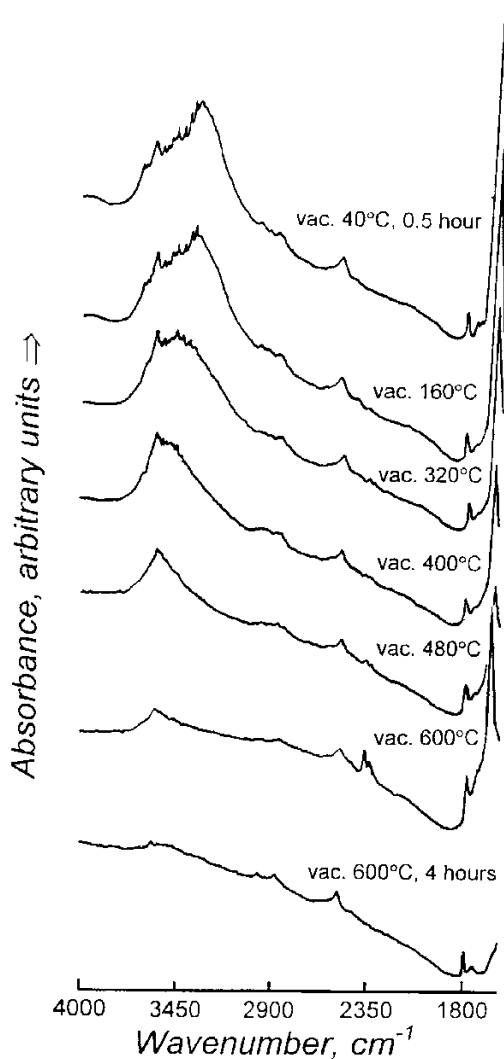


Fig. 12. The B-cancrinite calcined in vacuum (crystallization conditions of B-cancrinite: T=300°C, 0.1 Na<sub>2</sub>CO<sub>3</sub> solution; see Text-fig. 14 for bands value)

and from dilute solution (0.1M). Two steps in the dehydration are observable. The dehydration of the sample is a very slow process up to 240°C and results in a reduction of the broad band (3200-3580 cm<sup>-1</sup>). The structure first releases water that is weakly bonded to the framework (adsorbed water ~3260 cm<sup>-1</sup>). Aluminium at the surface needs sodium to compensate the charge. Sodium adsorbs water. The dehydration process is much faster above 400°C, and ends at 560°C (Text-fig. 12). The sharp band (~3600 cm<sup>-1</sup>) does not change its position up to 560°C, but its intensity decreases slowly. Above this temperature, the band position is initially slightly shifted towards lower frequen-

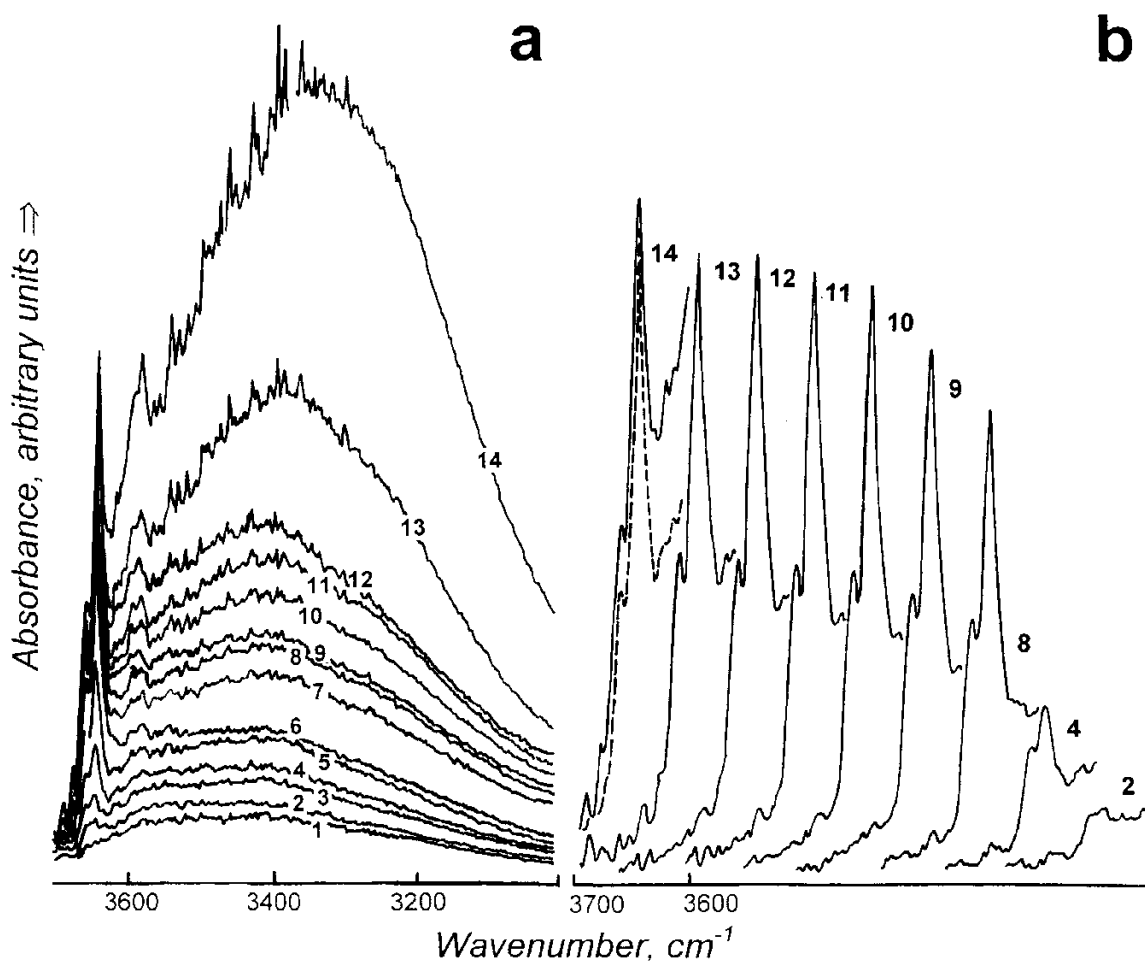


Fig. 13. The IR spectra of adsorbed water in B-cancrinite (crystallization conditions of B-cancrinite:  $T=300^{\circ}\text{C}$ ,  $0.1\text{M Na}_2\text{CO}_3$  solution)  
**a** – The OH stretching area. Explanations: spectra 1-14 respectively show water adsorption under following conditions: 0.01mbar (water pressure)/1min, 0.01mbar/10min, 0.1mbar/1min, 0.1mbar/10min, 1mbar/1min, 1mbar/10min, 5mbar/1min, 5mbar/10min, 10mbar/1min, 10mbar/10min, 10mbar/30min,  $p_{\text{max}}$ /1min,  $p_{\text{max}}$ /10min,  $p_{\text{max}}$ /1h; **b** – The IR spectra of hydroxyl groups (the same explanations as for Fig. 13a; spotted line – sample after degassing)

cies and then the band eventually disappears. Displacement of the band position can be caused by thermal vibrations of the molecules. Thermal vibration makes the hydrogen bonding  $\text{H}\cdots\text{O}_2$  stronger because the  $\text{H}-\text{O}_1$  bond length becomes longer and the  $\text{H}\cdots\text{O}_2$  shorter. The hydrogen bonding takes on a more ionic character. Some cation migration seems to occur during this stage of the dehydration process. Residual bands at  $3582\text{ cm}^{-1}$  and  $3500\text{ cm}^{-1}$  disappear after prolonged (4h) calcination at  $600^{\circ}\text{C}$ . In the water bending vibration region the  $\sim 1640\text{ cm}^{-1}$  band splits into three:  $\sim 1740\text{ cm}^{-1}$ ,  $\sim 1680\text{ cm}^{-1}$  and  $\sim 1630\text{ cm}^{-1}$ . The first one remains as a residual peak even after prolonged calcination.

Adsorption of water molecules results in relatively fast increase of the sharp band intensity. The sharp band position, compared with that in the activation process moves from  $\sim 3600\text{ cm}^{-1}$  to  $3640\text{ cm}^{-1}$  (Text-fig. 13a-b). Another phenomenon is increasing intensity of the broad band in the OH stretching vibration area and a split sharp band  $\sim 1670\text{--}1638\text{ cm}^{-1}$  in the water bending area. After completion of the adsorption process the sample were degassed for 0.5h in the vacuum. The area of the broad band (OH stretching vibration) decreases markedly and becomes asymmetrical (Text-fig. 14). In the water bending region two distinct bands  $\sim 1638$  and  $1670\text{ cm}^{-1}$  show two preferential sites of water adsorption. The sharp band at  $\sim 3645\text{--}60\text{ cm}^{-1}$  is also split

into two peaks. The IR spectra do not reveal any changes in the  $\text{CO}_3^{2-}$  environment due to the dehydration and rehydration process.

*B-cancrinite crystallized at  $T=300^\circ\text{C}$  in 1M  $\text{Na}_2\text{CO}_3$  solution*

The activation process of B-cancrinite (grown from the more concentrated 1M solution at  $300^\circ\text{C}$ )

proceeds generally in a similar manner to that of B-cancrinite formed in a dilute solution, but is much slower. Reduction of the low frequencies bands occurs before the  $\sim 3600\text{ cm}^{-1}$  band disappears. The residual peaks at  $\sim 3580\text{ cm}^{-1}$  and  $\sim 1740\text{ cm}^{-1}$  remain even after 4h calcination at  $600^\circ\text{C}$  (Text-fig. 15). The dehydration process changes the environment of the  $\text{CO}_3^{2-}$  groups. In the poorly resolved area at  $\sim 1500\text{ cm}^{-1}$  with three overlapping bands:  $1501\text{ cm}^{-1}$ ,  $1461\text{ cm}^{-1}$  and  $1386\text{ cm}^{-1}$ , the last peak loses its intensity due to sample calcination (Text-fig. 16). Adsorption of water does not restore the previous structure of the  $\text{CO}_3^{2-}$  chain.

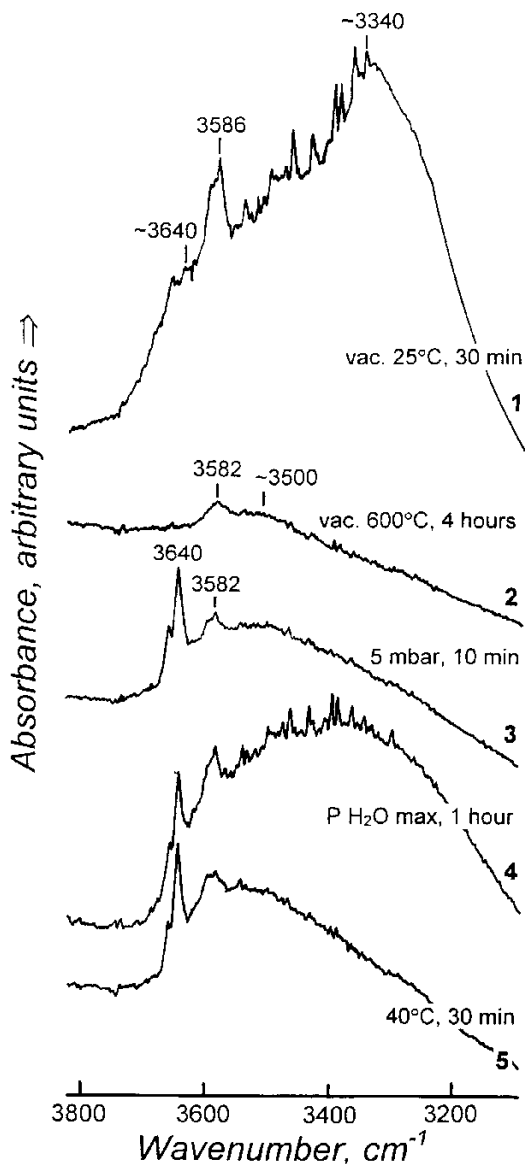


Fig. 14. The IR spectra of dehydrated and rehydrated B-cancrinite (crystallization conditions of B-cancrinite:  $T=300^\circ\text{C}$ , 0.1M  $\text{Na}_2\text{CO}_3$  solution); Explanations: 1 – Sample before calcination, 2 – Sample after calcination, 3 – Sample after rehydration (water pressure 5mbar/10min), 4 – Sample after rehydration ( $p_{\text{max}}$ /1h), 5 – Sample after degassing ( $40^\circ\text{C}/0.5\text{h}$ )

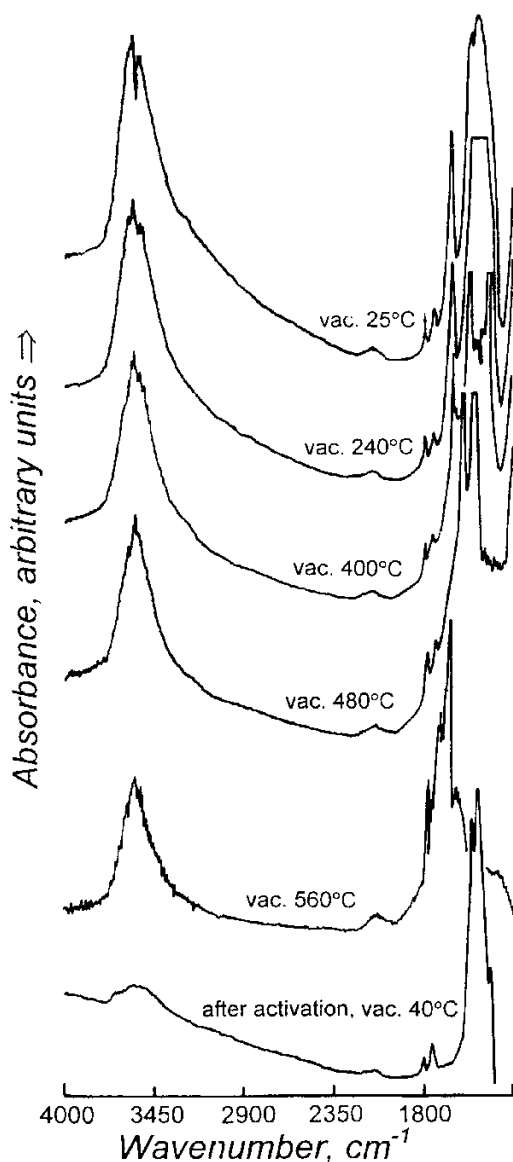


Fig. 15. Activation of B-cancrinite synthesized at  $300^\circ\text{C}$  in 1M  $\text{Na}_2\text{CO}_3$  solution (for band values see Text-fig. 18)

The adsorbed water does not restore the former OH stretching vibration spectrum either. Water enters the structure very slowly. It gives rise to a sharp bipartite peaks ( $3645\text{ cm}^{-1}$ ,  $3660\text{ cm}^{-1}$ ) which probably originates from isolated OH groups (Text-fig. 17). Increasing water pressure up to 10 mbar changes only the peak intensity. This peak is not

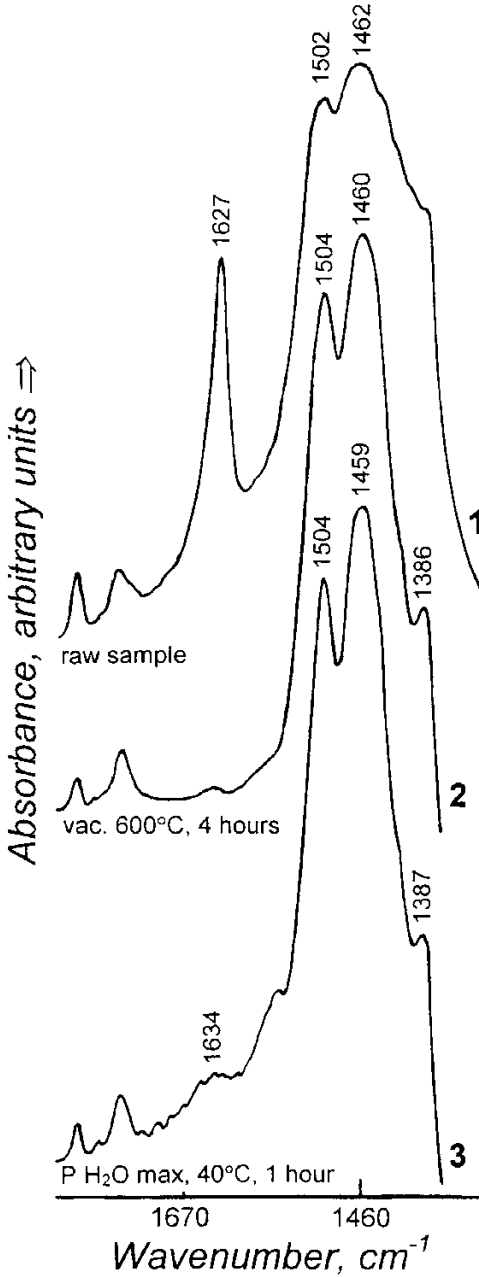


Fig. 16. The  $\text{CO}_3^{2-}$  vibrational range of B-cancrinite  
 Explanations: 1 – Sample before calcination, 2 – Sample calcined in vacuum for 4h at  $600^\circ\text{C}$ , 3 – Sample after rehydration ( $40^\circ\text{C}/p_{\text{max}}/1\text{h}$ )

accompanied by any other in the water bending area. Adsorption under maximum water pressure adds a very broad band which vanishes after sample degassing (Text-fig. 18).

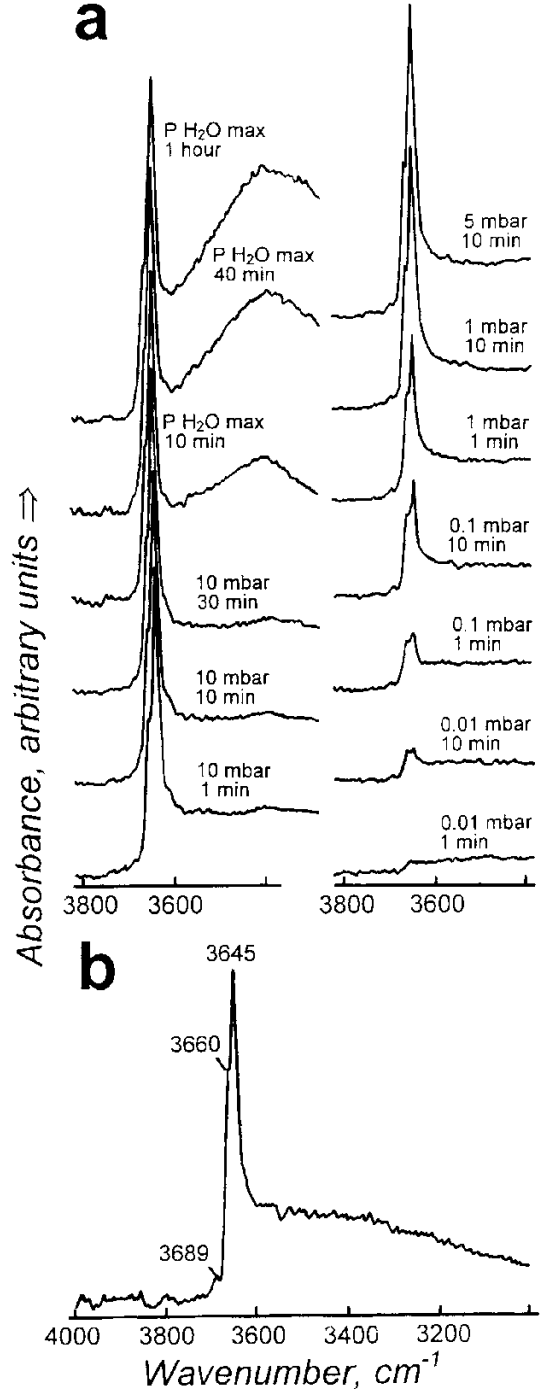


Fig. 17. The IR spectra of adsorbed water in B-cancrinite (crystallization conditions of B-cancrinite:  $T=300^\circ\text{C}$ ,  $1\text{M Na}_2\text{CO}_3$  solution)  
 a – The OH stretching area, b – The IR spectrum of adsorbed water in the same sample after degassing

*B-cancrinite crystallized at  $T=550^{\circ}\text{C}$  in  $1\text{M}$   $\text{Na}_2\text{CO}_3$  solution*

The release of water from the structure in this case is more impeded. The big channel is filled with  $\text{CO}_3^{2-}$  groups. Water squeezes through the blocked channel. There is no preferred sequence to the disappearance of any of the bands. They all disappear simultaneously and uniformly. Water is present in the structure practically up to  $520^{\circ}\text{C}$ .

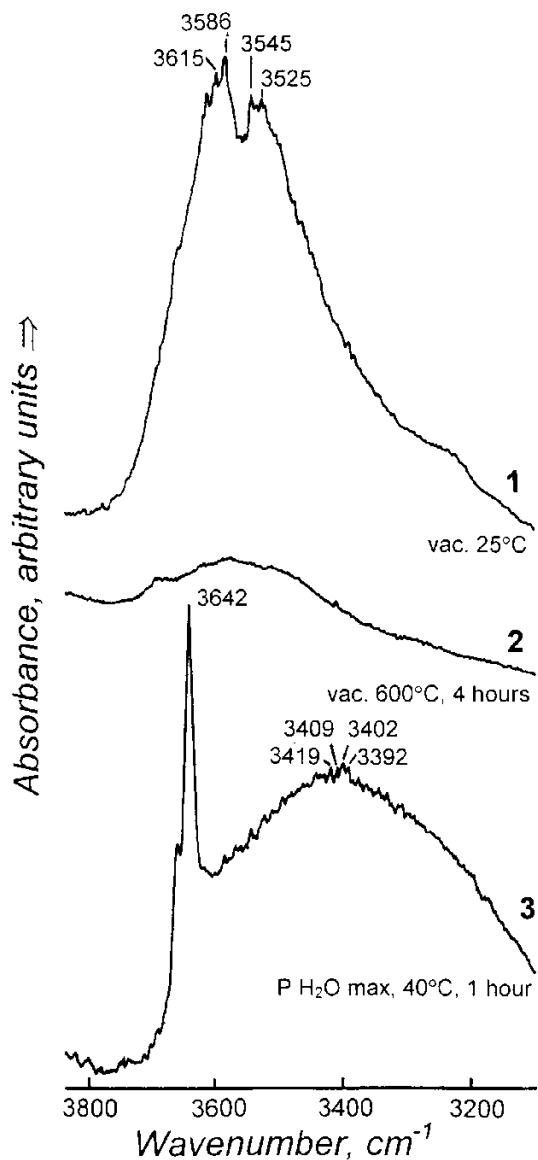


Fig. 18. The IR spectra of dehydrated and rehydrated B-cancrinite (crystallized at  $300^{\circ}\text{C}$  in  $1\text{M}$   $\text{Na}_2\text{CO}_3$  solution)

Explanations: **1** – Sample before calcination, **2** – Sample after calcination, **3** – Sample after rehydration ( $p_{\text{max}}/1\text{h}$ ), **4** – Sample after degassing ( $40^{\circ}\text{C}/0.5\text{h}$ )

The IR bands originating from its relicts remain visible even after the evacuation. The adsorption is not able to push much water into the structure. Only a small amount of water enters the structure as isolated OH groups. Most of the water is adsorbed at the crystal surface and is removed due to degassing.

*A-cancrinite crystallized at  $550^{\circ}\text{C}$ ,  $400^{\circ}\text{C}$  in  $1\text{M}$   $\text{Na}_2\text{CO}_3$  solution and at  $550^{\circ}\text{C}$  in  $0.5\text{M}$   $\text{Na}_2\text{CO}_3$  solution*

In all these samples dehydration and rehydration processes take place in a similar manner. The broad band in the OH stretching vibration region reduces its area earlier than the sharp  $\sim 3600\text{ cm}^{-1}$  band. Reduction of the broad band area is accompanied by a shift towards higher frequencies. The sharp band maintains its position and decreases its intensity on heating up to  $500^{\circ}\text{C}$ . At  $550^{\circ}\text{C}$  only relict  $3490\text{ cm}^{-1}$  and  $\sim 1740\text{ cm}^{-1}$  bands remain. The activation changes the superstructure of the big channel. Adsorption of water causes the appearance of a broad asymmetric band in the OH stretching vibration region and a split band in the water

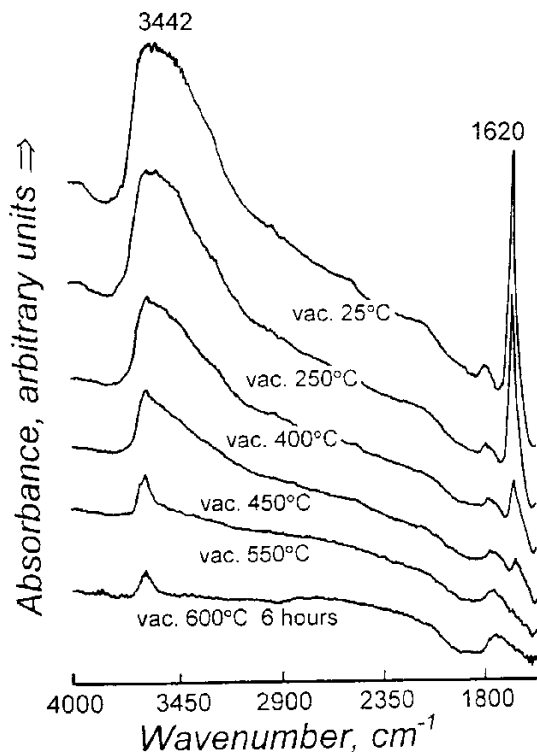


Fig. 19. Analcime calcined in vacuum (crystallization conditions of analcime:  $T=400^{\circ}\text{C}$ ,  $0.1\text{M}$   $\text{Na}_2\text{CO}_3$  solution)

bending region. The broad asymmetric band (in the 3000-3700  $\text{cm}^{-1}$  range) has its sloping side shifted towards lower frequencies. After the degassing the intensity of the band decreases markedly, but its shape does not change. The  $\sim 1648 \text{ cm}^{-1}$  band keeps its split character.

*Analcime sample crystallized at 400°C in 0.1M  $\text{Na}_2\text{CO}_3$  solution*

The activation of analcime causes a uniform decline of the low frequency part of the IR spectrum (Text-fig. 19). At 400°C the broad band gains one peak at  $\sim 3623 \text{ cm}^{-1}$ . This peak remains

visible throughout the whole process and corresponds to relict water after the evacuation. The evacuation between 400-600°C changes only its intensity. The water bending vibration peak decreases without any split, and disappears at 500°C. The adsorption almost restores the water environment in the crystal (Text-fig. 20). It produces an asymmetric broad band in the OH stretching vibration region and a sharp band at  $\sim 1630 \text{ cm}^{-1}$  in the water bending region. The asymmetric broad band, with the maximum at  $\sim 3550 \text{ cm}^{-1}$  is accompanied by an enlarging band at  $3660 \text{ cm}^{-1}$ . Both bands merge at 10mbar water pressure (Text-fig. 20).

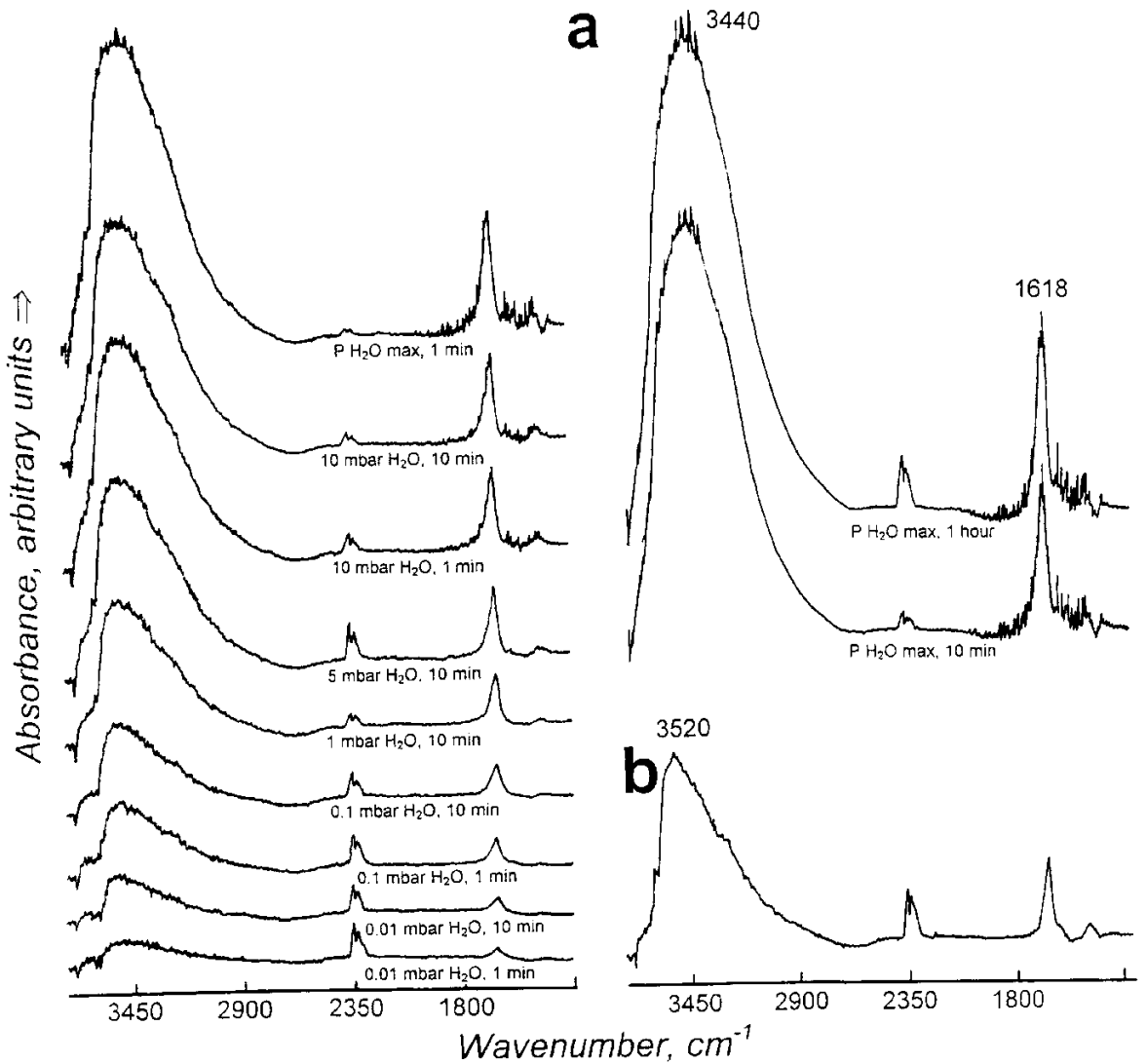


Fig. 20. The IR spectra of adsorbed water in analcime

a – The OH stretching area, b – The IR spectra of adsorbed water in analcime after degassing

## Dehydration – DTG-TG, DSC study

Thermogravimetric analyses and differential scanning calorimetry were carried out on 20 cancrinite and 5 analcime samples. Characteristic data from DTG-TG and DSC curves of cancrinites and analcimes are summarised in Table 9.

The DTG-TG and DSC analyses were performed by means of a fully computerised Du Pont Thermal Analyst 2100 with Thermogravimetric Analyser 951 and Differential Scanning Calorimeter 910.

The data were collected under the following conditions:

- DTG method: sample weight 20-30 mg, heating range 20-950°C (rate 10 deg/min) in an argon atmosphere,
- DSC method: sample weight 10mg, heating range 20-700°C (rate 10 deg/min), in an argon atmosphere.

The first comprehensive explanation of cancrinite thermal behaviour was given by HASSAN (1996) and therefore I describe my own data with reference to his data and interpretation. In the A and B-cancrinite the DTG-TG signals generally reveal four stages in their thermal behaviour. At least three of these stages indicate water loss. The

fourth could indicate the loss of the supercell (HASSAN 1996) and/or loss of hydroxyl groups (BUHL 1991). The first signal, at ~70-140°C indicates loss of the water adsorbed at the surface. It is present in almost all A and B-cancrinite samples as a split signal. Although this water is very weakly bonded to the zeolite framework (for enthalpy value *see* Table 9), the split signal (at ~86°C and ~113°C) shows that there are two preferential adsorption sites in the cancrinite structure (Text-fig. 21). The next signal appears at 302-360°C and, according to HASSAN (1996), it originates from the H<sub>2</sub>O(I) loss. DTG curves show a very broad peak in this area. H<sub>2</sub>O(II) leaves the structure in the temperature interval 670-770°C (the range of the midpoint temperature). DTG curves usually show a narrow peak in this area. HASSAN (1996) has determined H<sub>2</sub>O(II) loss to occur at 683°C. Between 820-870°C (midpoint temperatures) the loss of superstructure and /or dehydroxylation process is noticeable. HASSAN (1996) has observed this process in the temperature range ~838-888°C without any peak on DTG curves.

DTG-TG and DSC curves show some differences in the case of cancrinite structure formed under high and low temperature as well as in the more concentrated and diluted solution. Cancrinites grown in the more concentrated solu-

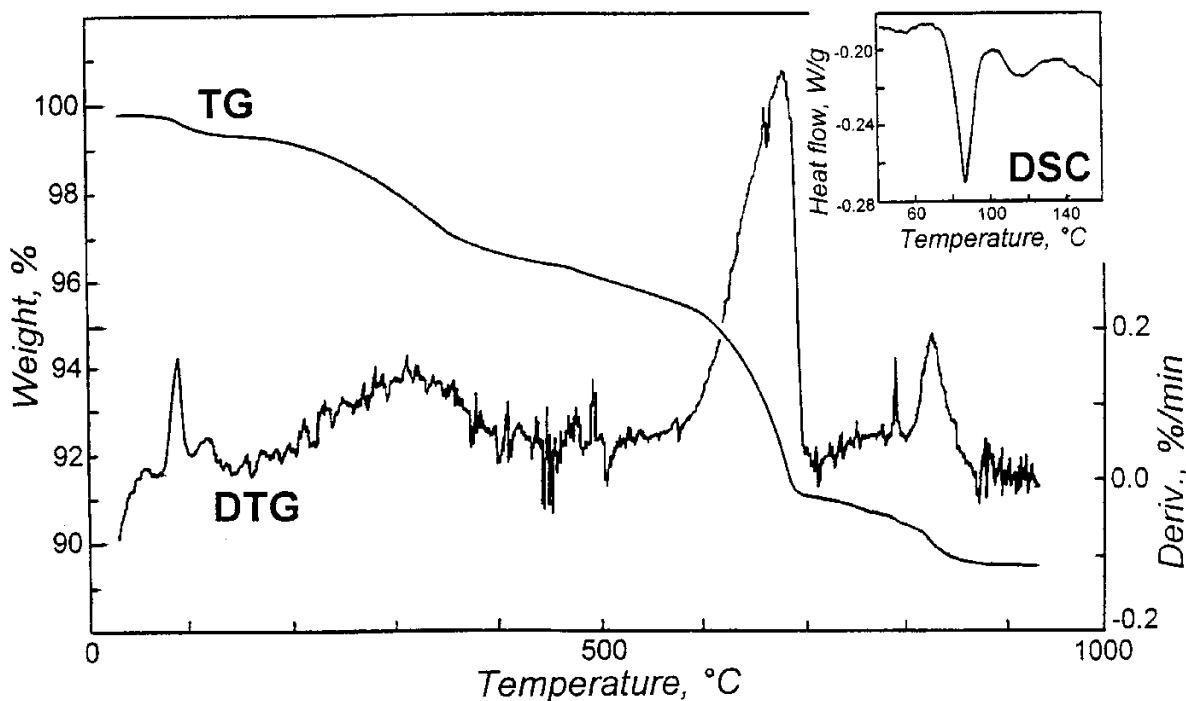


Fig. 21. The DTG-TG and detail of DSC curves of B-cancrinite (synthesis conditions: T=350°C, 0.1M Na<sub>2</sub>CO<sub>3</sub> solution)

tion (1M Na<sub>2</sub>CO<sub>3</sub>) at 550°C do not reveal any signals on DTG-TG curves in the area corresponding to supercell loss or/and the dehydroxylation

process (Text-fig. 22 and Table 9). Additionally in the B-cancrinite belonging to this group water (both I and II) leaves the structure continuously in

Table 9. Data from the TG-DTG, DSC analyses of cancrinites and analcimes.

Peaks	Miscellaneous	TG	DSC
<b>B-CANCRINITE; synthesis conditions - T=550°C, 1M Na<sub>2</sub>CO<sub>3</sub> solution</b>			
1	Start T(°C)	56.4	54.3
	Onset T(°C)	73.1	67.2
	Midpoint T(°C)	86.5	78.0
	End T(°C)	96.2	
	Stop T(°C)	145.9	111.5
	%Wt loss	2.7	
	Enthalpy (J/g)		78.7
2	Start T(°C)	248.6	
	Onset T(°C)	589.9	
	Midpoint T(°C)	748.8	
	End T(°C)	807.5	
	Stop T(°C)	891.1	
	%Wt loss	7.9	
	Enthalpy (J/g)		
<b>B-CANCRINITE; synthesis conditions - T=400°C, 1M Na<sub>2</sub>CO<sub>3</sub> solution</b>			
1	Start T(°C)	67.8	70.5
	Onset T(°C)	81.8	79.0
	Midpoint T(°C)	87.5	86.6
	End T(°C)	98.2	
	Stop T(°C)	140.3	103.8
	%Wt loss	0.5	
	Enthalpy (J/g)		4.5
2	Start T(°C)	139.9	140.8
	Onset T(°C)	238.3	185.4
	Midpoint T(°C)	312.4	273.9
	End T(°C)	365.8	
	Stop T(°C)	450.4	390.6
	%Wt loss	3.1	
	Enthalpy (J/g)		36.6
3	Start T(°C)	450.0	559.5
	Onset T(°C)	629.7	603.7
	Midpoint T(°C)	671.7	669.8
	End T(°C)	684.1	
	Stop T(°C)	710.0	696.0
	%Wt loss	6.4	
	Enthalpy (J/g)		124.3
4	Start T(°C)	709.6	
	Onset T(°C)	796.5	
	Midpoint T(°C)	823.6	
	End T(°C)	842.4	
	Stop T(°C)	880.7	
	%Wt loss	1.3	
	Enthalpy (J/g)		

Peaks	Miscellaneous	TG	DSC
<b>B-CANCRINITE; synthesis conditions - T=550°C, 0.1M Na<sub>2</sub>CO<sub>3</sub> solution</b>			
1	Start T(°C)	75.7	80.1
	Onset T(°C)	84.8	82.3
	Midpoint T(°C)	138.6	140.5
	End T(°C)	220.6	
	Stop T(°C)	230.8	198.0
	%Wt loss	0.7	
	Enthalpy (J/g)		6.4
2	Start T(°C)	233.4	200.4
	Onset T(°C)	238.3	220.1
	Midpoint T(°C)	356.9	290.1
	End T(°C)	441.5	
	Stop T(°C)	450.4	380.2
	%Wt loss	3.3	
	Enthalpy (J/g)		103.6
3	Start T(°C)	457.9	
	Onset T(°C)	612.3	
	Midpoint T(°C)	772.3	
	End T(°C)	788.4	
	Stop T(°C)	810.1	
	%Wt loss	3.7	
	Enthalpy (J/g)		
4	Start T(°C)	809.8	
	Onset T(°C)	835.9	
	Midpoint T(°C)	848.7	
	End T(°C)	867.2	
	Stop T(°C)	930.3	
	%Wt loss	3.0	
	Enthalpy (J/g)		
<b>B-CANCRINITE; synthesis conditions - T=350°C, 0.1M Na<sub>2</sub>CO<sub>3</sub> solution</b>			
1	Start T(°C)	63.3	67.1
	Onset T(°C)	235.6	69.8
	Midpoint T(°C)	322.5	85.1
	End T(°C)	364.6	
	Stop T(°C)	486.1	95.5
	%Wt loss	4.4	
	Enthalpy (J/g)		1.3
2	Start T(°C)	486.3	177.6
	Onset T(°C)	632.9	173.3
	Midpoint T(°C)	675.6	315.3
	End T(°C)	688.2	
	Stop T(°C)	712.1	388.3
	%Wt loss	4.7	
	Enthalpy (J/g)		92.8

Peaks	Miscellaneous	TG	DSC
3	Start T(°C)	712.3	584.7
	Onset T(°C)	803.3	607.1
	Midpoint T(°C)	843.9	679.9
	End T(°C)	893.9	
	Stop T(°C)	930.8	702.6
	%Wt loss	2.0	
	Enthalpy (J/g)		132.7

**A-CANCRINITE; synthesis conditions**  
**- T=550°C, 1M Na<sub>2</sub>CO<sub>3</sub> solution**

1	Start T(°C)	73.7	69.3
	Onset T(°C)	83.9	78.0
	Midpoint T(°C)	88.2	86.1
	End T(°C)	92.8	
	Stop T(°C)	101.5	99.6
	%Wt loss	0.4	
	Enthalpy (J/g)		9.4
2	Start T(°C)	102.5	99.6
	Onset T(°C)	108.3	
	Midpoint T(°C)	111.2	112.2
	End T(°C)	117.3	
	Stop T(°C)	135.2	127.74
	%Wt loss	0.3	
	Enthalpy (J/g)		3.8
3	Start T(°C)	136.2	146.1
	Onset T(°C)	248.9	178.5
	Midpoint T(°C)	338.0	323.9
	End T(°C)	375.5	
	Stop T(°C)	435.6	420.6
	%Wt loss	8.7	
	Enthalpy (J/g)		216.6
4	Start T(°C)	436.7	
	Onset T(°C)	494.3	
	Midpoint T(°C)	529.0	
	End T(°C)	584.2	
	Stop T(°C)	700.1	
	%Wt loss	1.3	
	Enthalpy (J/g)		

**A-CANCRINITE; synthesis conditions**  
**- T=350°C, 1M Na<sub>2</sub>CO<sub>3</sub> solution**

1	Start T(°C)	67.3	63.6
	Onset T(°C)	78.6	67.2
	Midpoint T(°C)	86.8	82.7
	End T(°C)	99.7	
	Stop T(°C)	134.6	120.5
	%Wt loss	0.5	
	Enthalpy (J/g)		6.7
2	Start T(°C)	163.4	331.5
	Onset T(°C)	333.5	402.0
	Midpoint T(°C)	475.2	472.7
	End T(°C)	584.4	

Peaks	Miscellaneous	TG	DSC
3	Stop T(°C)	658.7	615.1
	%Wt loss	5.5	
	Enthalpy (J/g)		49.9
	Start T(°C)	656.2	
	Onset T(°C)	754.1	
	Midpoint T(°C)	789.9	
	End T(°C)	810.3	
4	Stop T(°C)	843.8	
	%Wt loss	3.4	
	Enthalpy (J/g)		
	Start T(°C)	843.7	
	Onset T(°C)	875.6	
	Midpoint T(°C)	906.8	
	End T(°C)	914.8	
4	Stop T(°C)	935.1	
	%Wt loss	2.3	
	Enthalpy (J/g)		

**ANALCIME; synthesis conditions -**  
**T=450°C, 0.5M Na<sub>2</sub>CO<sub>3</sub> solution**

1	Start T(°C)	73.7	69.3
	Onset T(°C)	83.9	78.04
	Midpoint T(°C)	88.2	86.1
	End T(°C)	92.8	
	Stop T(°C)	101.5	99.6
	%Wt loss	0.3	
	Enthalpy (J/g)		9.4
2	Start T(°C)	102.5	99.6
	Onset T(°C)	108.3	
	Midpoint T(°C)	111.2	112.2
	End T(°C)	117.3	
	Stop T(°C)	135.2	127.7
	%Wt loss	0.2	
	Enthalpy (J/g)		3.8
3	Start T(°C)	136.2	146.1
	Onset T(°C)	248.9	178.5
	Midpoint T(°C)	338.0	323.9
	End T(°C)	375.5	
	Stop T(°C)	435.6	420.6
	%Wt loss	6.9	
	Enthalpy (J/g)		216.6
4	Start T(°C)	436.7	
	Onset T(°C)	494.3	
	Midpoint T(°C)	529.0	
	End T(°C)	584.2	
	Stop T(°C)	700.1	
	%Wt loss	0.8	
	Enthalpy (J/g)		

**ANALCIME; synthesis conditions -**  
**T=350°C, 0.5M Na<sub>2</sub>CO<sub>3</sub> solution**

Peaks	Miscellaneous	TG	DSC
1	Start T(°C)	124.3	134.7
	Onset T(°C)	213.6	177.1
	Midpoint T(°C)	278.5	265.7
	End T(°C)	340.0	
	Stop T(°C)	422.0	379.7
	%Wt loss	7.3	
	Enthalpy (J/g)		128.4
2	Start T(°C)	533.0	
	Onset T(°C)	568.8	
	Midpoint T(°C)	592.6	
	End T(°C)	602.1	
	Stop T(°C)	614.4	
	%Wt loss	0.1	
3	Start T(°C)	614.7	
	Onset T(°C)	633.8	
	Midpoint T(°C)	654.8	
	End T(°C)	684.1	
	Stop T(°C)	0.1	
	%Wt loss		

Peaks	Miscellaneous	TG	DSC
Enthalpy (J/g)			
<b>ANALCIME; synthesis conditions - T=500°C, 0.1M Na<sub>2</sub>CO<sub>3</sub> solution</b>			
1	Start T(°C)	221.1	
	Onset T(°C)	291.1	
	Midpoint T(°C)	313.2	
	End T(°C)	405.9	
	Stop T(°C)	485.7	
	%Wt loss	5.4	
<b>ANALCIME; synthesis conditions - T=350°C, 0.1M Na<sub>2</sub>CO<sub>3</sub> solution</b>			
1	Start T(°C)	73.2	109.7
	Onset T(°C)	219.1	161.0
	Midpoint T(°C)	294.9	278.4
	End T(°C)	360.8	
	Stop T(°C)	504.7	394.1
	%Wt loss	7.9	
	Enthalpy (J/g)		148.8

the temperature range ~250-890°C (Text-fig. 22). In the B-cancrinites, the midpoint temperatures of all peaks are usually slightly shifted towards lower T values in the samples grown under low temperature (300-350°C) than in the samples grown under

high temperatures. The opposite tendency appears in the samples of the A-cancrinites. Another relationship can be observed in the case of samples of the B-cancrinites grown at the same temperature from diluted and concentrated solution (Table 9),

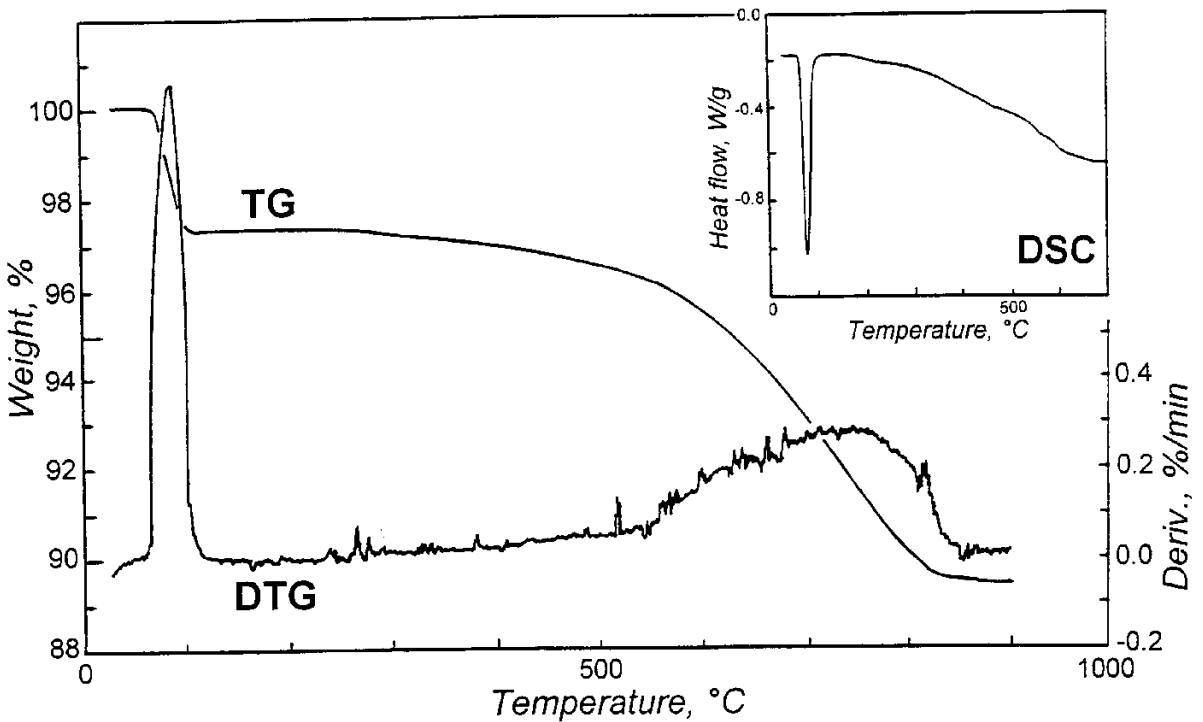


Fig. 22. The DTG-TG and DSC curves of B-cancrinite (synthesis conditions: T=550°C, 1M Na<sub>2</sub>CO<sub>3</sub> solution)

namely that the midpoint temperature of all peaks is usually slightly shifted towards higher value in the DTG-TG curves of cancrinites synthesized from diluted solution. The data are supported by enthalpy values determined for the process of  $H_2O(I)$  and  $H_2O(II)$  release (Table 9).

The relationship between  $H_2O(I)$  and  $H_2O(II)$  in the cancrinites is not constant. In the B-cancrinite crystallized from more concentrated solution (1M  $Na_2CO_3$ , at  $550^\circ C$ )  $H_2O(II)$  is absent. Whole water behaves like  $H_2O(I)$ . B-cancrinite grown in the most diluted solution at  $300^\circ C$  has almost equal

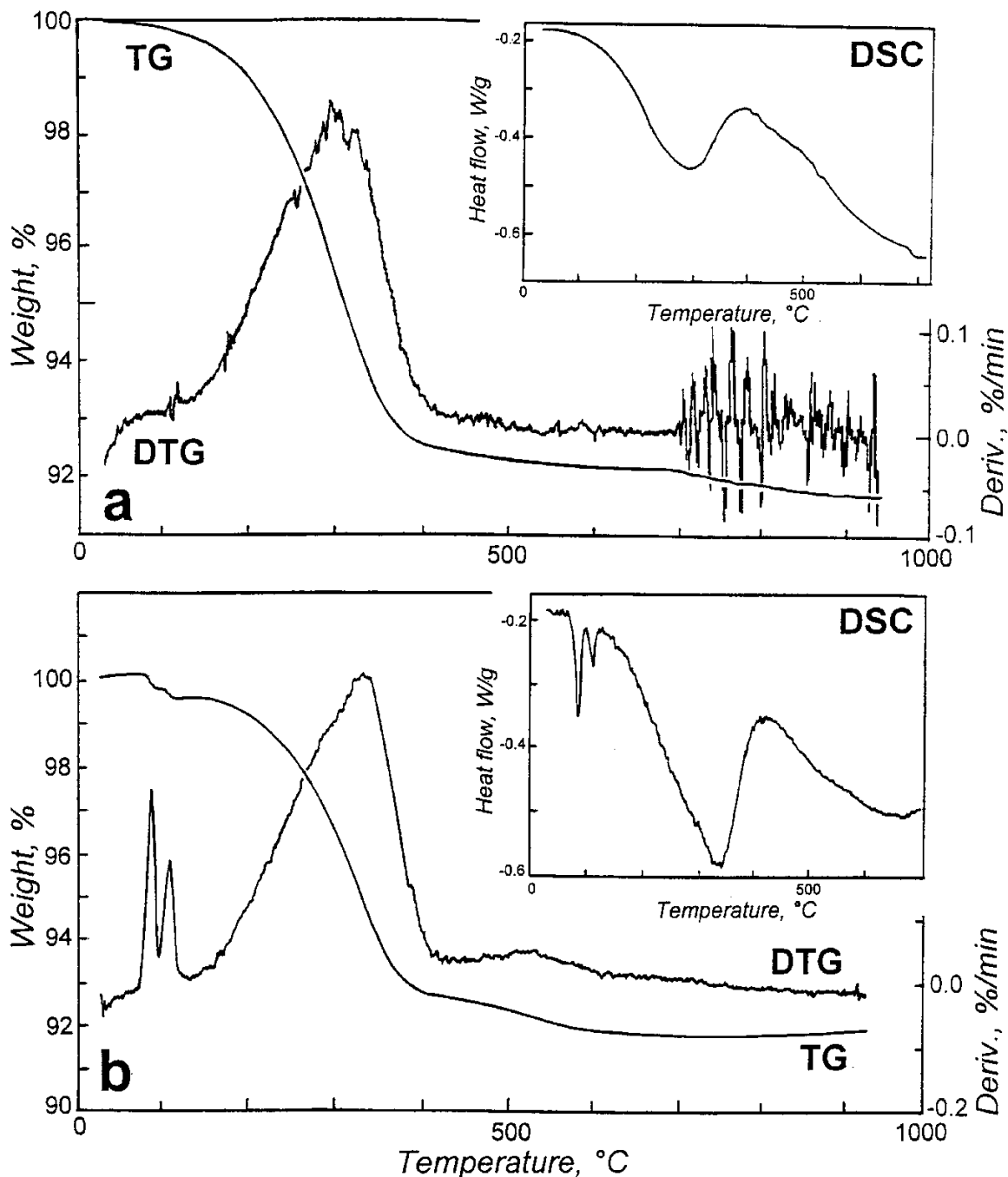


Fig. 23. The DTG-TG and DSC curves of analcimes

**a** – synthesis conditions:  $T=300^\circ C$ , 0.1M  $Na_2CO_3$  solution, **b** – synthesis conditions:  $T=450^\circ C$ , 0.5M  $Na_2CO_3$  solution

amount of  $\text{H}_2\text{O(I)}$  and  $\text{H}_2\text{O(II)}$ . In the A-cancrinite formed under the same conditions  $\text{H}_2\text{O(I)}$  dominates. The amount of  $\text{H}_2\text{O(II)}$  increases in the A-cancrinite samples synthesized at low temperature.

The last signal on the DTG/TG curves seems to correspond to loss of the supercell. The DTG peak corresponding to changes in supercell structure is usually a broad one. In some samples of B and A-cancrinites (except those crystallized at  $T=550^\circ\text{C}$  from 1M  $\text{Na}_2\text{CO}_3$  solution) the broad peak additionally gains one or two sharp-pointed signals. Changes in the superstructure of the big channel were also observed in these samples during the activation process monitored by IR. The samples show the presence of residual IR bands (in the  $3000\text{--}3700\text{ cm}^{-1}$  and  $1740\text{ cm}^{-1}$  area) of the spectra after the activation. It is possible that there are OH or  $\text{OH}_3$  groups in the structure of these cancrinites.

The thermal behaviour of the analcimes is actually similar for all samples, but some differences are also noticed. Analcimes generally release water in a one-stage process. The midpoint temperature of the process approaches  $\sim 300^\circ\text{C}$  (Text-fig. 23). The temperature is somewhat lower in the analcimes formed under low temperatures ( $300\text{--}350^\circ\text{C}$ ). The amount of water is much bigger in the analcime formed in diluted solution and at low temperature ( $300\text{--}350^\circ\text{C}$ ). On the DTG-TG curves of analcime grown in the more concentrated solution ( $0.5\text{M Na}_2\text{CO}_3$ ), two other peaks at lower temperatures ( $<200^\circ\text{C}$ ) can be seen (Text-fig. 23b). The low temperature peaks can be attributed to adsorbed water. They show two preferential adsorption sites in the structure. Two weak peaks at higher temperatures ( $>400^\circ\text{C}$ ) can also be determined. The weight loss due to these processes is negligible (Table 9). The origin of the high temperature peaks ( $>400^\circ\text{C}$ ) is not clear. They suggest the presence of other  $\text{OH}_m$  groups as impurities. The activation energy for that sample is a bit larger ( $105.9\text{kJ/mol}$ ) than for the other analcimes ( $97\text{kJ/mol}$ ). LINE & *al.* (1995) gave the value of activation energy  $92\text{kJ/mol}$  for H-analcime. Analcime formed at  $350^\circ\text{C}$ , but in more concentrated solution ( $1\text{M Na}_2\text{CO}_3$ ), also shows some water adsorbed at the surface.

## THE $^1\text{H}$ MAS NMR STUDY

The  $^1\text{H}$  MAS NMR studies give information about the different kinds of water and hydroxyl protons present in the structure. Twelve samples of

B and A-cancrinites and two samples of analcime were selected for the  $^1\text{H}$  MAS NMR investigation. B and A-cancrinite samples represented extremely different synthesis conditions: 1M  $\text{Na}_2\text{CO}_3$  solution and  $T=550^\circ\text{C}$ ; 1M  $\text{Na}_2\text{CO}_3$  solution and  $T=300^\circ\text{C}$ ; 0.5M  $\text{Na}_2\text{CO}_3$  solution and  $T=550^\circ\text{C}$ ; 0.5M  $\text{Na}_2\text{CO}_3$  solution and  $T=300^\circ\text{C}$ ; 0.1M  $\text{Na}_2\text{CO}_3$  solution and  $T=550^\circ\text{C}$ ; 0.1M  $\text{Na}_2\text{CO}_3$  solution and  $T=300^\circ\text{C}$ . The analcime samples were grown in 0.1M  $\text{Na}_2\text{CO}_3$  solution at  $300^\circ\text{C}$  and  $400^\circ\text{C}$ .

Other NMR studies of proton environment as well as other elements interacting with proton in the aluminosilicate structures provide a reference for the present research. These are  $^1\text{H}$  MAS NMR study on hydrosodalite (BUHL & *al.* 1988, ENGELHARDT & *al.* 1987, 1992) and  $^{23}\text{Na}$  MAS NMR study on hydrosodalite and analcime (BUHL & *al.* 1988, ENGELHARDT & *al.* 1992, KIM & KIRKPATRICK 1998). The hydrosodalite structure show some similarities with cancrinite structure.

The  $^1\text{H}$  MAS NMR spectra were recorded at  $24^\circ\text{C}$  and 400MHz. The spectrum width was 100kHz. Chemical shifts were referenced to  $\text{TMS}=0\text{ppm}$ .

The  $^1\text{H}$  MAS NMR spectra of the B and A-cancrinites are generally similar. The signals have similar value of chemical shifts but their intensities vary. An exception is the spectrum of the B-cancrinite originating from the synthesis in 1M  $\text{Na}_2\text{CO}_3$  solution at  $T=550^\circ\text{C}$ . To present the features of the cancrinite spectra descriptions of the spectrum for the B-cancrinite sample grown in 1M  $\text{Na}_2\text{CO}_3$  solution at  $T=550^\circ\text{C}$  and spectrum for the A-cancrinite grown in 0.5M  $\text{Na}_2\text{CO}_3$  solution at  $T=550^\circ\text{C}$  are given.

The  $^1\text{H}$  MAS NMR spectrum of B-cancrinite (synthesized in 1M  $\text{Na}_2\text{CO}_3$  solution at  $T=550^\circ\text{C}$ ) consists of many overlapping signals (Text-fig. 24a). A range of chemical shifts results in a very broad peak area. The most intense peak appears at 3.29 ppm. It is accompanied by other signals, the main being at: 6.83, 15.96 and 18.5 ppm. The structure seems to possess many different protons. They are in different structural environments. The surrounding of each proton provides another electron shielding.

The spectrum of A-cancrinite (synthesized in 0.5M  $\text{Na}_2\text{CO}_3$  solution at  $T=550^\circ\text{C}$ ) reveals four signals: at 3.04 ppm, 4.14 ppm, 4.70 ppm and 6.21ppm (Text-fig. 24b). The most intense peak appears at 3.04 ppm. Peak intensity is proportional

to site occupancy. One of the protons environment is privileged in the structure. The signal is broad, which could indicate some disorder at this site. The intensities of next two signals (4.14 ppm and 4.70 ppm) are comparable. Both peaks are very well resolved. Both protons environments are then very well defined. The sites do not show any disorder. A very sharp signal usually originates from water the molecules of which are either very weakly hydrogen bonded or not involved in hydrogen bonding. The signal at 6.21 ppm is much weaker and broader than the others. There is also a trace of signal at -1.3 ppm (Text-fig. 25a). The chemical shift of this signal varies from -0.7 to 1.32 ppm in other sam-

ples of A and B-cancrinite. Analysing the IR spectra recorded at room temperature as well as taken during the dehydration and rehydration process and the DTG/TG data of cancrinites one can expect to find at least four distinctly different proton environments in the structure. The  $^1\text{H}$  MAS NMR measurements confirm this hypothesis.

Both analcime spectra are generally similar. The spectrum of analcime synthesized at lower temperature displays one additionally peak at 4.58 ppm which is absent from the spectrum of analcime grown at higher temperature. The spectra of analcime samples (synthesized in 0.1M  $\text{Na}_2\text{CO}_3$  solution at  $T=300^\circ\text{C}$ ) shows peaks at -1.24 ppm,

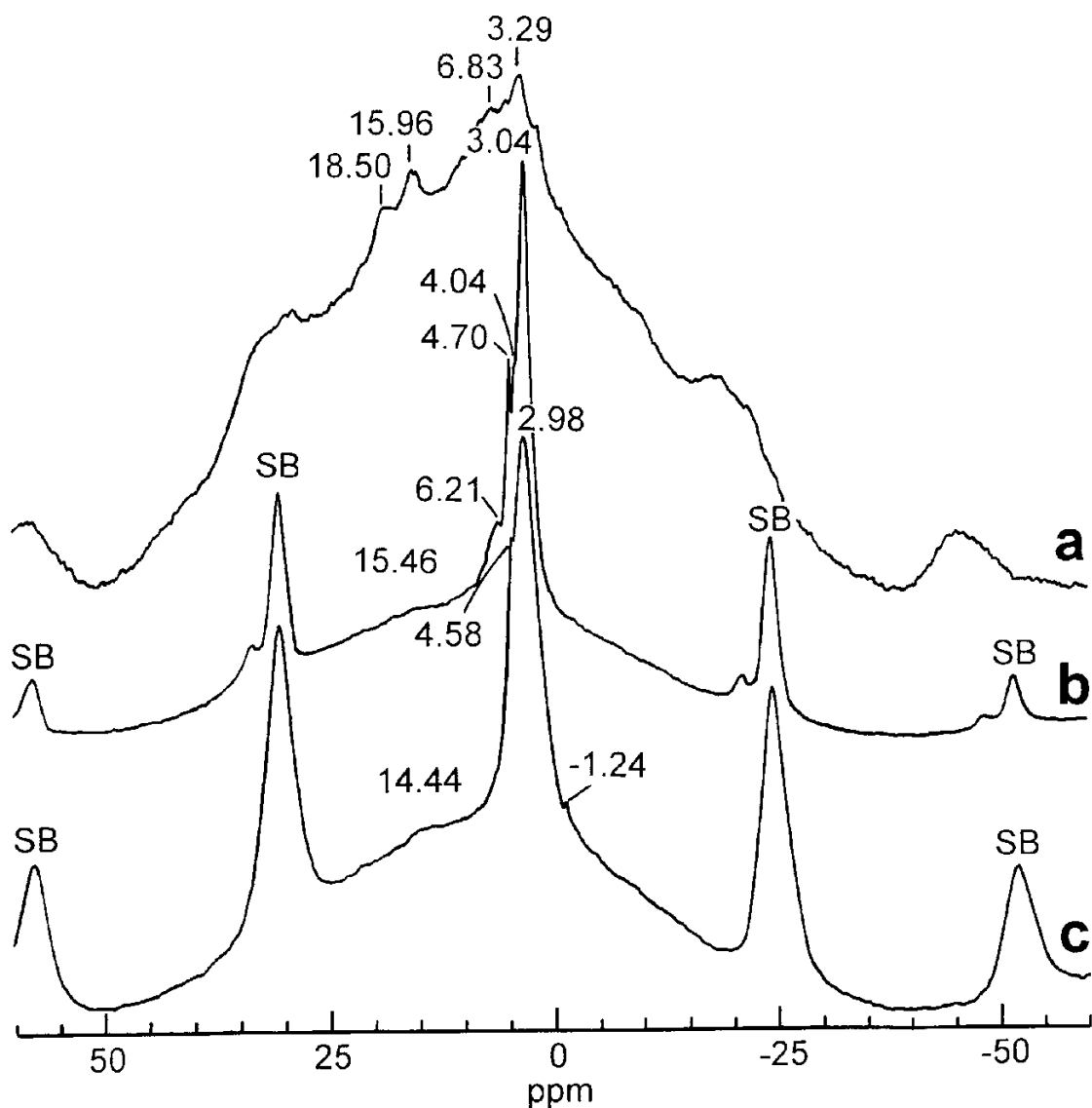


Fig. 24. The  $^1\text{H}$  MAS NMR spectra of cancrinite and analcime  
 a – B-cancrinite, b – A-cancrinite, c – analcime; Explanations: SB – spinning side bands

2.98 ppm and 4.58 ppm. All the peaks form one broad band with the maximum at 2.98 ppm suggesting some order-disorder on the proton site (Text-figs 24c and 25b). Even though there are three different protons in the structure, the environment of one of them dominates those of the other two. The signal at 4.58 ppm disappears in the samples synthesized at temperatures higher than 400°C.

BUHL & *al.* (1988) and ENGELHARDT & *al.* (1992) identified the 4.2-4.3 ppm chemical shift as a shift of liquid water and water in zeolites. The lines at ~4 ppm could also correspond to SiOHAl groups (ENGELHARDT & *al.* 1987). The impurity water or adsorbed water was assigned at 5 ppm. The higher field shift at ~3 ppm accompanied by -1.2 ppm was attributed to H<sub>2</sub>O and OH groupings in the hydrosodalite structure (BUHL & *al.* 1988).

Hydrosodalite structure containing only OH groups gave a signal at -6.5 ppm.

## RESULTS AND DISCUSSION

The aim of the present research work was to find possible connections between water environment in the zeolite structure and physico-chemical conditions leading to the formation of this structure. A positive answer can be given to the question regarding the existence of such connections. Although there are some connections the relation between water environment and the physico-chemical conditions of the structure formation is not a simple one. According to the results of my research work the amount water incorporated into the structure depends on the synthesis conditions. Low temperature synthesis products contain more water than high temperature reaction products. The same relation is to some extent true for the crystals formed in solution with either low or high salt concentration. The IR signals originating from hydrogen bonded water are shifted towards higher frequencies in the low temperature synthesis products. This means that the hydrogen bonding in low temperature synthesis products is weaker. Water is probably held in the channel due to the participation of one water molecule in double hydrogen bonding (EMIRALIEV & JAMZIN 1982).

Water position in synthesized crystals depends on modification of some unit buildings in the structure. The structure formation depends in turn on many factors. One of them is the structure of the source material, defects in that structure, microcracks and so on. The above mentioned circumstances cause variation in the progress of the reaction during the same period of time. The type of zeolitic structure that appears as a reaction product also depends on the reaction temperature, chemical constituents in the solution and chemical composition of the source material. All these factors determine the activity and speciation of the components in the hydrothermal system. The reaction temperature determines the kinetics of silicon and aluminium transport in the system. Due to differences in the silicon and aluminium behaviour, the low temperature syntheses favour analcime whereas high temperature syntheses favour cancrinite crystallization. The activity of other components in the solutions also influences the type of zeolitic structure that crystallizes. High CO<sub>3</sub><sup>2-</sup> concentration in

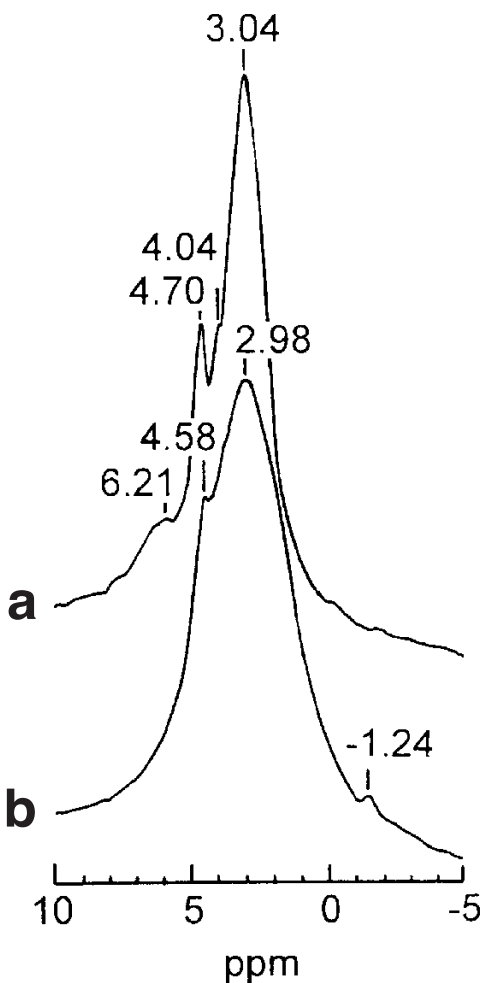


Fig. 25. Detail of A-cancrinite (a) and analcime (b) <sup>1</sup>H MAS NMR spectrum

the solution inhibits analcime formation even if silicon activity in the system is sufficient to promote such a crystallization. Temperature and  $\text{CO}_3^{2-}$  concentration in the solution also controls the type of superstructure of the anion chain in the big cancrinite channel. A similar role is played by the sodium and calcium activity. Cancrinites formed at high temperature are rich in calcium. The products of low temperature syntheses contain more sodium. The type of crystal that appears depends on the mineral/water ratio. A low solution content in the system results in the crystallization of nepheline instead of cancrinite.

Synthesized analcimes do not show any differences in chemical composition. Under experimental conditions the stability field of analcimes is much more limited than that of cancrinites. Changes in the physico-chemical conditions are reflected in the habit of the analcime crystals. Various chemical composition and various superstructure modifications of the anion clusters in the big channel cause changes in water position in cancrinite crystals. Water environment in the analcimes seems to be similar.

The water in the cancrinite structure has been determined as  $\text{H}_2\text{O(I)}$  and  $\text{H}_2\text{O(II)}$  (HASSAN, 1996a, b). The present research work confirms that classification. There are at least two different kinds of hydrogen-bonded water in the cancrinite structure. The presence of at least two kinds of molecular water is confirmed by the IR signals in the water bending area. The signal at  $\sim 1640\text{ cm}^{-1}$  splits into three parts during the calcination process ( $1638\text{ cm}^{-1}$ ,  $1670\text{ cm}^{-1}$  and  $1740\text{ cm}^{-1}$ ). One of the bands belongs neither to  $\text{H}_2\text{O(I)}$  nor to  $\text{H}_2\text{O(II)}$ . This suggests that not all of the O-H relations occur as  $\text{H}_2\text{O(I)}$  or  $\text{H}_2\text{O(II)}$ . This observation is in agreement with the conclusions of EMIRALIEV & JAMZIN (1982) and GALITSKI & *al.* (1978) that there must also be other  $\text{OH}_m$  ( $m=1, 2, 3$ ) groups in the structure. These groups are probably involved in the superstructure unit of the big channel. Some of the  $\text{OH}_m$  groups leave the structure in the temperature interval corresponding to the loss of the supercell. The dehydration process, as shown by the IR measurements, does not remove those groups. Their presence after the calcination is manifested by the  $\sim 1740\text{ cm}^{-1}$  peak in the water bending vibration area and relics of a peak in the stretching vibration area. The DTG/TG analysis additionally hints at some molecular water adsorbed at the mineral surface and located in two preferential sites. Adsorbed water usually leaves the structure at  $T=70\text{--}140^\circ\text{C}$ .

The resonance  $^1\text{H}$  signal at  $\sim 5\text{ ppm}$  can be attributed to adsorbed water.

Correlation of  $\text{H}_2\text{O(I)}$  and  $\text{H}_2\text{O(II)}$  behaviour in the cancrinite structure with the conditions of the structure formation is the most important problem, because the sum of both kinds of water comprises almost the entire water content. The position of the adsorbed water and  $\text{OH}_m$  groups in the structure does not vary significantly with run conditions so it is of less importance. The IR, DTG/TG and NMR investigations presented in this work give much more precise characteristics of  $\text{H}_2\text{O(I)}$  and  $\text{H}_2\text{O(II)}$ . According to the obtained results the molecules of  $\text{H}_2\text{O(I)}$  show some order-disorder. Molecules of  $\text{H}_2\text{O(II)}$  seem to be located in two different environments. HASSAN'S (1996a, b) data indicate that, due to the dehydration process,  $\text{H}_2\text{O(I)}$  disappears prior to  $\text{H}_2\text{O(II)}$ . The dehydration process, as shown by the respective IR measurements, as well as by the IR spectra recorded at room temperature, make it possible to assign this water better. The very broad IR signal with the maximum intensity at  $\sim 3450\text{ cm}^{-1}$  may be attributed to  $\text{H}_2\text{O(I)}$ . The signal disappears during the activation (IR data) in the temperature interval corresponding to the  $\text{H}_2\text{O(I)}$  dehydration temperature obtained from DTG/TG analysis. The peak is also very broad. The DTG/TG analyses and the analyses of the deconvoluted OH stretching vibration region in the IR spectra lead to the conclusion that the  $\text{H}_2\text{O(I)}$  molecules are located in different positions and that the hydrogens of those molecules interact via hydrogen bonding with the oxygens of the Si-Al framework. Thus the spectra suggest disorder at the water position. According to the results of EMIRALIEV & JAMZIN (1982) only two of the three sites around three-fold axis could be occupied by water. Interaction of the disordered water molecules with the Al-Si framework gives rise to a broad IR band. The H-O1 and H .....O2 distances vary considerably for different  $\text{H}_2\text{O(I)}$  molecules ( $2.7\text{Å--}3\text{Å}$ ). The Na1 distance to framework oxygens is  $2.4\text{--}2.8\text{Å}$ . The H-O1 distance achieves its maximum value ( $1\text{Å}$ ) in the  $\text{H}_2\text{O(I)}$  for B-cancrinite sample formed at  $550^\circ\text{C}$  ( $1\text{M Na}_2\text{CO}_3$  solution) and decreases with reducing run temperature and solution concentration down to  $0.96\text{Å}$ . In the high temperature cancrinite sample ( $550^\circ\text{C}$ ;  $1\text{M Na}_2\text{CO}_3$  solution), all of the water behaves like  $\text{H}_2\text{O(I)}$ . Each water molecule appears in a slightly different environment. Several  $^1\text{H}$  MAS NMR signals in the spectrum confirm this idea. In the remaining cancrinite, it is very probable that the  $^1\text{H}$

MAS NMR signal at  $\sim 3$  ppm can be attributed to  $\text{H}_2\text{O(I)}$ . The signal shows some order-disorder on the proton site. This signal may be also influenced by another H environment that does not belong to  $\text{H}_2\text{O(I)}$ .

The  $\text{H}_2\text{O(II)}$  is much more sensitive to the synthesis conditions than  $\text{H}_2\text{O(I)}$ . The IR spectra recorded at room temperature and during the dehydration process allow me to attribute the sharp bands ( $\sim 3530\text{--}70\text{ cm}^{-1}$  and  $\sim 3600\text{--}3630\text{ cm}^{-1}$ ) to  $\text{H}_2\text{O(II)}$ . The  $\text{H}_2\text{O(II)}$  appears in a very small or trace amounts in high temperature run products. Its amount in the grown crystals increases with falling run temperature and falling salt concentration in the solution. According to the DTG/TG data, in the low temperature reaction products, the  $\text{H}_2\text{O(II)}$  amount is almost equal to that of  $\text{H}_2\text{O(I)}$ . In fact the integrated intensity of  $\text{H}_2\text{O(II)}$  IR bands is always lower than that of  $\text{H}_2\text{O(I)}$ . Some water molecules which structurally belong to  $\text{H}_2\text{O(I)}$  may leave the channel cavity with some delay. The position of the  $\text{H}_2\text{O(II)}$  is better defined than that of the  $\text{H}_2\text{O(I)}$ . Two sharp IR and  $^1\text{H}$  MAS NMR (at  $\sim 4$  ppm) signals indicate two different hydrogen environments. According to the signal, the protons do not show any disorder on their sites. The sites are very well defined. Various IR, as well as  $^1\text{H}$  MAS NMR, signals are not of equal intensity. It is probable that the molecules of  $\text{H}_2\text{O(II)}$  have two H-H orientations in the channel cavity. Some doubts arise about the  $\text{H}_2\text{O(II)}$  location, i.e. which channel is occupied by this water type? HASSAN (1996a, b) believes it is the six-membered channel. EMIRALIEV & JAMZIN (1982) found only one type of water in the six-membered channel. They located some  $\text{OH}_m$  ( $m=1, 2, 3$ ) groups in the big channel. Both these sets of data are not compatible. HASSAN (1996a, b) investigated cancrinite from a silica-deficient rock from Bancroft, EMIRALIEV & JAMZIN (1982) worked on hydrothermal synthesis product. Although refining the structure of cancrinite produced at high temperature in concentrated solution (SŁABY 1994) gave data similar to those of the Bancroft cancrinite (GRUNDY & HASSAN 1982), this refinement does not locate the water position. All that can be stated is that both crystals possess a similar Al-Si framework and a similar sodium and calcium position. EMIRALIEV & JAMZIN (1982) studied a synthesis product, so their data are more comparable with the present research. Precise superstructure model, but not comparable with EMIRALIEV & JAMZIN (1982) data, was given by HASSAN & BUSECK (1992). The present research

deals with a range of cancrinite crystals. The spectroscopic data suggest appearance of various superstructure units in the big channel. Some of them resemble cancrinite investigated by HASSAN & BUSECK (1992), whereas others resemble that investigated by EMIRALIEV & JAMZIN (1982). Valuable conclusions can be drawn from the dehydration process carried out within the present research, and monitored by the IR technique. The dehydration process induced in some cancrinite samples causes changes in the superstructure of the anion chain in the big channel. It is quite obvious that  $\text{H}_2\text{O(II)}$  is much more responsible for those changes, because the process is much better pronounced in cancrinites with a higher  $\text{H}_2\text{O(II)}$  content. In the sample formed at  $550^\circ\text{C}$  (in 1M  $\text{Na}_2\text{CO}_3$  solution), the water behaves like  $\text{H}_2\text{O(I)}$ . Water molecules leave the structure without any changes in the twelve-membered channel superstructure. The channel is filled with  $\text{CO}_3$  anions. The rehydration process does not produce any results. Water cannot enter the structure through a blocked channel. By contrast the samples with a large  $\text{H}_2\text{O(II)}$  content adsorb water relatively easily. The  $\text{H}_2\text{O(II)}$  enters the structure before the  $\text{H}_2\text{O(I)}$ . The framework and anions chains in the channel are somewhat distorted. The adsorbed water possess a character of isolated OH groups. The  $\text{H}_2\text{O(I)}$  accumulates at the surface but does not occupy sites in the six-membered channel. It is very unlikely that both kinds of water were present in the six-membered channel before the dehydration process, since the rehydration procedure is capable of permitting only  $\text{H}_2\text{O(II)}$  to enter the crystal structure. It is worth noting that  $\text{H}_2\text{O(I)}$  should have a better chance of reappearing in the channel. Its molecules can choose one of the three potentially available places around  $\text{P}_3$ . The six-membered channel seems to be blocked after dehydration. The twelve-membered channel in turn allows  $\text{H}_2\text{O(II)}$  to enter. The molecules occupy strictly defined sites. They are not those occupied by  $\text{H}_2\text{O(II)}$  before the activation because the superstructure is modified due to the calcination process (compare values of the sharp IR bands in the stretching vibration area of OH before calcination and after adsorption). Adsorption restores  $\text{H}_2\text{O(II)}$  but cannot restore  $\text{H}_2\text{O(I)}$ .

In the A and B-cancrinites crystallized at  $550^\circ\text{C}$  and from more concentrated solution the  $\text{H}_2\text{O(I)}$  dominates. The  $\text{H}_2\text{O(II)}$  appears in trace amounts. The dehydration process modifies the superstructure of the A-cancrinite only. The modification

results in H<sub>2</sub>O(I) adsorption. The B-cancrinite grown in similar conditions preserves its big channel superstructure during the dehydration process. The route for the H<sub>2</sub>O(I) to reappear during the rehydration is blocked.

The correlation between the amount of sodium in cancrinite crystals and the H<sub>2</sub>O(II) content in the structure gives additional valuable information. The correlation is positive, the more sodium, the bigger H<sub>2</sub>O content. Increase in sodium content causes replacement of Ca cations in the big channel through Na<sup>2+</sup> (GRUNDY & HASSAN 1982). The ordering pattern of the supercell includes inter-channel cations, anions and vacancies. The H<sub>2</sub>O(II) appears in the structure with larger sodium and smaller CO<sub>3</sub> groups content. Both constituents are involved in the formation of the supercell unit. According to HASSAN's (1996a, b) data, it is reasonable to place the H<sub>2</sub>O(II) in the six-membered channel. The present research leads to the conclusion that the possibility of associating H<sub>2</sub>O(II) with Na<sup>2+</sup> cannot be excluded. However this statement requires further investigation. Neutron diffraction data on samples showing different big channel environment are necessary.

The water environment in the analcime crystals is distinctly different in the high and low temperature reaction products. Crystals synthesized at low temperature reveal a bigger water amount in the structure. The IR spectra of analcimes crystallized at high temperature (550°C, 0.1 M Na<sub>2</sub>CO<sub>3</sub> solution) display three bands in the OH stretching vibration region. Lowering of the run temperature results in the appearance of additional OH groups with well defined position (the fourth band ~3630cm<sup>-1</sup>). The integrated intensity of the fourth band is four times bigger in the IR spectra of the low temperature analcime than in the corresponding spectra of the analcime formed at higher temperature. The NMR spectra show three different proton environments in the analcime structure. Two of the peaks (at 2.98 ppm and 4.58 ppm) can be attributed to molecular water. Variation in peak intensity correlate well with changes of IR band intensity in the OH stretching vibration area in the analcime samples. The first <sup>1</sup>H resonance signal might be correlated with the broad IR band (~3440cm<sup>-1</sup>) and the second one (at 4.58 ppm) with the ~3630cm<sup>-1</sup> band. The site giving rise to the second narrow peak is better defined. The third <sup>1</sup>H resonance signal points to another OH<sub>m</sub> cluster. Because water in the analcime structure shows a wide range of order-disorder, even more compli-

cated IR or NMR spectra can be expected. LIBOWITZKY & ROSSMAN (1997) presented OH stretching vibration region of analcime crystal composed of five bands.

The dehydration and rehydration processes give evidence that in the structure of the investigated analcimes at least two different kinds of OH<sub>m</sub> groups exist. As in the case of cancrinite, the water can be determined as H<sub>2</sub>O(I) and H<sub>2</sub>O(II). Dehydration and rehydration proceeds in two stages (see activation and adsorption of analcime monitored by IR measurements). The paths of the both processes differ. The hydrogen-bonded water H<sub>2</sub>O(I) leaves the structure first. This is shown in the IR spectra by the disappearance of broad band. The second type of water, H<sub>2</sub>O(II), visible in the IR spectrum as the 3636cm<sup>-1</sup> band, remains in the structure longer. Relict of the water persist even after prolonged calcination. Dehydration causes changes in sodium position and coordination (BAKAKIN & *al.* 1994, KIM & KIRKPATRICK 1998). The adsorbed water molecules enter the modified structure. The IR spectra recorded on the initial stages of rehydration reveal two preferential sites in the structure where water molecules are located. Some of these molecules are located on sites showing order-disorder (broad band from hydrogen-bonded water). The positions of others are better defined. The sharp band can arise from interaction with cations. Two types of water in analcime were found by FRANK-KAMENETSKAYA & *al.* (1997) in the study of unit cell parameters as a function of temperature.

Two stages of dehydration are easily discernible only on IR spectra. The DTG/TG method is not sensitive enough to detect the dual character of the water position. Careful analysis of the shape of the TG curve in some samples allows the second type of water to be located. The curve is asymmetric, with the sloping part at lower temperatures and the steep part at higher temperatures. In some samples water adsorbed at the surface demonstrates two preferential sites.

## CONCLUSIONS

Water position in the cancrinite and analcime structure is sensitive to the physico-chemical conditions of the structure formation. Water assignment can therefore provide helpful information concerning the origin of the crystals.

Activity of the chemical constituents in the solution determines the type of structure formed.

Activity and speciation of the components in a hydrothermal system is highly dependent on synthesis temperature.

The cancrinites and the analcimes formed under lower temperatures incorporate more water than those formed at higher temperature.

The most sensitive building unit to formation conditions in the cancrinite-like minerals is the twelve-membered channel. The superstructure originates from different ordering, orientation and substitution of Na<sub>2</sub>, Ca, CO<sub>3</sub> groups and vacancies. The structures of cancrinites grown at high temperature (550°C, 1M Na<sub>2</sub>CO<sub>3</sub> solution) show a different superstructure pattern from those grown at low temperature (300°C, 1M Na<sub>2</sub>CO<sub>3</sub> solution). The former are rich in Ca cations and CO<sub>3</sub> anions. The latter demonstrate a decrease in Ca cations and CO<sub>3</sub> anions and an increase in sodium cations.

The water environment in cancrinite is composed of different OH<sub>m</sub> clusters. The main forms of them are H<sub>2</sub>O(I) and H<sub>2</sub>O(II). H<sub>2</sub>O(I) shows some disorder at the site. It predominates in high temperature synthesis products. The H<sub>2</sub>O(II) position is well defined. It may have two different H-H orientations in the channel cavity. The amount of H<sub>2</sub>O(II) increases gradually in the synthesized structure with decreasing run temperature. The lower the synthesis temperature the weaker is the interaction of H<sub>2</sub>O(II) with the framework atoms. An increase of the H<sub>2</sub>O(II) content is correlated with the amount of Na, Ca, and CO<sub>3</sub> groups in the structure. The correlation is positive for sodium cations, and negative for both of the other two components. The H<sub>2</sub>O(II) behaviour during dehydration and rehydration processes suggests that the H<sub>2</sub>O(II) may be involved in the superstructure unit in the big channel. Besides H<sub>2</sub>O(I) and H<sub>2</sub>O(II), traces of other OH<sub>m</sub> groups are identified.

The water environment in analcimes, synthesized at low and high temperatures, differs significantly. In analcime, as in cancrinite, at least two types of water appear. Analcime crystals formed at high temperatures show only one type of hydrogen-bonded water H<sub>2</sub>O(I). The second type, H<sub>2</sub>O(II), appears in low temperature synthesis products. The position of this type of water is better defined. The NMR spectra of low temperature analcimes display apart from both types of water additionally a third hydrogen environment. Spectra of high temperature crystals demonstrate, on average, one hydrogen environment.

Water position in the cancrinite and analcime crystals indicates the conditions of their origin.

Even though there are obvious differences in water environment in high and low temperature run products, the relation between the water position and the physico-chemical conditions of crystal formation is a complex one. The water environment in the synthesized crystals depends indirectly on source material structure, reaction temperature, solution composition and others. All those factors exert an influence on the new structure being built. The relative importance of various factors on the relation differs and is often not very easy to assess. Temperature seems to be the main factor influencing the relation. Another factor, of less significance, is salt concentration in the solution.

### Acknowledgments

This research work received financial support from KBN Project No 605/PO4/9508. The author is highly indebted to Prof. Dr W. FRANKE for introducing into the experimental method of hydrothermal synthesis, and would like to thank the referees for their careful inspection of the work and many valuable remarks. Dr M. DEREWIŃSKI, Dr E. CZERWOSZ and Dr K. WOŹNIAK are gratefully acknowledged for very valuable discussion. Thanks are due to Dr E. UTZIG, Dr W. PASŁAWSKA and Dr R. DIDUSZKO for assistance with the TG and X-ray analyses. Special thanks are directed to Prof. Dr. A. RADWAŃSKI, who has helped enormously to prepare the manuscript for publication. Appreciated is also the help of Dr A. KOZŁOWSKI in drafting many of the diagrams.

### REFERENCES

- ABE, H., AOKI, M. & KONNO, H. 1973. Synthesis of analcime from volcanic sediments in sodium silicate solution. Experimental studies on the water-rock interaction. *Contr. Mineral. and Petrol.*, **42**, 81-92. Berlin – Heidelberg.
- ALEKSEYEV, V.A., MEDVEDEVA, L.S., PRISYAGINA, N.I., MESHALKIN, S.S. & BALABIN, A.I. 1997. Change in the dissolution rates of alkali feldspars as a result of secondary mineral precipitation and approach to equilibrium. *Geochim. et Cosmochim. Acta*, **61**, 1125-1142. Oxford.
- ANDERSON, G.M. & CERMIGNANI, C. 1991. Mineralogical and thermodynamic constraints on the metasomatic origin of the York River nepheline gneisses, Bancroft, Ontario. *Can. Mineral.*, **29**, 965-980. Ottawa.
- ANDERSON, G.M. & BURNHAM, C.W. 1983. Feldspar solubility and the transport of aluminum under meta-

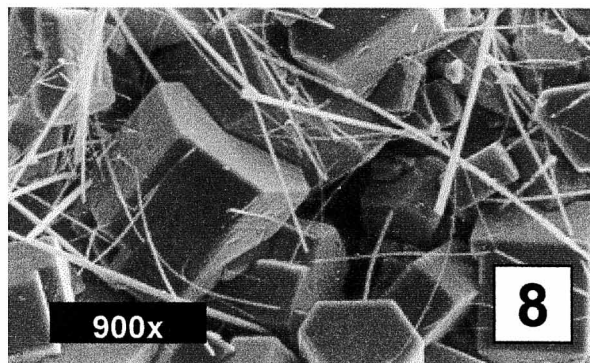
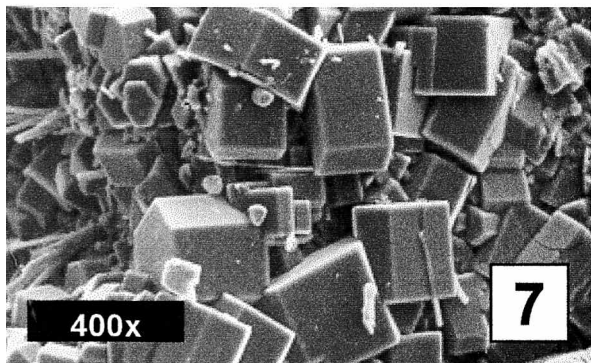
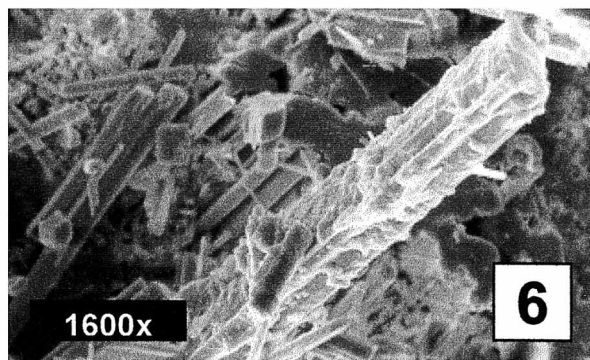
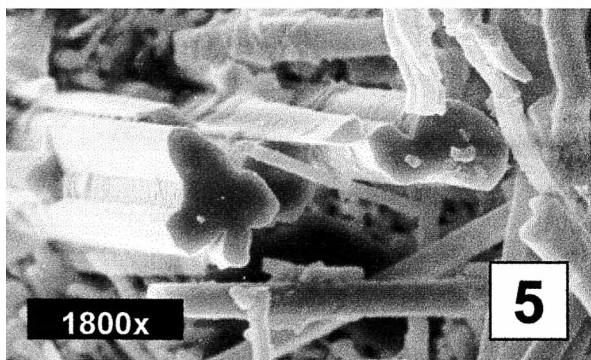
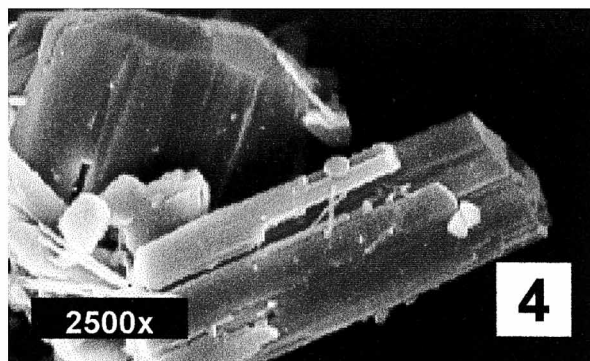
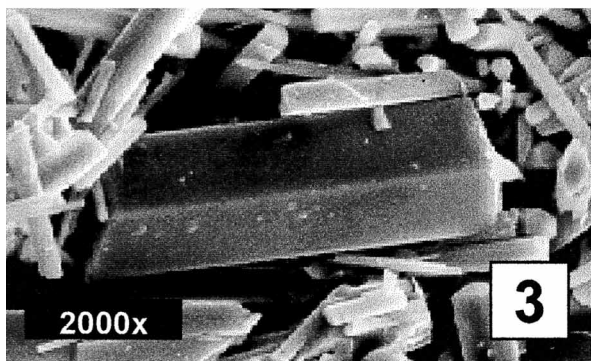
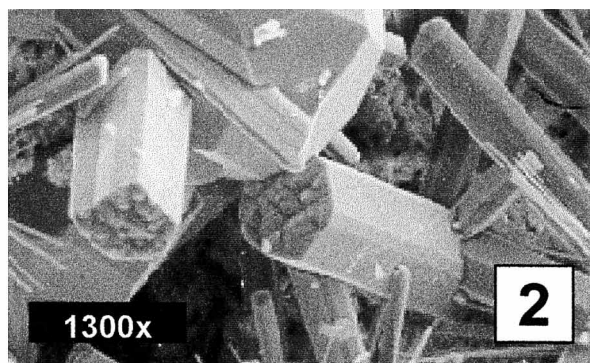
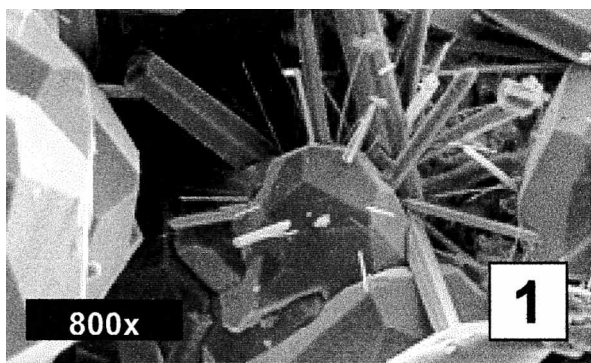
- morphic conditions. *Am. J. Sci.*, **283-A**, 283-297. New Haven.
- BAKAKIN, V.V., ALEXEEV, V.I., SERYOTKIN, YU.V., BELITSKY, I.A., FURSENKO, B.A. & BALKO, V.P. 1994. Crystal structure of dehydrated analcime. Plane four-fold Na-coordination. *Dokl. Akad. Nauk*, **339**, 520-524. Moscow.
- BALLIRANO, P., MARAS, A. & BUSECK, P.R. 1996. Crystal chemistry and IR spectroscopy of Cl- and SO<sub>4</sub>-bearing cancrinite-like minerals. *Amer. Miner.*, **81**, 1003-1012. Washington, D.C.
- BARTH-WIRSCHING, U. & HÖLLER, H. 1989. Experimental studies on zeolite formation conditions. *Eur. J. Mineral.*, **1**, 489-506. Stuttgart.
- BRADY, P.V. & WALTHER, J.V. 1989. Controls on silicate dissolution rates in neutral and basic pH solutions at 25°C. *Geochim. et Cosmochim. Acta*, **53**, 2823-2830. Oxford.
- BUHL, J.CH. 1991. Synthesis and characterization of the basic and non-basic members of the cancrinite-natrodavyne family. *Thermochimica Acta*, **178**, 19-31. Amsterdam.
- BUHL, J.CH., ENGELHARDT, G., FELSCHE, J., LUGER, S. & FOERSTER, H. 1988. <sup>23</sup>Na MAS-NMR and <sup>1</sup>H MAS-NMR studies in the hydro-sodalite system. *Ber. Bunsenges. Phys. Chem.*, **92**, 176-181. Weinheim.
- CASEY, W.H., WESTRICH, H.R., ARNOLD, G.W. & BANFIELD, J.F. 1989. The surface chemistry of dissolving labradorite feldspar. *Geochim. et Cosmochim. Acta*, **53**, 821-832. Oxford.
- CERMIGNANI, C. & ANDERSON, G.M. 1983. The plagioclase exchange reaction in carbonate solution in carbonate solutions and application to nephelinization. *Am. J. Sci.*, **283-A**, 314-327. New Haven.
- DIAKONOV, I., POKROVSKI, G., CASTET, S., SCHOTT, J. & GOUT, R. 1994. Experimental study of Na-Al complexing in hydrothermal solutions. *Mineral. Mag.*, **58A**, 227-228. London.
- DUBANSKA, V. & RYKL, D. 1983. Hydrothermal synthesis of analcime due to albite decay. *Acta Montana*, **62**, 27-42. Prague. [In Czech].
- EMIRALIEV, A. & JAMZIN, I.I. 1982. Refining of carbonate-cancrinite structure by means of neutron diffraction data. *Kristallografiya*, **27**, 51-55. Moscow. [In Russian].
- ENGELHARDT, G., FELSCHE, J. & SIEGER, P. 1992. The hydrosodalite system Na<sub>6+3x</sub>[SiAlO<sub>4</sub>]<sub>6</sub>(OH)<sub>x</sub>·nH<sub>2</sub>O: Formation, phase composition, and de- and rehydration studies by <sup>1</sup>H, <sup>23</sup>Na, <sup>29</sup>Si MAS-NMR spectroscopy in tandem with thermal analysis, X-ray diffraction, and IR spectroscopy. *J. Am. Chem. Soc.*, **114**, 1173-1182. Washington, D.C.
- ENGELHARDT, G., JERSCHKEWITZ, H.-G., LOHSE, U., SARV, P., SAMOSON, A. & LIPPMAN, E. 1987. 500 MHz <sup>1</sup>H-MAS n.m.r. studies of dealuminated HZSM-5 zeolites. *Zeolites*, **7**, 289-291. Guildford.
- FERRARIS, G., JONES, D.W. & YERKES, J. 1971. A neutron diffraction study of the crystal structure of analcime, NaAlSi<sub>2</sub>O<sub>6</sub>·H<sub>2</sub>O. *Z. Kristallogr.*, **135**, 240-252. München.
- FOIT, F.F., JR., PEACOR, D.R. & HEINRICH, E.W. 1973. Cancrinite with a new superstructure from Bancroft, Ontario. *Can. Mineral.*, **11**, 940-951. Ottawa.
- FRANK-KAMENETSKAYA, O.V., GORDIENKO, V.V., KAMINSKAYA, T.N., ZORINA, M.L. & KOSTITSYNA, A.V. 1997. Water in crystal structure of minerals of the analcime – pollucite isomorphous series NaAlSi<sub>2</sub>O<sub>6</sub>·H<sub>2</sub>O – CsAlSi<sub>2</sub>O<sub>6</sub>·H<sub>2</sub>O. *Proceedings of the Russ. Min. Soc.*, **2**, 62-71. Moscow.
- GALITSKI, W.J., GRETSCHUSCHNIKOV, B.N. & SOKOLOV, J.A. 1978. On the water form in the cancrinite. *Jour. Inorg. Chem.*, **23**, 3152-3154. Moscow. [In Russian].
- GIAMPAOLO, C. & LOMBARDI, G. 1994. Thermal behaviour of analcimes from two different genetic environments. *Eur. J. Mineral.*, **6**, 285-289. Stuttgart.
- GERSON, A.R. & ZHENG, K. 1997. Bayer process plant scale: transformation of sodalite to cancrinite. *J. of Cryst. Growth*, **171**, 209-218. Amsterdam.
- GHOBARAKAR, H. & FRANKE, W. 1986. The morphology of analcime. *Cryst. Res. Technol.*, **21**, 1071-75. Berlin.
- GRUNDY, H.D. & HASSAN, I. 1982. The crystal structure of a carbonate-rich cancrinite. *Can. Mineral.*, **20**, 239-251. Ottawa.
- GUNNER, W.K. & BURR, S.W. 1946. Nephelized paragneisses in the Bancroft area, Ontario. *J. Geol.*, **54**, 137-168. Chicago.
- HASSAN, I. & BUSECK, P.R. 1992. The origin of superstructure and modulations in cancrinite. *Can. Mineral.*, **30**, 49-59. Ottawa.
- HASSAN, I. 1996a. The thermal behaviour of cancrinite. *Can. Mineral.*, **60**, 949-956. Ottawa.
- 1996b. Thermal expansion of cancrinite. *Mineral. Mag.*, **34**, 893-900. London.
- HELLMANN, R. 1994. The albite – water system: Part I. The kinetics of dissolution as a function of pH at 100, 200, and 300°C. *Geochim. et Cosmochim. Acta*, **58**, 595-611. Oxford.
- 1995. The albite – water system: Part II. The time evolution of the stoichiometry of dissolution as a function of pH at 100, 200, and 300°C. *Geochim. et Cosmochim. Acta*, **59**, 1669-1697. Oxford.
- HERMELER, G., BUHL, J.CH. & HOFFMANN, W. 1991. The influence of carbonate on the synthesis of an intermediate phase between sodalite and cancrinite. *Catalysis Today*, **8**, 415-426. Amsterdam.

- HOCELLA, JR., M.F., PONADER, H.B., TURNER, A.M. & HARRIS, D.W. 1988. The complexity of mineral dissolution as viewed by high resolution scanning. Auger microscopy: Labradorite under hydrothermal conditions. *Geochim. et Cosmochim. Acta*, **52**, 385-394. Oxford.
- HÖLLER, H. & WIRSCHING, U. 1980. Experiments on the formation of zeolites from nepheline and nephelinite. *In*: L.V.R. REES (Ed.), Proc. 5th Int. Conf. Zeolites. Heyden, pp. 164-170. London.
- JARCHOW, O. 1965. Atomanordnung und Strukturverfeinerung von Cancrinit. *Z. Kristallogr.*, **122**, 407-422. München.
- KARLSSON, H.R. & CLAYTON, R.N. 1990. Oxygen isotope fractionation between analcime and water: An experimental study. *Geochim. et Cosmochim. Acta*, **54**, 1359-1368. Oxford.
- & — 1991. Analcime phenocrysts in igneous rocks: Primary or secondary? *Amer. Miner.*, **76**, 189-199. Washington, D.C.
- KHUNDADZE, A.G., SENDEROV, E.E. & KHITAROV, N.I. 1970. Experimental data on composition of synthetic analcimes. *Geochem.*, **5**, 588-600. Moscow.
- KIM, Y. & KIRKPATRICK, R.J. 1998. High-temperature multi-nuclear NMR investigation of analcime. *Amer. Miner.*, **83**, 339-347. Washington, D.C.
- KUBICKI, J.D., SYKES, D. & ROSSMAN, R. 1993. Calculated trends of OH infrared stretching vibrations with composition and structure in aluminosilicate molecules. *Phys. Chem. Minerals*, **20**, 425-432. Berlin – Heidelberg.
- LIBOWITZKY, E. & ROSSMAN, G. 1997. An IR absorption calibration for water in minerals. *Amer. Miner.*, **82**, 1111-1115. Washington, D.C.
- LINE, CH., PUTNIS, A., PUTNIS, CH. & GIAMPAOLO, C. 1995. The dehydration kinetics and microtexture of analcime from two parageneses. *Amer. Miner.*, **80**, 268-279. Washington, D.C.
- LINE, C.M.B., WINKLER, B. & DOVE, M.T. 1994. Quasielastic incoherent neutron scattering study of the rotational dynamics of the water molecules in analcime. *Phys. Chem. Minerals*, **21**, 451-459. Berlin – Heidelberg.
- LO, H.-J. 1987. The grain size effect on the synthesis of analcime from the glassy basalt. *Memoir of the Geol. Soc. of China*, No **8**, 87-94. Beijing.
- LUHR, J.F. & KYSER, T.K. 1989. Primary igneous analcime: The Colima minettes. *Amer. Miner.*, **74**, 216-223. Washington, D.C.
- MAZZI, F. & GALLI, E. 1978. Is each anacime different? *Amer. Miner.*, **63**, 448-460. Washington, D.C.
- MERLINO, S. 1984. Feldspathoids: their average and real structures. *In*: W.L. BROWN (Ed.), Feldspars and feldspathoids, pp. 435-470. Reidel Publishing Company.
- MUNDUS, C., MULLER-WARMUTH, W. & BUHL, J.CH. 1996. Crystallization of the basic sodalite under hydrothermal conditions studied by MAS-NMR, XRD and DTA/DTG. *Eur. J. Mineral.*, **8**, 231-239. Stuttgart.
- NAKAMOTO, K., MARGHOSHES, M. & RUNDLE, R.E. 1955. Stretching frequencies as a function of distances in hydrogen bonds. *J. Am. Chem. Soc.*, **77**, 6480-6488. Washington, D.C.
- NOVAK, A. 1974. Hydrogen bonding in solids. *In*: J.D. DUNITZ, P. HEMMERICH, R.H. HOLM, J.A. IBERS, C.K. JORGENSEN, J.B. NEILANDS, D. REINEN & R.J.P. WILLIAMS (Eds), Structure and bonding 18: Large molecules, pp. 177-216. Springer; New York.
- PEARCE, T.H. 1993. Analcime phenocrysts in igneous rocks: Primary or secondary? – Discussion. *Amer. Miner.*, **78**, 225-229. Washington, D.C.
- PECHAR, F. 1988. The crystal structure of natural monoclinic analcime (NaAlSi<sub>2</sub>O<sub>6</sub>·H<sub>2</sub>O). *Z. Kristallogr.*, **184**, 63-69. München.
- 1989. Hydrothermal analcime synthesis at 10MPa isobar. *Cryst. Res. Technol.*, **24**, 871-877. Berlin.
- PUTNIS, A., PUTNIS, CH. & GIAMPAOLO, C. 1994. The microtexture of analcime phenocrysts in igneous rocks. *Eur. J. Mineral.*, **6**, 627-632. Stuttgart.
- SŁABY, E. 1994. Cancrinite formation as a product of oligoclase alteration in carbonate solution – an experimental approach. *Eur. J. Min.*, **6-1**, p. 271. Stuttgart.
- SŁABY, E., KOZŁOWSKI, A., CZERWOSZ, E., DIDUSZKO, R. & BANERJEE, A. 1995. Investigation of synthetic fluid inclusions in hydrothermal analcimes. *Bol. de la Soc. Esp. de Miner.*, **18-1**, 235-236. Madrid.
- SOKOLOV, N.D. 1964. Vodornaya svyaz. *Nauka*; Moscow.
- TAYLOR, W.H. 1930. The structure of analcite (NaAlSi<sub>2</sub>O<sub>6</sub>·H<sub>2</sub>O). *Z. Kristallogr.*, **74**, 1-19. München.
- UEDA, S. & KOIZUMI, M. 1979. Crystallization of analcime solid solutions from aqueous solutions. *Amer. Miner.*, **64**, 172-179. Washington, D.C.
- ZHENG, K., GERSON, A.R., ADDAI-MENSAH, J. & SMART, R.St.C. 1997. The influence of sodium carbonate on sodium aluminosilicate crystallization and solubility in sodium aluminate solutions. *J. of Cryst. Growth*, **171**, 197-208. Amsterdam.

## PLATE 1

Habit of experimentally grown **cancrinite** and **nepheline**

- 1 — Aggregate of acicular cancrinite growing on analcime (run conditions: 8 days synthesis,  $T=450^{\circ}\text{C}$ ,  $0.5\text{M Na}_2\text{CO}_3$  solution; source material – acid plagioclase)
- 2 — Cancrinite – combination of two prisms (run conditions:  $T=550^{\circ}\text{C}$ ,  $1\text{M Na}_2\text{CO}_3$  solution; source material – acid plagioclase)
- 3 — Cancrinite – single prism (run conditions:  $T=450^{\circ}\text{C}$ ,  $0.5\text{M Na}_2\text{CO}_3$  solution; source material – basic plagioclase)
- 4 — Cancrinite – combination of prism with pyramid and pedion (run conditions:  $T=450^{\circ}\text{C}$ ,  $0.5\text{M Na}_2\text{CO}_3$  solution; source material – basic plagioclase)
- 5-6 — Crystal cluster of cancrinite (run conditions:  $T=550^{\circ}\text{C}$ ,  $1\text{M Na}_2\text{CO}_3$  solution; source material – basic plagioclase)
- 7 — Nepheline (run conditions: 12 days synthesis,  $T=550^{\circ}\text{C}$ ,  $1\text{M Na}_2\text{CO}_3$  solution, W/M ratio 5; source material – acid plagioclase)
- 8 — Short hexagonal prisms of nepheline with cancrinite needles (run conditions: 12 days synthesis,  $T=600^{\circ}\text{C}$ ,  $1\text{M Na}_2\text{CO}_3$  solution, W/M ratio 5; source material – acid plagioclase)

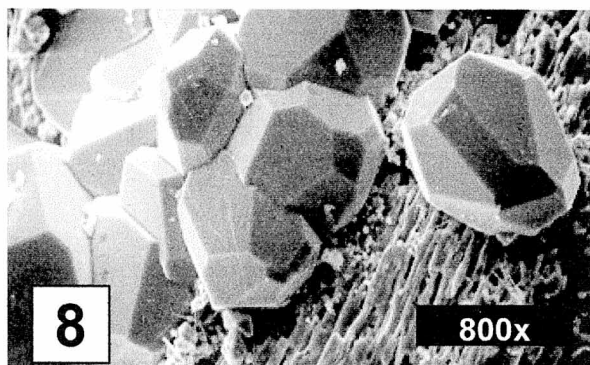
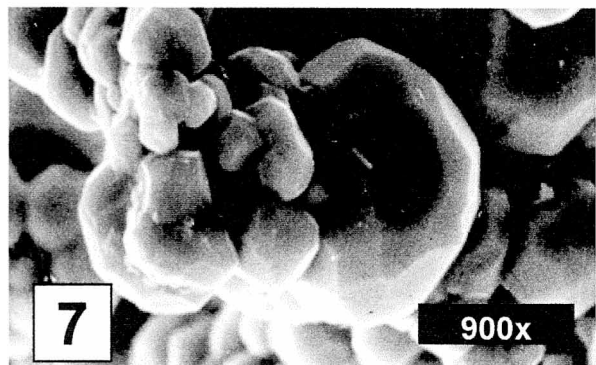
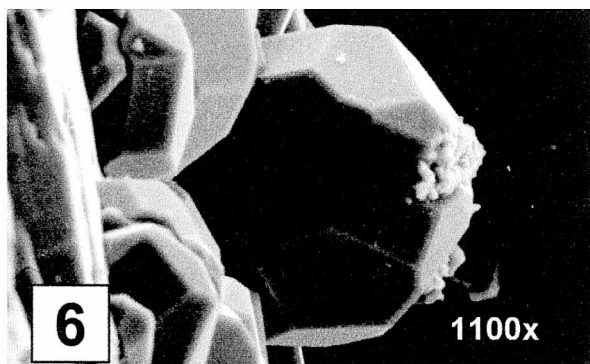
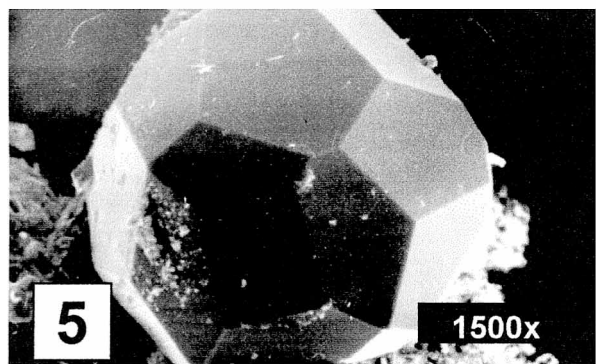
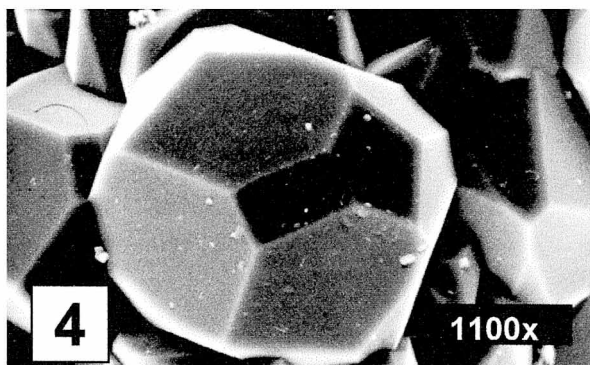
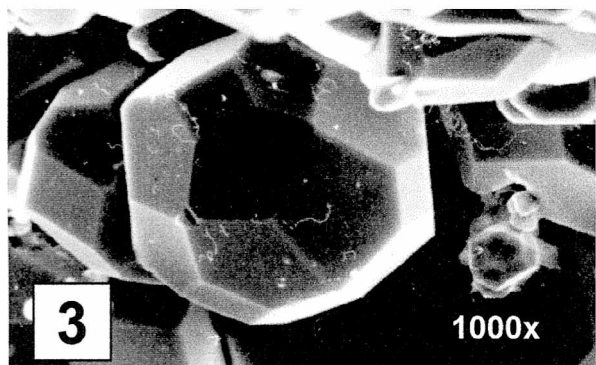
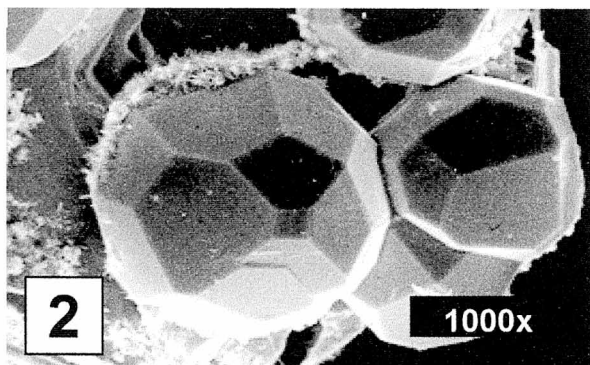
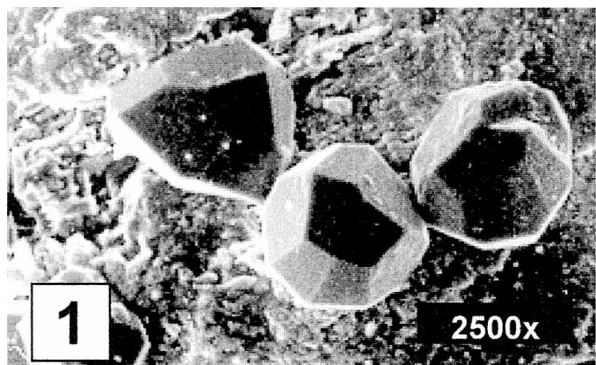


Habit of experimentally grown **cancrinite** and **nepheline**

## PLATE 2

Habit of experimentally grown **analcime**

- 1 — Analcime – deltoicositetrahedron (run conditions: T=450°C, 1M Na<sub>2</sub>CO<sub>3</sub> solution)
- 2 — Analcime – combination of deltoicositetrahedron with cube (run conditions: T=400°C, 0.5M Na<sub>2</sub>CO<sub>3</sub> solution)
- 3-4 — Analcime – combination of deltoicositetrahedron with cube (run conditions: T= 300°C, 0.5M Na<sub>2</sub>CO<sub>3</sub> solutions)
- 5-6 — Analcime – combination of deltoicositetrahedron with cube (run conditions: T=300°C, 0.1M Na<sub>2</sub>CO<sub>3</sub> solution)
- 7 — Analcime – combination of deltoicositetrahedron with cube and probably tetrakisohedron (run conditions: T=300°C, 0.5M NaHCO<sub>3</sub> solution)
- 8 — Analcime (run conditions: 4 days synthesis, 400°C, 0.5M Na<sub>2</sub>CO<sub>3</sub> solution)



Habit of experimentally grown analcime